Cranfield University

Clair Atterbury.

Investigation into the manipulation of the properties of Indium Tin Oxide (ITO) coatings.

School of Applied Science.

MSc. Ultra Precision Technologies.

Cranfield University

School of Applied Science

MSc Thesis. Ultra Precision Technologies

2007 - 2008

Clair Atterbury

Investigation into the manipulation of the properties of Indium Tin Oxide (ITO) coatings.

Supervisors: Prof John Nicholls and Mr Phil Hatchett

Academic Year 2007 to 2008

This thesis is submitted in partial fulfilment of the requirements for the degree of MSc Ultra Precision Technologies.

ABSTRACT

This thesis investigates the manipulation of the properties of Indium Tin Oxide (ITO) coatings. This is carried out with a combination of Experimental and Theoretical work. The coating of ITO onto a glass substrate was both theoretically modelled and the practical work analysed to observe the effects. Observation of the effects on the output parameters when depositing a single layer of ITO via Electron beam evaporation onto a glass substrate multiple times with varying conditions was carried out. The amount of ITO required to produce optimum % transmission and the deposition conditions required to provide <20 Ω/□ and <100 Ω/□ were investigated.

This study then considered the addition of a single layer of an additional coating both theoretically and practically to maximise the %T for the wavelength ranges under consideration. From this, the ideal refractive index for the additional coating to maximise the %T for the ranges was deduced. Progression was then made to consider multiple layers. Theoretical work carried out on the addition of extra layers and the deduction of the optimal refractive index implied that overall, Cryolite would produce the best average %T across the ranges considered.

In addition to this, the results of ITO deposition via Evaporation and sputtering were examined to determine the difference the technique used has upon the coating produced.

DEDICATION

I would like to dedicate this work to my parents who have supported me through this MSc and throughout my life. I would also like to dedicate this work to the memory of Leah Bushell who has also supported me through the important times in my life and my memory of her will always be with me throughout my MSc and life.

Without their kind support, I would not have got as far as I have.

ACKNOWLEDGMENTS

I would like to thank the following people for their kind help during my project:

- Dr Chris Sansom and all of the Precision Engineering department at Cranfield
- Mr Phil Hatchett and Mrs Gail Hatchett
- Prof John Nicholls
- Ms Sharon Mcguire
- Dr John Mitchell and UPSII generally
- Ms Christine Kimpton
- Mr Andrew Dyer
- Diamond Coatings

Table of Contents

LIST OF ILLUSTRATIONS

LIST OF TABLES

1 Introduction

1.1 The project

This project involves the investigation of Indium Tin Oxide (ITO) coatings and the manipulation of their % Transmission (over the visible and the immediately neighbouring ranges) and Sheet Resistivity. The main deposition method considered will be Ion Assisted Vapour Deposition. Sputtering will also be considered for comparative purposes.

Chapter 1 introduces the project and considers the project aims and objectives.

Chapter 2 investigates prevalent literature available on this subject.

The Experimental and Theoretical work carried out is reported and discussed in chapters 3 & 4.

Chapter 5 discusses the results obtained in chapters 3 and 4.

Chapter 6 then moves on to form Conclusions and make Recommendations for future work.

Unfortunately, the application of this work can not be discussed for commercial reasons.

1.2 Aims and Objectives

The aims and objectives of this project are as follows:

- To review theoretical model of the effects of adding a layer of ITO onto a glass substrate

- Observation of the effects on the output parameters when depositing a single layer of ITO via Electron beam evaporation onto a glass substrate multiple times with varying conditions
- Determination of the ITO deposition conditions required to provide <20 Ω/□
- Determination of the ITO deposition conditions required to provide <100 Ω/□
- Determination of the effects of adding coatings to maximise %T by theoretical modelling
- Observation of the results of depositing coatings onto the ITO to maximise %T by Evaporation
- Examination of the results of ITO deposition via IAD and sputtering to determine the difference the technique used has upon the coating produced
- The primary %T values to be considered in this project are the values it takes over the visible range

2 Literature Review

2.1 Indium Tin Oxide (ITO)

A Transparent Conducting Oxide (TCO) can be defined as a thin film that is transparent to visible light and conducts electricity (Subrahmanyam, 2002).

Indium Oxide is a transparent ceramic material with the following structure:

Figure 1 Indium Oxide

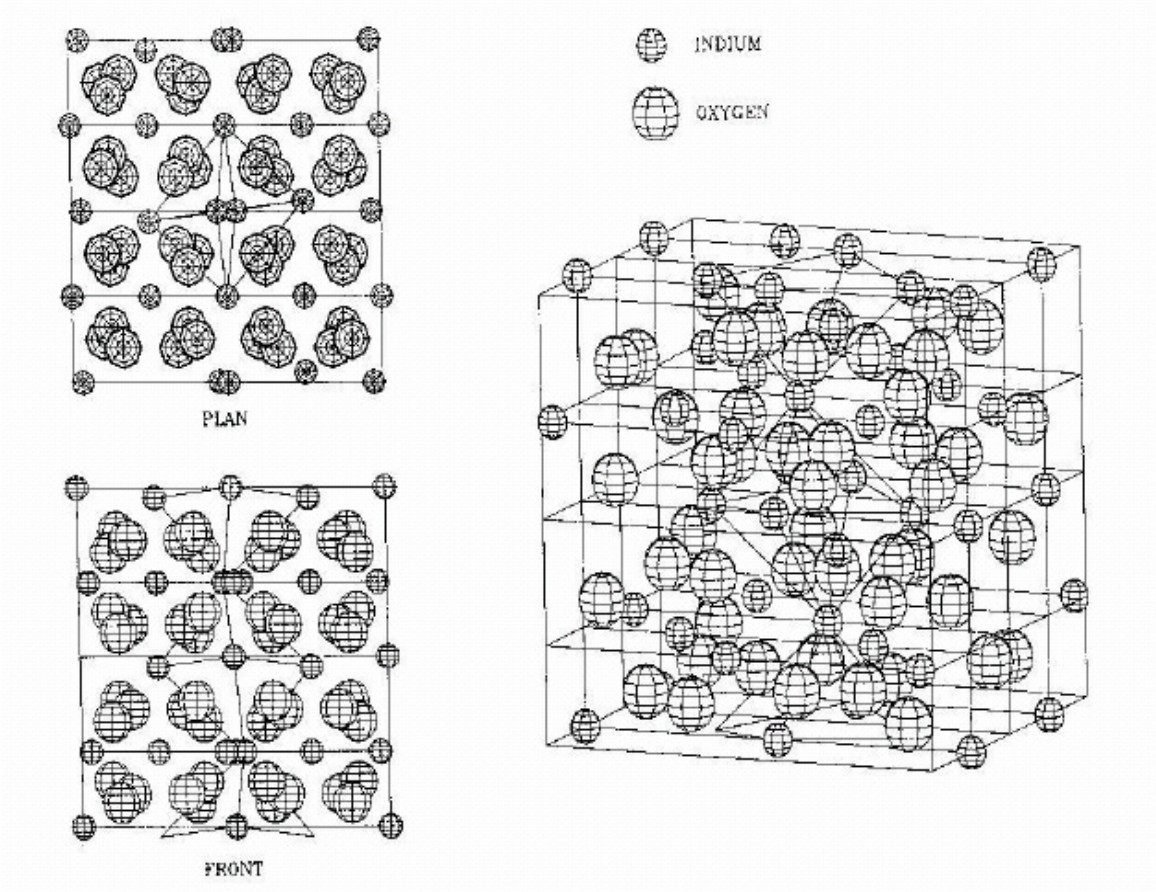

(Source Zhou, 2005)

Indium Oxide maintains its transparency when it is doped with Tin. The addition of tin has the desirable effect of making the material conductive by increasing a number of free electrons present (Eite *et al*, 2004). Indium Oxide doped with Tin, commonly known as Indium Tin Oxide (ITO) is a TCO. Depending upon the temperatures involved, ITO can take the following forms (Lawson, 2008):

- Room temperature deposition results in an amorphous ITO coating (a-ITO).
- At temperatures above about 150^{o}C, ion bombardment results in the nucleation of small crystal sites. The overall result being the production of Polycrystalline ITO films (p-ITO). Heating to about 200^{o}c also produces a polycrystalline structure. p-ITO has a very smooth surface profile.

There are numerous techniques for depositing ITO. This will be reviewed below.

2.2 Review of commonly employed ITO coating techniques

A review of the prevalent ITO literature reveals that the following techniques have been used to apply ITO coatings:

1. **Physical processes e.g. Dip Coating** (Piao *et al,* 2006, Chen *et al*, 2005, Agerter *et al*, 2003, Al-Dahoudi *et al*, 2003, Goebbet *et al*, 1999, TakÅhashi *et al*, 1997, Nishio *et al*, 1996), **Spin Coating** (Psuja *et al*, 2007, Al-Dahoudi *et al*, 2006, Han *et al*, 2005, Hong *et al*, 2004), **Spray Coating** (Goebbet *et al*, 1999, Bisht *et al*, 1999), **Direct gravure printing** (Puetz *et al*, 2005)

2. **Laser based processes e.g. Pulsed laser deposition** (Viespe *et al*, 2007, Teghil *et al*, 2007, Ngaffo *et al*, 2007)

3. **Arc Discharge deposition** (Chen *et al*, 2004, Niino *et al*, 2002)

4. **Chemical Vapour Deposition** (Goebbet *et al*, 1999), Chemical Solution Deposition (Yun *et al*, 2005)

5. **Physical Vapour Deposition:**

    a) **Sputtering e.g. RF** (Boycheva *et al*, 2007, Bertran *et al*, 2003), **DC** (Shen *et al*, 2006, Boehme *et al*, 2005), **Magnetron** (Lee *et al*, 2007, De Bosscher *et al*, 2005, Gao *et al*, 2001, Strumpfel *et al*, 2000, Kusano *et al*, 1998, Lippens *et al*, 1998, Wu *et al*, 1997, Baouchi, 1996), **High Vacuum Sputter roll coating** (Mayr, 1986), **Pulse package sputtering** (Gnehr *et al*, 2005), **Cyclotron resonance plasma sputtering** (Yasui *et al*, 2001)

    b) **Evaporation techniques e.g. Electron Beam deposition** (Raoufi *et al*, 2008, Fallah *et al*, 2006), **Ion Assisted Deposition** (Wang *et al*, 1999, Yu *et al*, 2008, Lee *et al*, 1999)

The references given in each case illustrate examples where the application of the technique has been discussed. This thesis will be focussing on the Physical Vapour deposition route of Electron Beam Evaporation (with Ion Assisted Vapour Deposition). Sputtering of ITO will also be considered. Sputtering and Evaporation with Ion Assisted Vapour Deposition are the most common techniques applied today (AtoZ of materials, Cerac technical publications). These techniques are therefore considered in more detail below.

2.2.1 Electron Beam Evaporation

According to Bashir (1998), the process of evaporation involves heating a solid to a sufficiently high temperature that vaporisation occurs. This process is

followed by the solid recondensing onto a cooler substrate. Evaporation is a physical vapour deposition process that can be achieved via various heating mechanisms such as radiation, eddy currents, electron beam bombardment, a laser beam or electrical discharge (Bunshah, 1980). The Electron beam bombardment heating method will be focussed upon in this section as this is the technique used in this work.

The process of electron beam evaporation is illustrated in Figure 2. According to Smith (1995), the process of Electron beam evaporation is as follows. Electrons are emitted from a hot filament and their acceleration is induced via the high voltage applied as is illustrated in Figure 3. The electron beam is deflected by a magnetic field. The filament is hidden and the beam is deflected to make it take the desired path to ensure that the filament does not sit in the path of the evaporant. The crucible is typically water cooled to minimise outgassing or melting complications. The accelerated electrons impact the evaporant with a power that is sufficient to heat most materials to greater than 1000^{o}C (Traub, 2008). Pellicori (2002) feels that heating of over 1200^{o}C can commonly be achieved. The use of a suitable evaporant would thus result in vaporisation of that evaporant and recondensation onto the substrate.

Pellicori (2002) states that this method is the most common method used to deposit ITO due to the suitability of the temperatures involved.

Figure *4* illustrates an electron beam evaporation gun in operation.

Figure 2 Process of Electron Beam Evaporation

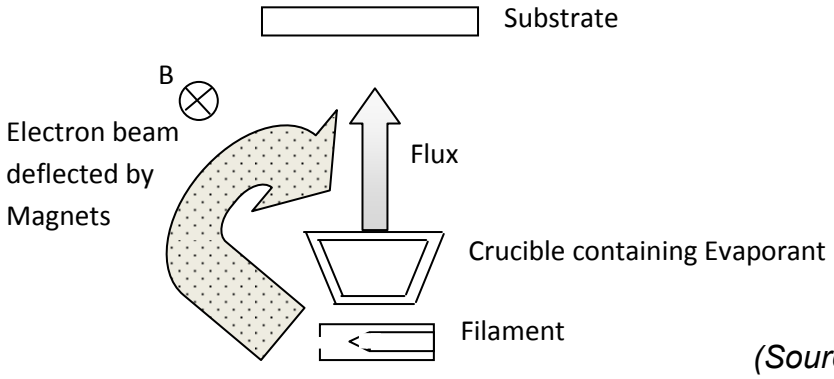

(Source – Traub, 2008)

Figure 3 Typical Electron beam evaporation gun

(Source Hatchett, 2008)

Figure 4 Electron beam Evaporation Gun in operation

(Source Hatchett, 2008)

2.2.2 Ion Assisted vapour Deposition

Ion assisted Vapour deposition is used to assist Physical Vapour Deposition processes such as Sputtering or Evaporation (Hirvonen, 2004). In this section, the Physical Vapour Deposition process considered is Electron beam evaporation (as discussed in the previous section). In conjunction with Electron Beam Evaporation, ions are used to assist the process. A typical ion assisted vapour deposition chamber where this is carried out is illustrated in Figure 5. It can be seen that in addition to the electron beam gun discussed in the previous section, there is also an ion source present that typically produces a low energy broad ion beam (Hirvonen, 2004). Other important features are the substrate heaters that are used to heat the substrate to the desired temperature and the thickness monitor that in conjunction with the IC/5 determines the thickness of coating that has been deposited on the substrate. The substrate dome is the housing for the substrates and is rotated at the desired speed by the substrate drive.

Figure 5 Typical Ion Assisted Vapour Deposition Chamber

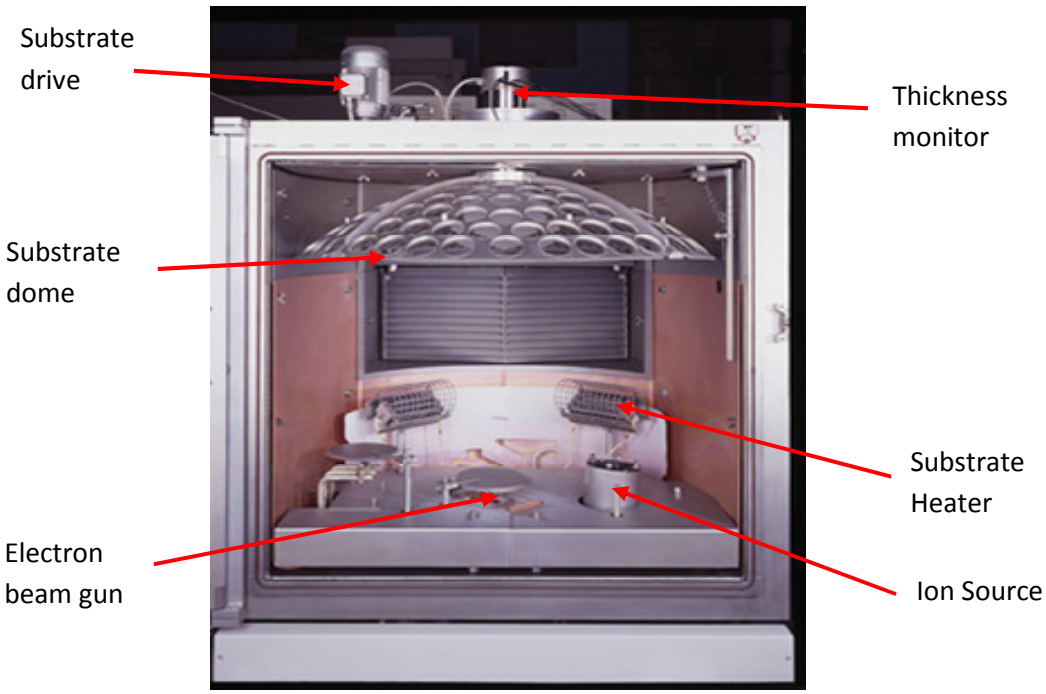

(Source – Hatchett, 2008)

Hirvonen (2004) feels that the energetic ions used in ion assisted deposition play various beneficial roles in thin film coating processes. These benefits can be divided into two main categories. These categories are generic effects of thin film growth and Chemical effects on growth. The Generic effects of ion assistance on thin film growth are as follows:

- Enhanced adhesion
- Texture modification
- Nucleation
- Stress control
- Densification
- Surface morphology and patterning

The Chemical effects of ion assistance on thin film growth are:

- Stoichiometry and synthesis control.

2.2.3Sputtering

Sputtering is again a physical vapour deposition process. The basic process of sputtering is illustrated in Figure 6.

Figure 6 Process of Sputtering

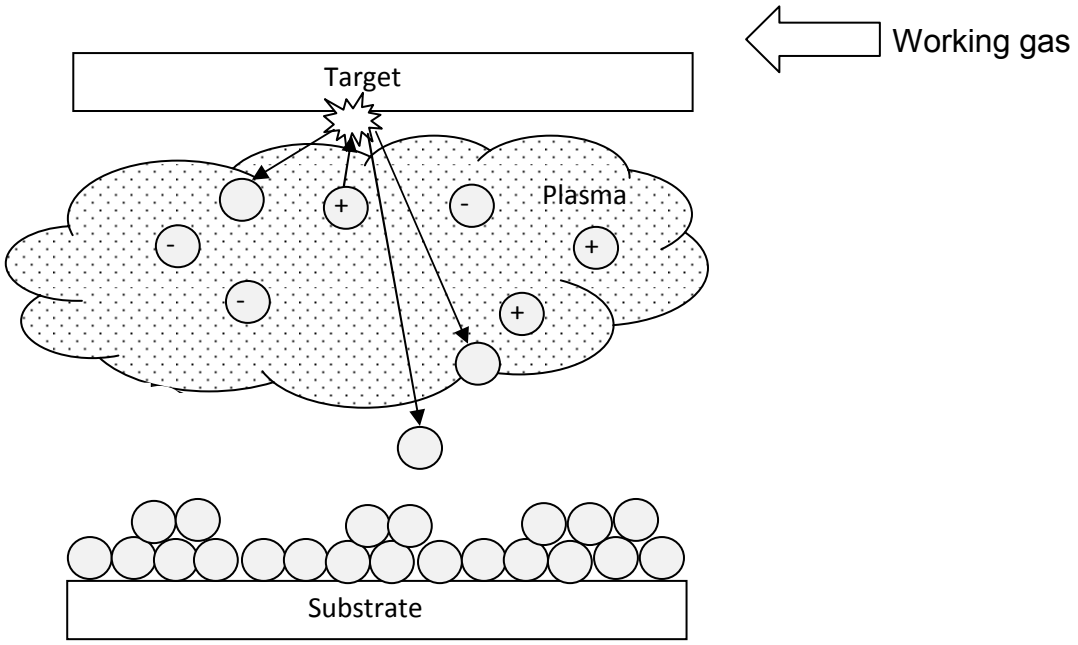

(Source Bunshah, 1980)

The basic process of sputtering consists of positively charged ions (typically created from a working gas (usually Argon) and a glow discharge) striking a target resulting in the dislodging of target atoms which then condense onto the substrate (Bunshah, 1980). Magnetic fields produced from magnets can be used to enhance the process by localising the plasma to provide optimum performance (Traub, 2008).

2.2.4 Comparison of Evaporation and Sputtering

Traub (2008) performed a comparative study between Evaporation and Sputtering. In this study, the technique which conformed to the features in each case was identified. The results of this were as follows:

Table 1 Comparison of Evaporation and Sputtering Techniques

Feature considered	Evaporation	Sputtering
Highest rate	☑	
Highest film density		☑
Highest purity films produced	☑	
Best Adhesion		☑
Lowest film stress	☑	
Best Step coverage		☑
Highest film thickness uniformity	☑	
Lowest material consumption		☑
Lowest material investments	☑	
Lowest x-ray emissions		☑
Best thickness control	☑	
Best Compound deposition control		☑

2.3 Single Layer ITO deposition and analysis of factors that effect the properties of the ITO layer reported in the literature

The literature demonstrates that people have considered the effect of limited variables in their deposition process and the effect that they have on the single layer ITO coating produced.

Liu, Mihara, Matsutani, Asanuma, Kiuchi (2003), Liu, Matsutani, Asanuma, Kiuchi (2003), Liu *et al* (2002), Pokaipisit and Morton *et al* (1999) have all utilised Ion assisted Deposition to deposit a single layer of ITO and considered the effect on certain variables on the results produced.

Liu, Mihara, Matsutani, Asanuma, Kiuchi (2003) considered the effects that Evaporation rate, Substrate Temperature, Oxygen Ion beam energy and density had on the results observed over the wavelength range of 200 and 1000nm.

Liu, Matsutani, Asanuma, Kiuchi (2003) investigated the effects of the varying the acceleration voltage and current densities of the oxygen ions produced using an electron cyclotron resonance source. The differences that occur when the deposition was carried out at room temperature and 200^{o}C were also observed.

Liu *et al* (2002) reported the effects that variables such as thickness and growth rate had on the results achieved.

Pokaipisit (undated) looked at the variables of ion beam energy density, oxygen flow rate and substrate temperature.

Morton *et al* (1999) considered variables such as deposition rate, oxygen flow, and drive current on the sheet resistivity produced.

The effect of certain variables has also been considered for other deposition techniques:

Amirishahbazi *et al* (2005) and Bashar (1998) considered the effect of certain variables on the resulting single layer of ITO produced via Sputtering. Bashar

(1998) performed a more comprehensive study encompassing a wider range of variables.

Kim *et al* (2005) reported the effect of certain variables on the deposition of a single layer of ITO via pulsed laser deposition.

Regarding the analysis of variables, it can be seen from the literature that different variables have been studied in isolation for various specific deposition systems and methods. It is for this reason that the author has decided in this thesis to perform a more comprehensive study considering all of the major variables that can be altered and observed on the LAB600 and their effects on the results rather than just considering the variables that are assumed to have a greater dependence.

Unfortunately, with all of the studies reported in the literature, the authors had either different or undisclosed sheet resistivity requirements (and thus thicknesses). Unless the required sheet resistivity matches the sheet resistivity requirements of this thesis, a direct comparison of the Transmission and Resistivity results can not be successfully performed as is demonstrated by all of studies mentioned above that demonstrate that the variables chosen have an effect on the results obtained. To do more work with this, the conditions given in the literature would need to be replicated to enable direct comparisons to be performed. This was not possible with the constraints placed on this work and it is for this reason that the results from the papers are not shown.

2.4 Layers reported to have been employed with ITO in an attempt to maximise the %T observed in the visible region

Dobrowolski *et al* (1987) and SPO (2000) both report the deposition of a single layer of SiO_2 on top of an existing layer of ITO in an attempt to improve the %T observed in the visible region.

Morton *et al* (1999) again looked at the results of a single layer of SiO_2. However, in this case, a layer of Al_2O_3 was also introduced between the substrate and the ITO in an attempt to further improve the results.

Gilo *et al* (1999) on the other hand considered the addition of a single layer of MgF_2 whose thickness ranged between 50 to 250 nm to the existing ITO layer again in an attempt to maximise the %T.

Dever *et al* (1998) takes this work a step further and considered the co-deposition of ITO and MgF_2.

Stetson (2006) on the other hand proposed a more complex multilayer stack arrangement consisting of both TiO_2 and SiO_2 again with the aim of maximisation of %T across the visible range.

It can be seen from this section that the most commonly reported coating materials to have been applied in an attempt to maximise the %T of ITO in the visible region are SiO_2, TiO_2 and MgF_2. It is for this reason that this thesis will initially consider the addition of these layers to the ITO as a starting point in the quest to maximise the %T.

2.5 Data used in theoretical section

All the plots in this section were produced with Essential Macleod.

2.5.1 ITO Data Sources

The four main sources of ITO that were used in the theoretical section were obtained from Essential Macleod. The data and the original source for each set of data is given below:

2.5.1.1 ITO DATA 1

The data referred to as ITO data 1 was obtained from Essential Macleod. It was originally sourced from: http://windows.lbl.gov/materials/chromogenics/default.htm.

The values it provided for refractive indices and Extinction coefficients are illustrated on the following page:

Figure 7 Plot of Refractive index and Extinction Coefficient for ITO data 1

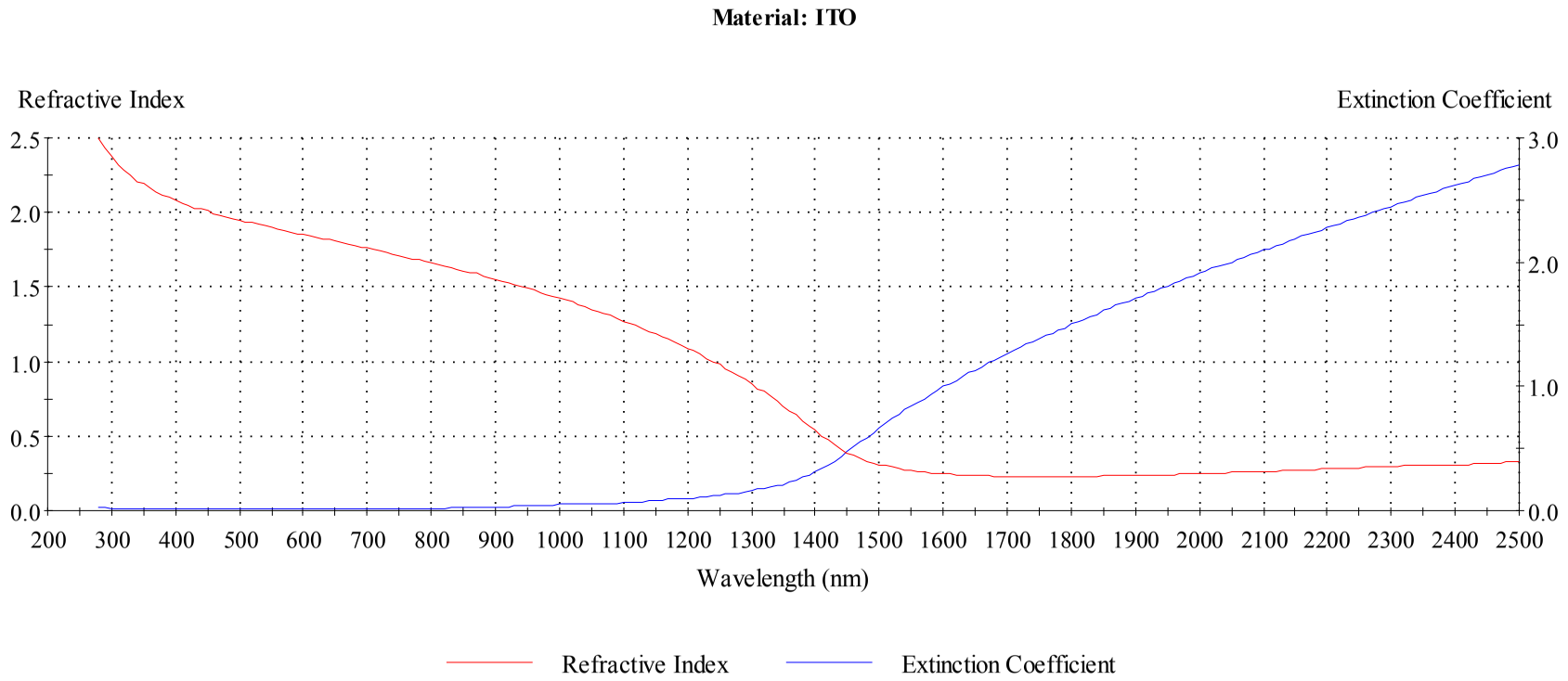

2.5.2.2 ITO DATA 2

The data referred to as ITO data 2 was obtained from Essential Macleod. No original source was listed.

The values it provided for refractive indices and Extinction coefficients are illustrated on the following page:

Figure 8 Plot of Refractive index and Extinction Coefficient for ITO data 2

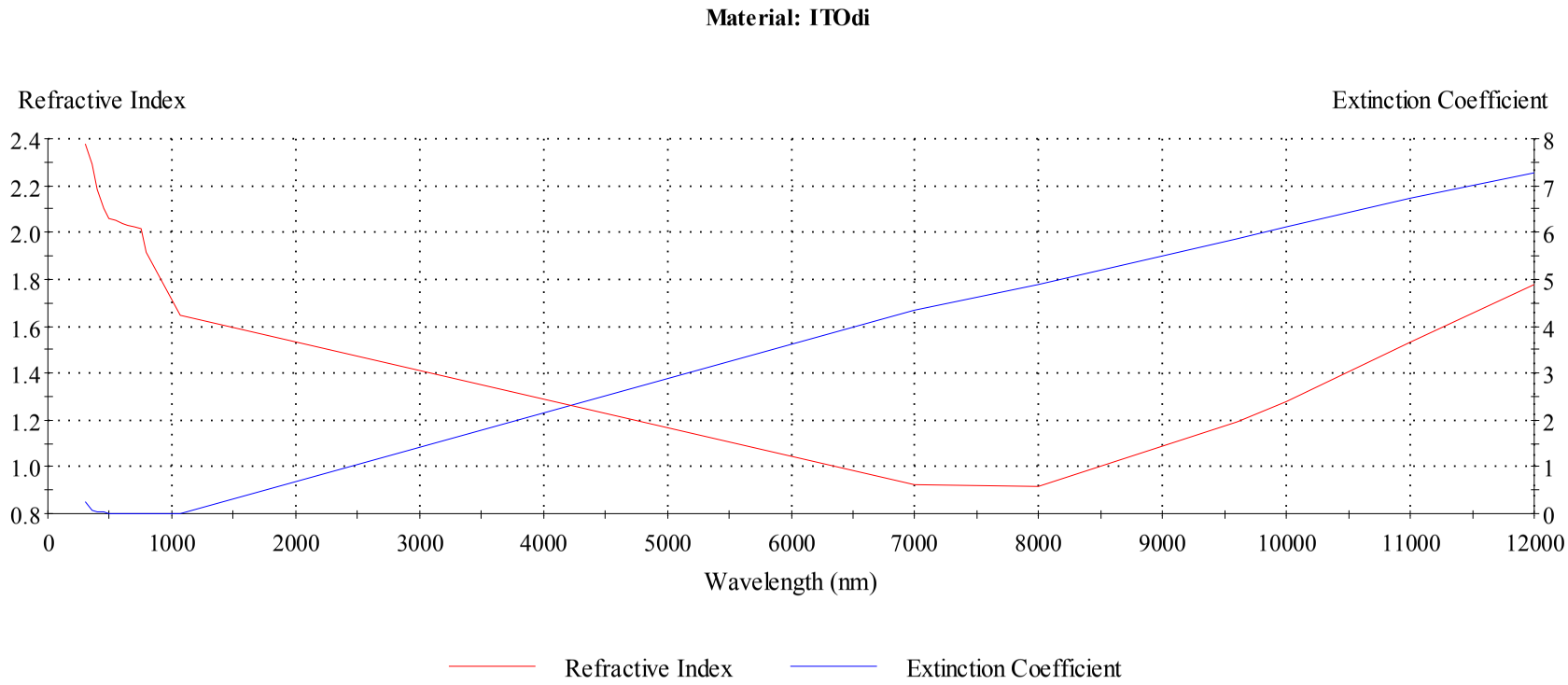

2.5.2.3 ITO DATA 3

The data referred to as ITO data 3 was obtained from Essential Macleod. It was originally sourced from the SOPRA Database

The values it provided for refractive indices and Extinction coefficients are illustrated on the following page:

Figure 9 Plot of Refractive index and Extinction Coefficient for ITO data 3

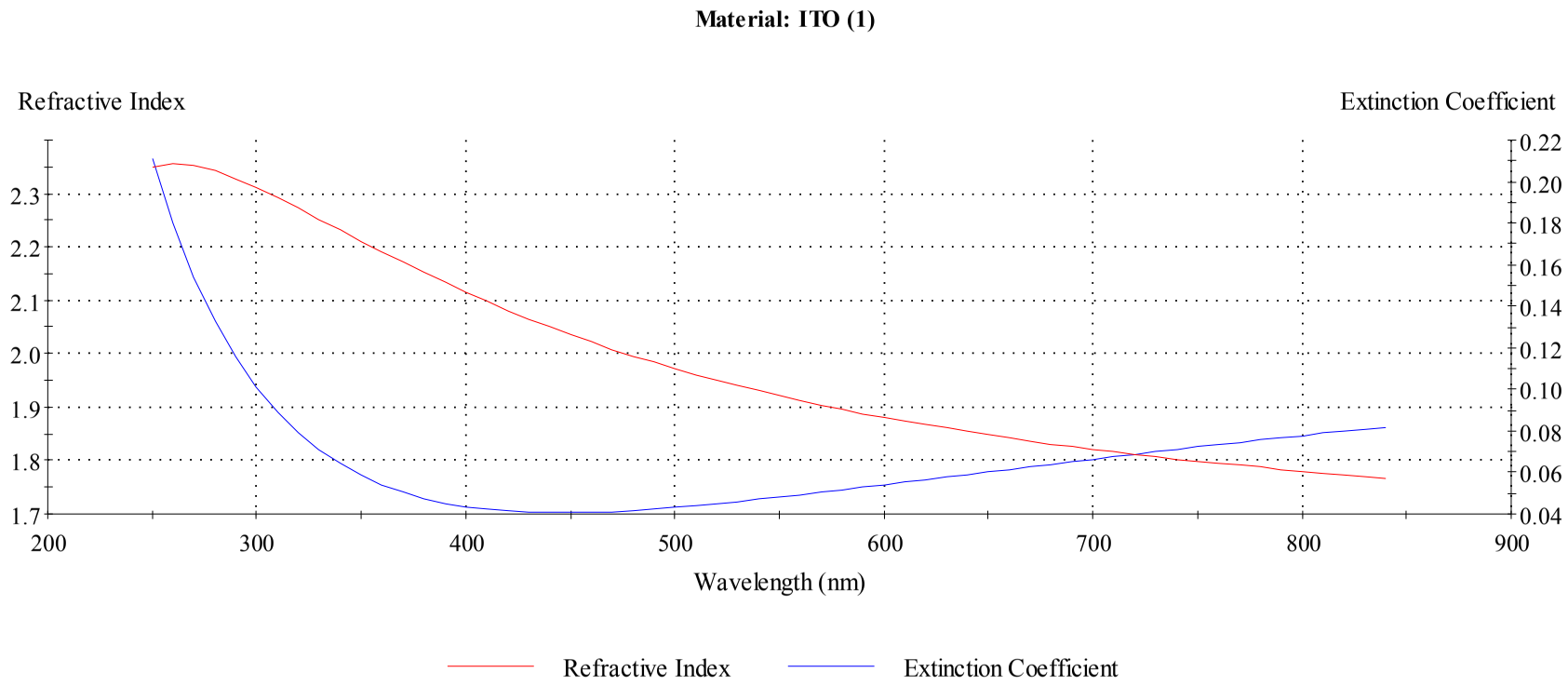

2.5.2.4 ITO DATA 4

The data referred to as ITO data 4 was obtained from Essential Macleod. It was originally sourced from Hoppe, H, N S Sariciftci, and D Meissner, Optical constants of conjugated polymer/fullerene based bulk-heterojunction organic solar cells. Molecular Crystals & Liquid Crystals, 2002. 385: p. [233]/113-[239]/119.

The values it provided for refractive indices and Extinction coefficients are illustrated below:

Figure 10 Plot of Refractive index and Extinction Coefficient for ITO data 4

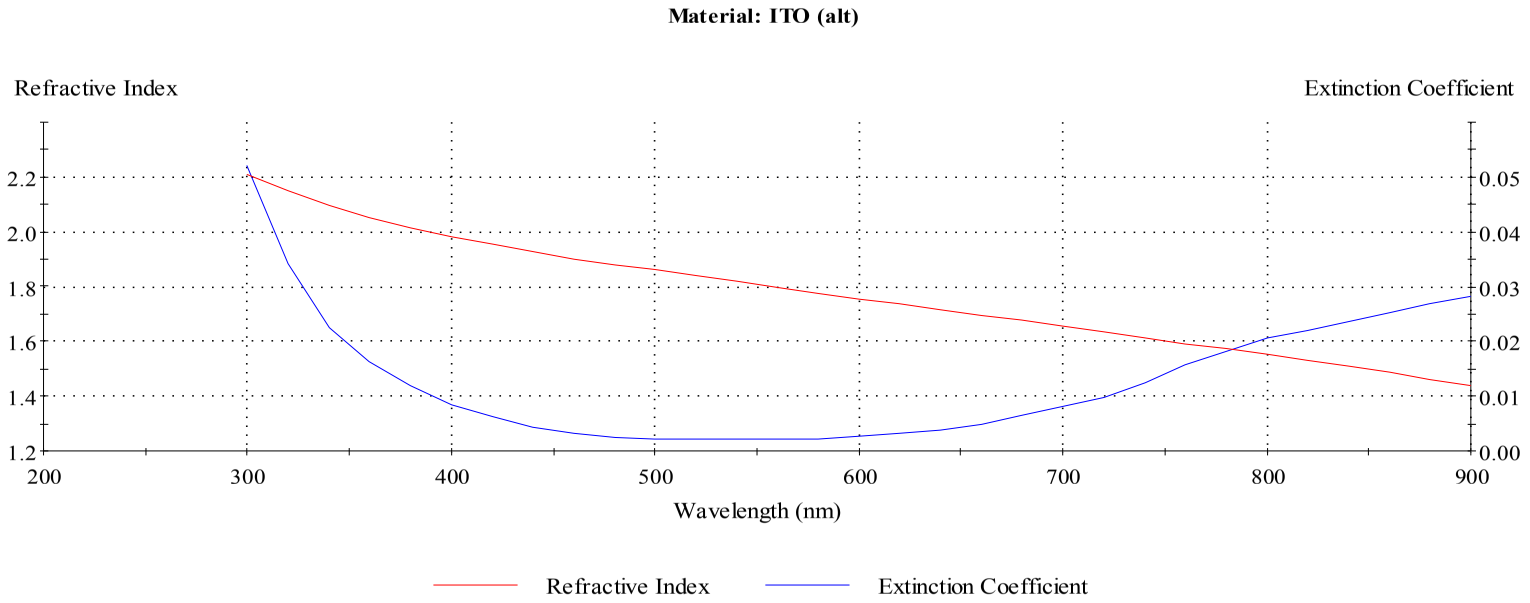

It can be seen from the four sources of ITO data here that there are discrepancies between the different sets of data. Each set of data was therefore used for each consideration in the theoretical work to enable a comparison to be made.

2.5.2 Other data used in the theoretical section

2.5.3.1 SiO_2

The refractive index and extinction coefficient data used for SiO_2 was sourced from Essential Macleod. The original source of the data was from Palik, Edward D. Handbook of the Optical Constants of Solids I. Academic Press, 1985 and p 12. Palik, Edward D. Handbook of the Optical Constants of Solids II. Academic Press, 1991, p753.

2.5.3.2 TiO_2

The refractive index and extinction coefficient data used for TiO_2 was sourced from Essential Macleod.

2.5.3.3 MgF_2

The refractive index and extinction coefficient data used for MgF_2 was sourced from Essential Macleod. The original source of the data was from the SOPRA database.

2.5.3.4 Cryolite

The refractive index and extinction coefficient data used for MgF_2 was sourced from Essential Macleod. NPL (2008) concurred with Essential Macleod that the refractive index values were accurate.

2.6 Review of Coating analysis techniques employed in this project and the reasoning for applying them to the ITO coatings

With all the available coating analysis techniques that can be employed, the choice of which techniques to use is numerous. This section addresses the techniques employed in this thesis and explains the reasoning behind the decision to use them.

2.6.1 Atomic Force Microscopy (AFM)

According to Whitehouse (2002), the AFM can be used to investigate the topography of various surfaces by means of a very small stylus and cantilever and a means of measuring the deflection of the tip of the cantilever as is illustrated in the figure below:

Figure 11 Typical Atomic Force probe

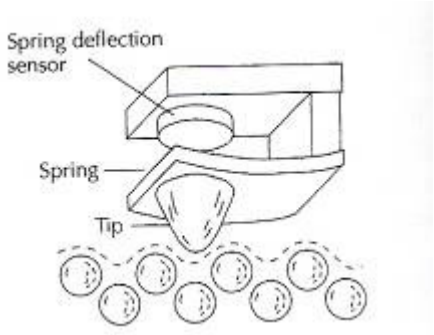

(Source Whitehouse, 2002)

Yun *et al* (2004) reports that Surface roughness deteriorates the conductivity and homogeneity of ITO thin films. It is for this reason that Yun *et al* (2004) etched their ITO coating surface to make it smoother in an attempt to minimise

this effect. This work implies that average surface roughness is therefore an important parameter to consider. The unetched sample reported in the work of Yun *et al* (2004) had an average surface roughness of approximately 4.8Å, whereas optimum etching produced an average roughness of approximately 3Å.

In this thesis, the author therefore decided to use the AFM on a selection of samples to determine the average roughness in each case so that a comparison could be made between the different coating techniques and different sample thicknesses.

2.6.2 Scanning Electron Microscopy (SEM)

Whitehouse (2002) reports that the SEM is essentially a microscope that utilises electrons rather than light. Whitehouse (2002) feels that the advantages of electrons are that the electron beams have a comparatively small spread meaning that the SEM has a smaller numerical aperture and a very good depth of field.

The SEM was chosen as an analysis technique in this thesis as it is useful to know the actual thickness of the coatings produced rather than just assuming the thickness entered into the IC/5 controller unit is accurate. The SEM is a very versatile tool that can show much more than this, but this report focuses on this small aspect of the SEM as this was the aspect of interest here.

3 Application

ITO finds very wide and varied applications in various market sectors. Applications of ITO are wide and varied. The applications can range from L-3 Wescam Imaging systems right the way across the spectrum to novel applications such as the production of Star Wars style light sabres (Azo Nano, 2005) like the one illustrated below:

Figure 12 Star Wars style light sabre

(Source Sagecroft Technologies, 2008)

The application of this work is the coating of certain windows of the L-3 Wescam stabilized multi-spectral airborne imaging systems. The source of the information in this section is L-3 Wescam (2008).

L-3 Wescam produces a variety of these imaging systems. An example of a typical L-3 Wescam imaging system is shown on the following page:

Figure 13 MX-15

(Source: L-3 Wescam, 2008)

The example shown above is the MX15. It incorporates the following features:

- Colour daylight camera with zoom capabilities. Below are examples of images produced with the ‘day spotter’.

Figure 14 Day spotter images

Wide  Very Narrow 

(Source L-3 Wescam, 2008)

- Monochromatic night camera. The pictures on the following page illustrate the benefits of images produced with the night spotter:

Figure 15 Comparison of Day Spotter and night spotter

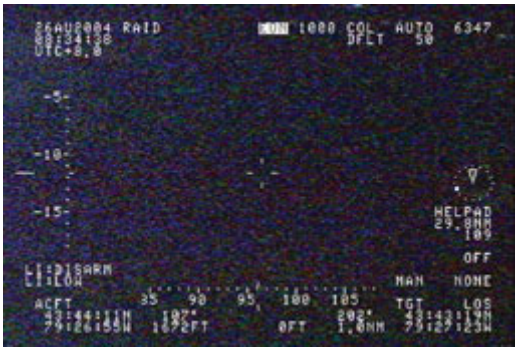

Night time: Using Day Spotter

Night time: Using Night Spotter

(Source: L-3 Wescam, 2008)

- Laser illumination

Figure 16 Benefits of combining the night spotter and laser illumination

No light: using spotter only

No light: using laser illuminated night spotter

(Source L-3 Wescam, 2008)

- Laser range finding capabilities
- The enhanced range local area processing (ELAP) haze penetration capabilities are illustrated on the following page:

Figure 17 ELAP Haze penetration capabilities

Before: With haze

After: With ELAP Processing

(Source L-3 Wescam, 2008)

The applications of L-3 Wescam imaging systems are wide and varied. Examples of applications are listed below:

- Defence – Imaging systems are used for the collection, analysis and dissemination of visual intelligence providing a faster, more accurate stream of dynamic visual information, thus making them an invaluable tool for the following defence sectors:
    - Army
    - Navy
    - Air force
    - Marines
    - Coast Guard

- Homeland security – Apart from the obvious application of Maritime security here, there is also the opportunity to facilitate search and rescue operations.
- Airborne law enforcement – The imaging system enhances the ability to carry out law enforcement and perimeter security. In addition to this, the

imaging system can be used by emergency medical services and other civil applications.

- Space – The imaging systems are in use at the International Space Station Alpha where they provide real-time images. Another space related application is the use of miniaturised Camera and transmission systems that provide information directly from astronauts' helmets.
- Sports – These imaging systems have provided unique coverage from numerous major sporting events including the Winter and Summer Olympic Games, Gymnastics, Cycling, Racing, Football, Golf, Hockey, Yachting, Swimming, Skiing and Baseball.

The requirements for the coatings under consideration in this project are high % transmission in the visible spectrum and neighbouring IR region and <20 and <100 ohms per square sheet resistivity. The project primarily focuses on the visible region but also considers the neighbouring region out of interest. Other relevant requirements are laid down by the use of the coating and the conditions it has to withstand (More detailed specifications can not be specified in this thesis due to their highly sensitive nature).

4 Experimental work

4.1 Methodology

This section focuses on the analysis of coatings produced at PJ Coatings with various conditions via Electron Beam Evaporation both with and with out Ion Assisted Vapour Deposition in a Leybold LAB600 (a photograph of the LAB600 is shown below):

Figure 18 Leybold LAB600

(Details of this technique are illustrated in section 2). The samples analysed in this section were produced in a clean room facility at PJ Coatings. The parameters entered into the IC/5 controller unit set to deposit these coatings are listed in Appendix A. This section also considers sputtered ITO samples (supplied by Diamond Coatings) for comparative purposes in section 4.5. Diamond Coatings did not supply the conditions that they used to sputter their samples for commercial reasons.

Transmission measurements (%T) were taken with a Cary Spectrophotometer. Measurements were taken to enable the study of the visible region and the adjacent area, as is laid out in the aims and objectives. The analysis looked at the average %T over the ranges 400-700nm, 450-900nm, 400-800nm and 700-

3000nm (the neighbouring infrared range is considered in addition out of interest as noticeable differences have been observed in %T measurements over this range).

The standard method used to determine sheet resistivity is to measure the resistance by placing the DVM probes on a 2”x1” test piece. The result of this is then divided by two to obtain a value for the ohms per square.

4.2 Results

This section presents the results from the Experimental work. The observations made from these results and resulting discussions are located in section 6.

4.2.1 Effects of deposition parameters on the output parameters when depositing a single layer of ITO via Electron beam evaporation onto a glass substrate multiple times with varying conditions

The ITO samples considered are shown in the photograph below:

Figure 19 The ITO samples

The reproducibility of the deposition conditions was evaluated statistically using the “Analysis of Variance” (ANOVA). ANOVA is a tool supplied by Microsoft

Excel that analyses the variance of data used to analyse the significance of variables on a result by returning an 'F value' and an 'F_{crit} value' for the rows and columns considered[1]. ANOVA two factor without replication was applied to the data in this thesis as no replication was present in the data analysed in each case. With the data in this thesis, two columns were considered for each ANOVA analysis procedure, one containing one of the variable types and the other containing one of the result types. This process was carried out for every variable and every result obtained in turn to individually assess the contribution of each variable to each result. The values of F were observed in each case and compared to F_{crit} for the columns. $F > F_{crit}$ means that the Variable column under consideration is significant to the selected result column. The bigger the value of F in relation to F_{crit}, the more significant the variable is to the result. Conversely, if $F < F_{crit}$, this means that the variable column considered is not significant to the result column considered (Note F and F_{crit} are referring to the F value and critical value of the F value respectively used in F tests for the equality of two standard deviations).

Table 2 summarises the values of F and F_{crit} for each variable and result considered in the ANOVA analysis. The highest and lowest value for each row in the table is shown in bold text.

The Results considered in this ANOVA analysis are Inner Resistivity, Outer Resistivity and Average %T for 400-700nm, 450-900nm, 400-800nm and 700-3000nm respectively. Even though the aims are to just consider the visible and near surrounding area, 700 – 3000nm was also considered here out of interest.

[1] Microsoft Excel 2007 Help Files

Table 2 Table summarising the values of F obtained in the ANOVA analysis (F_{crit} = 4 for all calculations (to 0 dp))

Variables → Results ↓	**Ar Flow**	**Pressure**	**O2 flow**	**Anode Voltage**	**Anode Current**	**Ion Assisted Deposition**	**Temp**	**ITO % Composition**	**Deposition rate**	**Thickness**
Inner Resistivity	115	114	67	**9**	120	122	**380**	124	112	119
Outer Resistivity	113	111	65	**8**	117	120	**413**	121	110	116
Average %T (400 - 700nm)	7460	9368	920	**8**	9003	9759	**10565**	9938	7115	9656
Average %T (450 – 900nm)	9991	12237	955	**10**	12187	13070	10251	**13218**	9675	12816
Average %T (400 – 800nm)	8473	10447	931	**9**	10270	11021	10200	**11217**	8106	10903
Average %T (700 – 3000nm)	513	403	57	**5**	514	504	**4388**	505	493	460

It can be seen that each result is affected by all of the variables considered to a greater or lesser extent. This implies that it is not very likely that any simple patterns will be present between the individual variables and their results. The next obvious step to this analysis would be to determine relationships between the variables that have the largest effect and the corresponding results (e.g. Temperature) to observe the effects because if any simple relationships between one variable and the results were present, they would most likely to be observed here. To perform this, each variable would have to be altered while all the other variables were held constant in a methodical manner for numerous runs. This unfortunately was not possible in this work as the number of practical hours where the equipment was available for use was severely limited.

4.2.2 Determination of the ITO deposition conditions required to provide <20 Ω/□

Out of all of the ITO coatings carried out with electron beam evaporation, the following parameters were found to provide an ITO coating with a sheet resistivity <20 Ω/□:

Table 3 Deposition conditions required to provide <20 Ω/□□

Date	Run	Thickness kA	Rate A/s	Material	Temperature '	IAD	Anode Current A	Anode Voltage V	O2 flow sccm	Pressure x 10-4 mbar	Ar flow sccm
60208	1	2	7.5	90 10 ITO	290	Yes	2	100	11.7	3	5.00
60208	2	2	7.5	90 10 ITO	290	Yes	2	100	11.9	3	5.00
10308	1	2	7.5	90 10 ITO	290	Yes	2	100	12.1	3.7	5.00
30308	1	2	7.5	90 10 ITO	290	Yes	2	100	11	3	5.00
100408	2	2	7.5	90 10 ITO	290	Yes	2	100	15.3	3.4	5.00
160508	1	2	1	90 10 ITO	290	No	0	0	40	4.8	0.00

The corresponding results obtained from these parameters from these were as follows:

Table 4 Results obtained when <20 Ω/□□ was achieved

Inner Resistivity ohms/sq	Outer Resistivity ohms/sq
15.5	17.5
17.5	19
16.7	19.35
19.3	19
16.3	17.5
19	19

4.2.3 Determination of the ITO deposition conditions required to provide <100 Ω/□

Out of all of the ITO coatings carried out with electron beam evaporation, the following parameters together provided an ITO coating which provided near to but less than100 Ω/□:

Table 5 Deposition conditions required to provide <100 Ω/□

Date	Run	*Thickness kA*	*Rate A/s*	*Material*	*Temperature °c*	*IAD*	*Anode Current A*	*Anode Voltage V*	*O2 flow sccm*	*Pressure x 10-4 mbar*	*Ar flow sccm*
70508	1	1	1	90 10 ITO	290	No	0	0	50	5.9	0.00

The corresponding results obtained from these parameters from these were as follows:

Table 6 Results obtained when <100 Ω/□□ was achieved

Inner Resistivity ohms/sq	**Outer Resistivity ohms/sq**
83	83

4.2.4 Attempt to maximise the %T with the addition of extra layers

The below table shows the results of the additional coatings that were deposited on the ITO coatings.

SiO_2, TiO_2 and MgF_2 were used as they are the most commonly reported coating materials to have been applied in an attempt to enhance the %T of ITO in the visible region.

No effect on ITO Resistivity was observed from the addition of any of the extra coatings applied.

Table 7 Additional coatings

Date	Run	AR Coating	ITO Thickness kA	AR Thickness kA	AR Deposition Rate A/s	%T 400 to 700 nm	%T 450 to 900 nm	%T 400 to 800 nm
120208	1	MgF2	1.8	0.70	10	99.7	98.9	99.5
250208	1	MgF2	0.5	1.00	10	100.5	100.6	100.3
40308	1	MgF2	0.5	1.00	10	100.4	100.5	100.2
40308	3	MgF2	0.5	1.10	10	98.5	99.7	98.7
80308	1	MgF2	0.75	1.03	10	91.0	88.6	88.1
120508	2	SiO2	2	1.00	5	97.8	97.8	97.8
130508	2	TiO2	2	2.00	3.5	102.6	103.1	102.7
140508	1	TiO2	2	0.09	2.5	103.0	102.7	102.9
		SiO2		0.46	5			
		TiO2		0.28	3.5			
		SiO2		0.18	5			
		TiO2		0.80	3.5			
		SiO2		0.16	5			
		TiO2		0.26	3.5			
		MgF2		1.02	10			

NB. The values shown to be over 100 in the last 3 columns reflects the effects that limitations and approximations of the method used to obtain the data have on the accuracy of the result obtained. Obviously they are not really over 100. The data is shown merely for comparative purposes to determine the AR coating that does the best job out of what was considered.

In each case, enhanced values of average %T were obtained for all of the wavelength ranges under consideration.

4.2.5 Examination of the results of ITO deposition via IAD and sputtering to determine the difference the technique used has upon the coating produced

Three ITO samples were sent to Cranfield University for Analysis via AFM and SEM. The samples chosen were one sputtered ITO sample and a 'thick' and 'thin' Evaporation sample (one with approx 200nm coating thickness and the other with approx 75nm coating thickness). These samples were chosen to get comparative information on the effects of the deposition method used and thickness of the ITO coatings. Ideally, more samples should have been investigated firstly to ensure that consistent results were obtained and secondly to determine the effect of other parameters. The intention of this section was however just a preliminary investigation that could lead to more detailed studies from the results of this where these factors would be taken into account.

4.2.5.1 Atomic Force Microscopy

Atomic Force Microscopy was used to look at the surface roughness of the three samples and to determine how this was affected by the method of deposition and to observe the variation with thickness of coating.

The results of this were as follows:

Figure 20 AFM Results for the ITO Sputtered sample

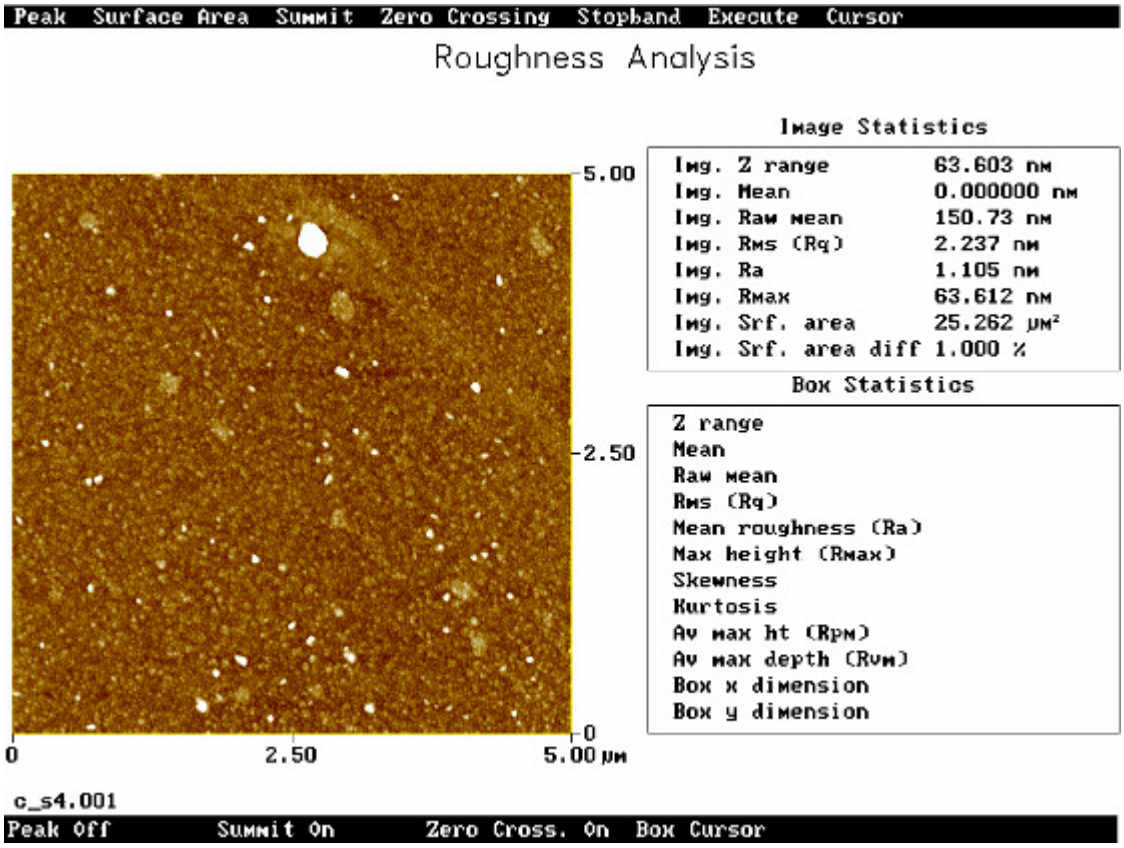

Figure 21 AFM results for the thin ITO Evaporation Sample

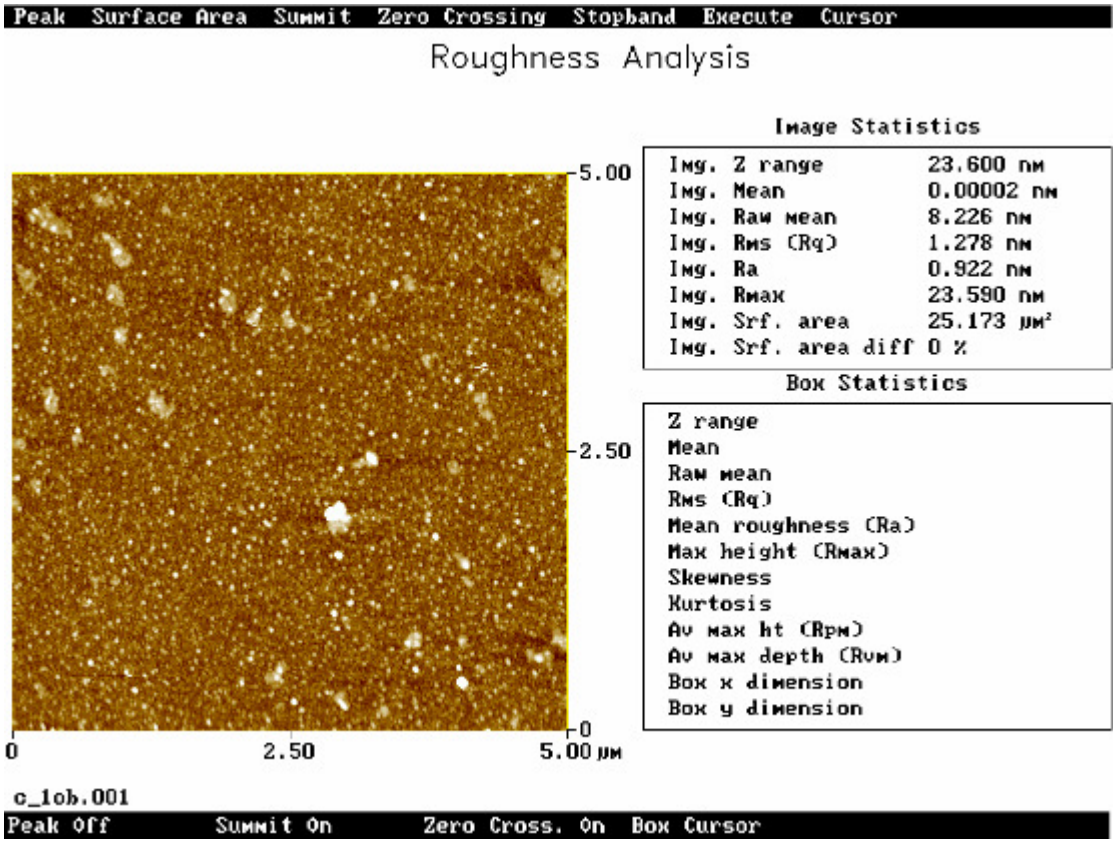

Figure 22 AFM results for the thick ITO Evaporation Sample

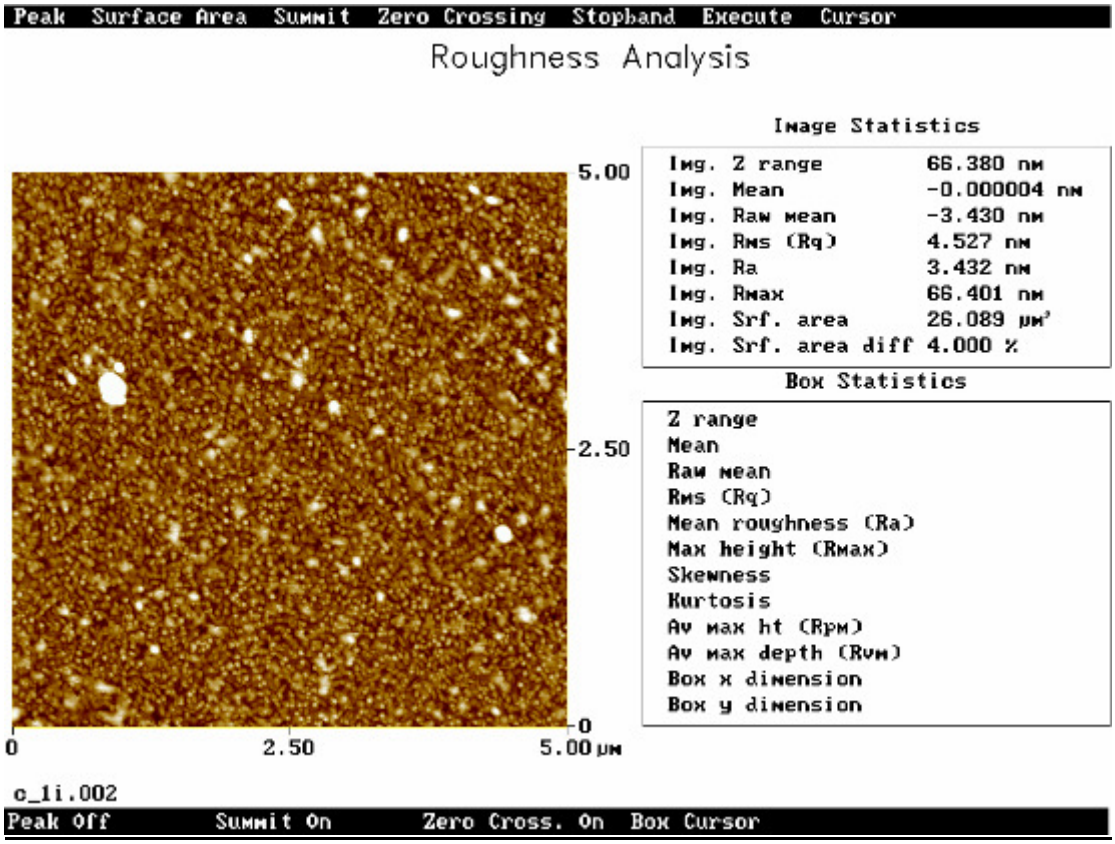

As this was only a preliminary study, not enough samples were taken to make conclusive observations. The purpose of this study was purely to determine whether such a study was required in the future as limitations on this work prevented this from being done. It can be seen from these results that more investigation is warranted as there appears to be a difference in average roughness observed with samples produced with different conditions and it is therefore recommended that this be studied further to see if this pattern was repeatedly observed.

4.2.5.2 Scanning Electron Microscopy

SEM work was conducted to observe the actual thickness of the ITO coatings in comparison to the thickness that was specified on the IC/5 controller. The results from this analysis are illustrated in figures 17-19.

Figure 23 SEM Results for the Sputtered ITO sample

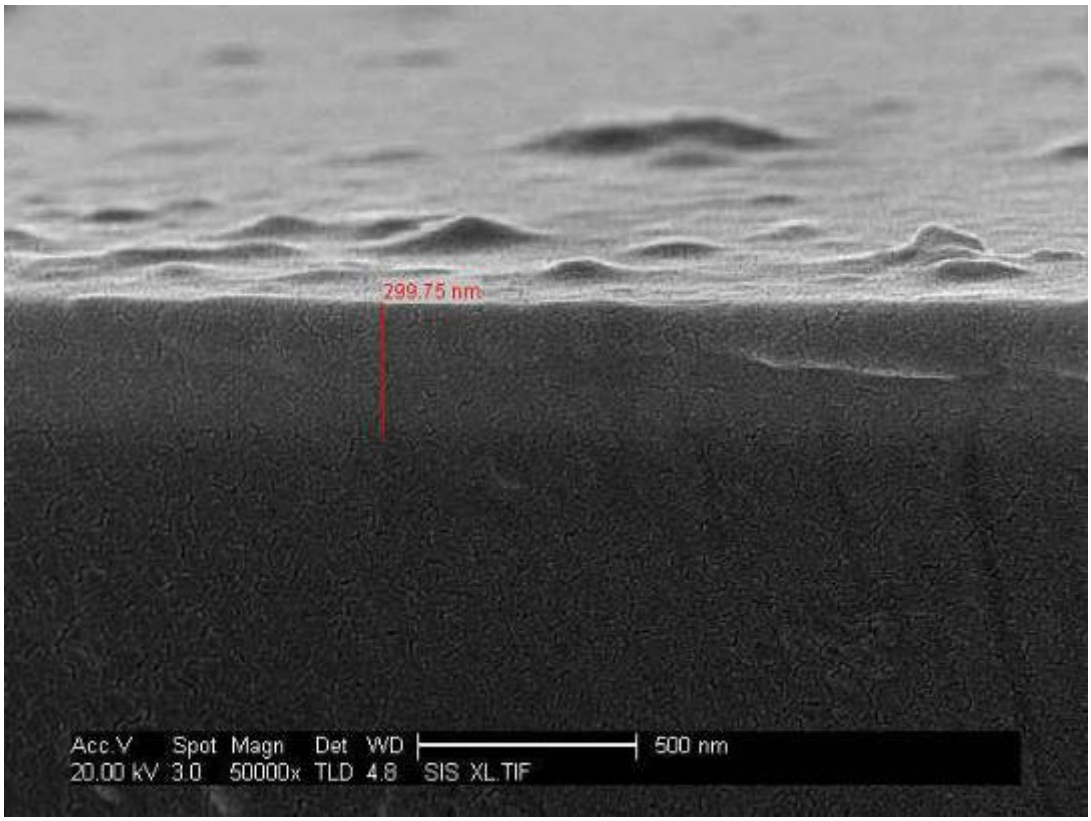

Unfortunately, Diamond coatings could not specify the thickness of the ITO coatings they set for commercial reasons so this could not be compared to the the achieved thickness of their coating.

Figure 24 SEM Results for the thin ITO evaporation sample

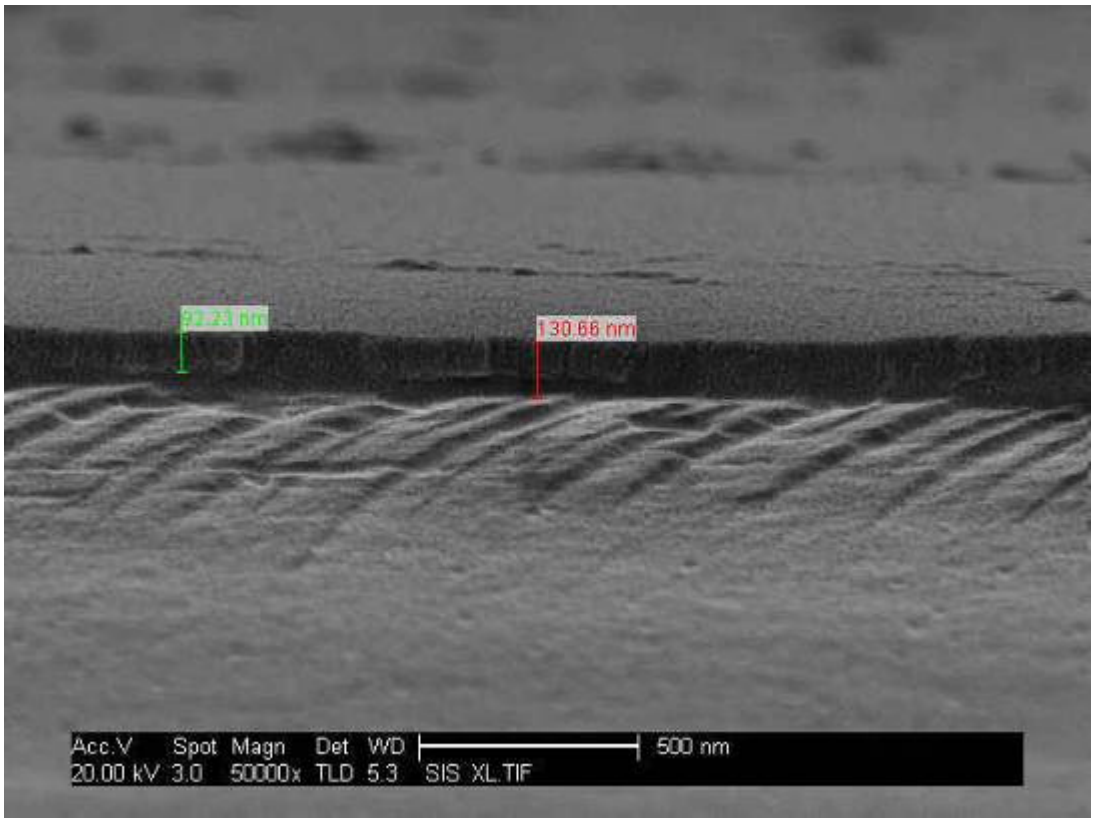

The thickness for this coating was set to 75nm on the IC/5 controller.

Figure 25 SEM Results for the thick ITO evaporation sample

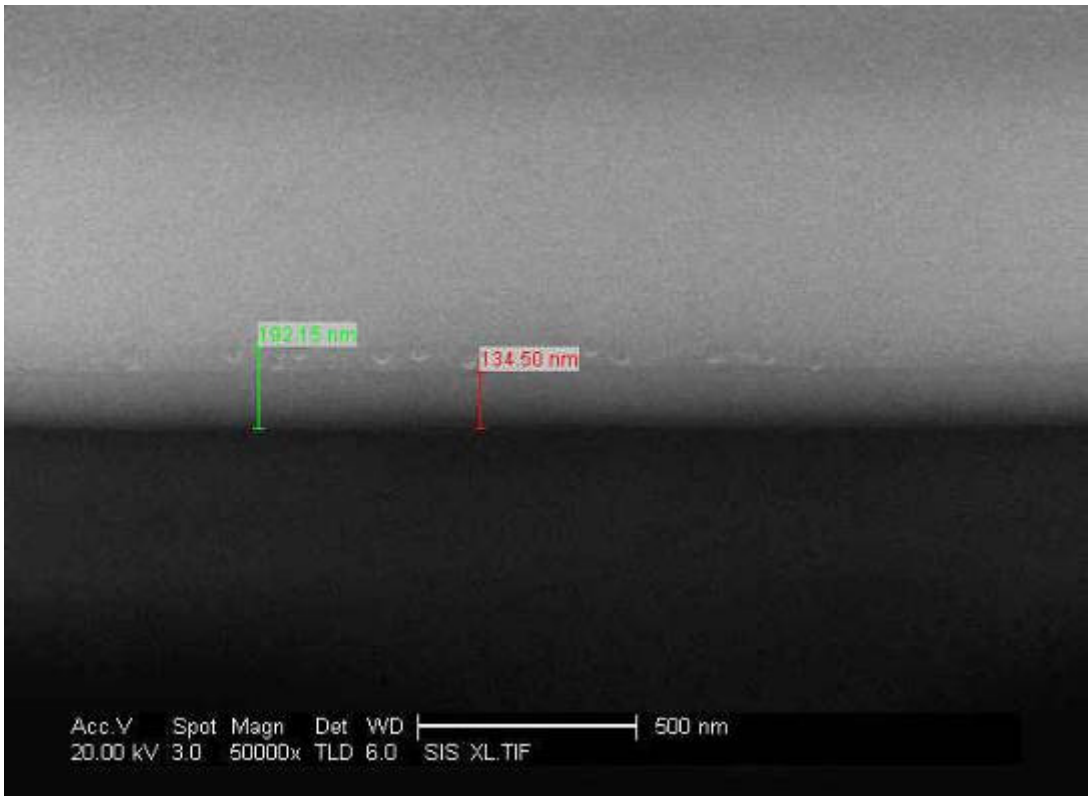

The thickness for this coating was set to 200nm on the IC/5 controller.

It can be seen with both the evaporation samples that a variation in thickness was observed across the sample. Again, this was a preliminary study, but it points towards the need for future work to be carried out in this field to determine what causes the variation in thickness and trying to eliminate it

5 Modelling ITO coating performance

5.1 Methodology

All analysis was carried out using Essential Macleod software. Analysis was performed with the Simplex Optimisation method provided by Macleod. All the diagrams shown in this section are from this software. The data sources used in these calculations are discussed in the literature review.

Analysis in this section was only carried out for the 400-700nm, 450-900nm (for three of the four data sets) and 400-800nm ranges as there is only one set of data here that would have met the 700-3000nm range requirements. It can be seen from the data that there are discrepancies between the different sets of data. Each set of data was used for each consideration in this section to enable a comparison to be made. It is for this reason that 700-3000nm was not considered here. Each range was considered separately for each section so that optimisation could be performed over each range separately. Optimisation was carried out with targets set every 25nm throughout each range.

5.2 Modelling Results

This section presents the modelling results. The observations made from these results and the resulting discussions are located in section 6.

5.2.1 Optimising the thickness of a single layer of ITO for %T

This section examines what thickness of ITO is required to give the optimum average %T for the wavelength ranges considered. The ITO on the substrate is illustrated in the figure below.

Figure 26 Illustration of the ITO on the Substrate

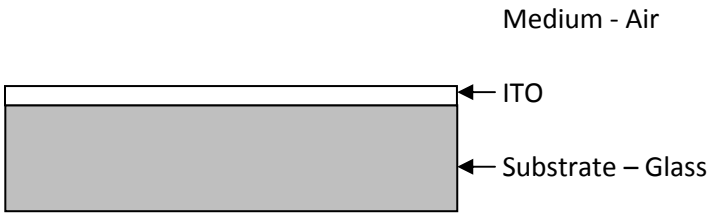

The results of this are shown in Table 8:

Table 8 Optimisation of %T by alteration of ITO thickness

Wavelength range /nm	ITO Data	Average %T across wavelength range	Optimum ITO Thickness /nm
400–700nm	1	88.4	117.02
400-700nm	2	84.6	114.43
400-700nm	3	79.6	105.73
400-700nm	4	91.5	120.68
450-900nm	1	88.8	132.41
450-900nm	2	76.3	137.78
450-900nm	4	92.0	136.79
400-800nm	1	88.1	116.74
400-800nm	2	83.9	119.59
400-800nm	3	79.0	102.15
400-800nm	4	91.3	120.03

5.2.2 Increasing the thickness to 2kÅ (200nm) to achieve the desired surface resistivity values

Even though the results in the previous section give thicknesses that exhibit the optimum average %T, unfortunately, these thicknesses do not meet the sheet resistivity requirements. To meet the sheet resistivity requirements, the ITO layer needs to be thickened. The effects of increasing the thickness of the ITO to 2kÅ is examined in this section.

Table 9 Effects of increasing the thickness of ITO to 2kÅ

Wavelength range /nm	ITO Data	ITO Thickness /kÅ	Average %T across wavelength range
400–700nm	**1**	**2**	**85.2**
400-700nm	**2**	**2**	**77.8**
400-700nm	**3**	**2**	**70.5**
400-700nm	**4**	**2**	**89.5**
450-900nm	**1**	**2**	**86.1**
450-900nm	**2**	**2**	**84.0**
450-900nm	**4**	**2**	**89.8**
400-800nm	**1**	**2**	**86.1**
400-800nm	**2**	**2**	**81.0**

400-800nm	**3**	**2**	**71.4**
400-800nm	**4**	**2**	**89.8**

5.2.3 Increasing the % Transmission through the addition of other layers to the ITO layer

According to Eite (2004), increasing the thickness of an ITO coating results in an increase in conductivity, a fall in transmission and an increase in cost (incurred via material costs and machine times). From the findings of Eite (2004), it therefore makes sense to primarily consider increasing the %T for the 20 Ohms/square samples as these samples are thicker and thus experience a lower % transmission. It is for this reason that all of the work carried out on maximising the %T in the remainder of this section has therefore focussed on an ITO thickness of 2kÅ (required for 20 Ohms/square).

5.2.3.1 Addition of a single layer

This section considers increasing the average % Transmission of ITO by adding an additional single layer. This situation is illustrated in Figure 27. The addition of a single layer of SiO_2, TiO_2 and MgF_2 is considered in turn (in tables 10-12). SiO_2, TiO_2 and MgF_2 were used as they are the most commonly reported coating materials to have been applied in an attempt to enhance the %T of ITO in the visible region (see section 2.4). It is for this reason that this thesis will initially consider the addition of these layers as a starting point in the quest to maximise the %T.

These materials have refractive indices both above and below the refractive index of ITO. For each material, the optimum thickness was deduced through Simplex analysis.

Figure 27 Illustration of the ITO and an additional layer

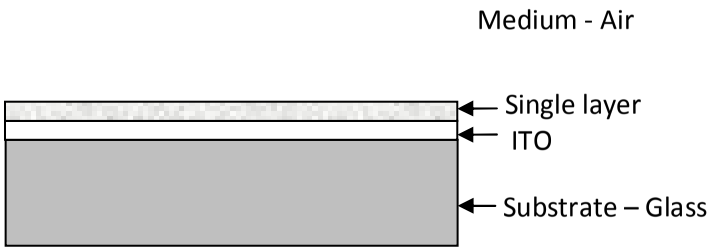

Table 10 Results of the addition of SiO_2

Wavelength range /nm	**ITO Data**	**ITO Thickness /kÅ**	**Average %T across wavelength range**	**Optimum SiO_2 Thickness /nm**
400–700nm	**1**	**2**	**92.2**	**86.60**
400-700nm	**2**	**2**	**87.8**	**88.67**
400-700nm	**3**	**2**	**77.1**	**87.31**

400-700nm	**4**	**2**	**95.5**	**80.75**
450-900nm	**1**	**2**	**91.8**	**89.83**
450-900nm	**2**	**2**	**91.7**	**93.73**
450-900nm	**4**	**2**	**94.3**	**88.34**
400-800nm	**1**	**2**	**92.1**	**87.20**
400-800nm	**2**	**2**	**88.9**	**89.86**
400-800nm	**3**	**2**	**77.1**	**88.28**
400-800nm	**4**	**2**	**94.9**	**82.05**

Table 11 Results of the addition of TiO_2

Wavelength range /nm	**ITO Data**	**ITO Thickness /kÅ**	**Average %T across wavelength range**	**Optimum TiO_2 Thickness /nm**
400–700nm	**1**	**2**	**80.3**	**108.93**
400-700nm	**2**	**2**	**77.3**	**95.59**
400-700nm	**3**	**2**	**67.1**	**123.96**

400-700nm	**4**	**2**	**83.2**	**107.52**
450-900nm	**1**	**2**	**80.2**	**148.86**
450-900nm	**2**	**2**	**79.3**	**129.31**
450-900nm	**4**	**2**	**83.1**	**151.66**
400-800nm	**1**	**2**	**80.8**	**157.06**
400-800nm	**2**	**2**	**78.4**	**150.59**
400-800nm	**3**	**2**	**67.5**	**155.13**
400-800nm	**4**	**2**	**83.4**	**158.79**

Table 12 Results of the addition of MgF_2

Wavelength range /nm	**ITO Thickness /kÅ**	**ITO Data**	**Average %T across wavelength range**	**Optimum SLAR Thickness /nm**
400–700nm	**2**	**1**	**92.6**	**91.46**
400-700nm	**2**	**2**	**87.6**	**93.10**
400-700nm	**2**	**3**	**77.4**	**92.28**

400-700nm	**2**	**4**	**96.1**	**85.67**
450-900nm	**2**	**1**	**92.3**	**96.17**
450-900nm	**2**	**2**	**91.9**	**99.07**
450-900nm	**2**	**4**	**95.0**	**95.15**
400-800nm	**2**	**1**	**92.6**	**92.76**
400-800nm	**2**	**2**	**89.1**	**94.40**
400-800nm	**2**	**3**	**77.4**	**94.03**
400-800nm	**2**	**4**	**95.6**	**89.04**

5.2.4 Optimisation of Refractive Index and Thickness for the addition of a Single Layer

Optimisation processes are good tools. It must however be remembered that they are only as good as their starting point. If the wrong starting point is chosen, optimisation can result in a local maximum instead of finding the true maximum. To minimise the chance of this, the above work was carried out to determine a good starting point for the optimisation of %T through manipulation of Refractive index and thickness. It showed that the MgF_2 gave the highest %T overall for all of the ranges out of all the single layers applied to the ITO. The Refractive index of MgF_2 was therefore used as the starting point for this analysis. This starting point was used in conjunction with Simplex optimisation in Essential Macleod to determine an optimised Refractive index and thickness for each case considered. The results of this are shown in Table 13 below:

Table 13 Optimisation of the refractive index and thickness for the addition of a single layer

Wavelength range /nm	ITO Data	Optimum Refractive Index for SLAR	Optimum SLAR Thickness /nm	Average %T for wavelength range
400–700nm	1	1.35452	93.57	92.7
400-700nm	2	1.42840	90.54	87.8
400-700nm	3	1.37595	92.93	77.4
400-700nm	4	1.32215	90.01	96.3
450-900nm	1	1.33534	101.63	92.4
450-900nm	2	1.40263	98.03	91.9
450-900nm	4	1.30834	103.14	95.3
400-800nm	1	1.33967	96.24	92.7
400-800nm	2	1.40417	93.24	89.1
400-800nm	3	1.35570	96.36	77.4
400-800nm	4	1.30834	94.06	95.8

5.2.5 Production of Symmetrical periodic layers to simulate the optimum Refractive indices and thicknesses

Wang (2006) feels that symmetrical periodic layers can offer equivalent indices that are unachievable with a single material. The next obvious step after obtaining optimised refractive indices and thicknesses is to find symmetrical periods made from common materials used in the visible region that can simulate the optimum refractive indices and thicknesses. The results of this for 400-700nm with ITO data 1 are shown below as a typical example:

Layer	Material	Physical Thickness (nm)
Medium	Air	
1	SiO2	33.75
2	TiO2	10.82
3	SiO2	33.75
4	ITO	200
Substrate	Glass	

Unfortunately, the above example of the results from this show that the physical thicknesses required for each layer are exceedingly small making accurate deposition of such thicknesses exceedingly difficult. This is illustrated in the Experimental section, where it could be seen that the actual thicknesses obtained compared to the thicknesses that were programmed got progressively less accurate when the thickness considered were smaller.

5.2.6 Finding a material that is closest to the optimum refractive index

The next step from this is to find a material with the closest refractive index to the optimum refractive indices calculated previously. This is carried out in Table 14.

Table 14 Materials with the nearest refractive index to the optimum refractive indices

Wavelength range /nm	ITO Data	Optimum Refractive Index	Nearest standard coating material[2]	Refractive index of coating material
400-700nm	1	1.35452	Na_3AlF_6 (Cryolite)	1.35
400-700nm	2	1.42840	SiO_2	1.46180
400-700nm	3	1.37595	MgF_2	1.38542
400-700nm	4	1.32215	Na_3AlF_6 (Cryolite)	1.35
450-900nm	1	1.33534	Na_3AlF_6	1.35

[2] Materials considered are listed in Essential Macleod under standard coating materials

			(Cryolite)	
450-900nm	2	1.40263	MgF_2	1.38542
450-900nm	4	1.30834	Na_3AlF_6 (Cryolite)	1.35
400-800nm	1	1.33967	Na_3AlF_6 (Cryolite)	1.35
400-800nm	2	1.40417	MgF_2	1.38542
400-800nm	3	1.35570	Na_3AlF_6 (Cryolite)	1.35
400-800nm	4	1.30834	Na_3AlF_6 (Cryolite)	1.35

It can be seen from the table that the data used in the theoretical studies plays a crucial role in determining the best course of action. This therefore reinforces the importance of examining the results from multiple sets of data to try to get a broader picture.

5.2.7 Cryolite studies

The most frequently occurring material in this table is Cryolite. The next step from here is therefore to model the use of a single layer of Cryolite for each wavelength range for each set of ITO data (see Figure 28). Figures 23 – 33 illustrate the

results for the different ITO data sets for the wavelength ranges under consideration. 2D plots of %T versus wavelength for normal incidence are given. Even though normal incidence is the primary consideration here, 3D plots are also shown to give more information for other angles. Circle diagrams (based at a design wavelength of 510nm) are also given to give a clearer picture of the effects the layers have. Table 15 then summarises these results.

Figure 28 Illustration of the addition of Cryolite to ITO

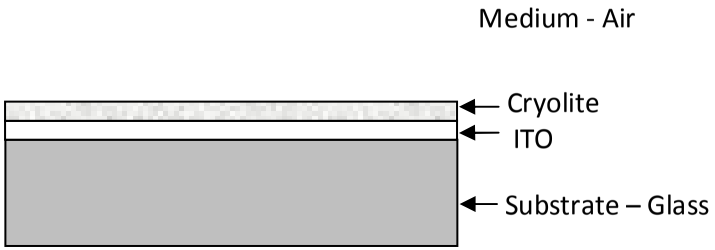

Figure 29 Results for ITO data 1 for 400-700nm

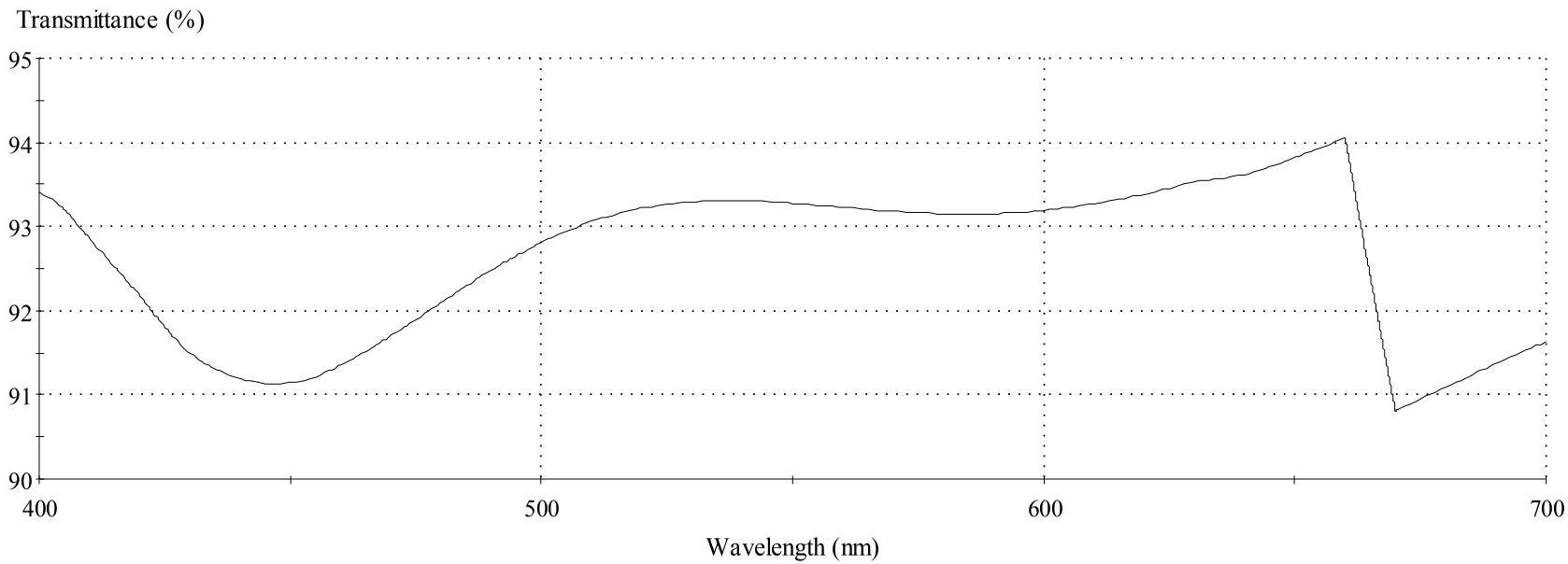
ITOsingleAR: Transmittance
Transmittance (%)
95
94
93
92
91
90
400
500
600
700
Wavelength (nm)

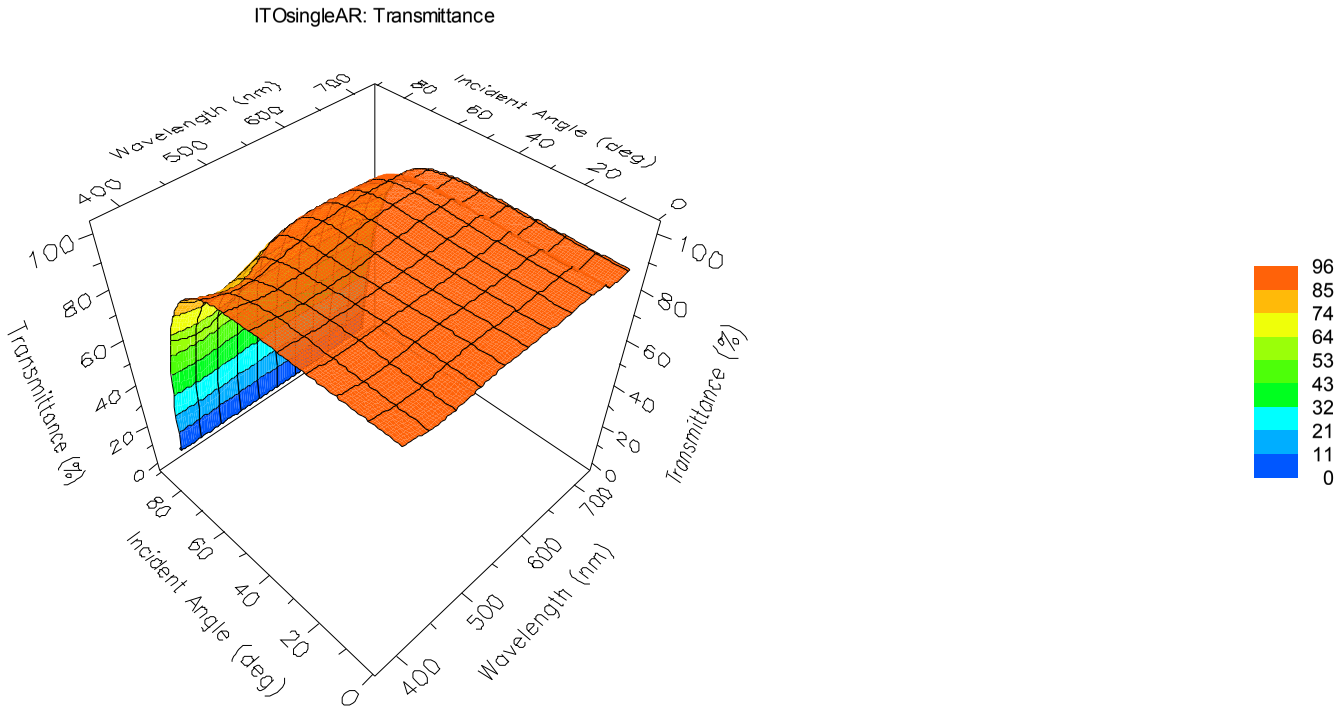
ITOsingleAR: Transmittance
Wavelength (nm)
400
500
600
700
Incident Angle (deg)
0
20
40
60
80
Transmittance (%)
0
20
40
60
80
100
96
85
74
64
53
43
32
21
11
0

ITOsingleAR: Reflection Coefficient

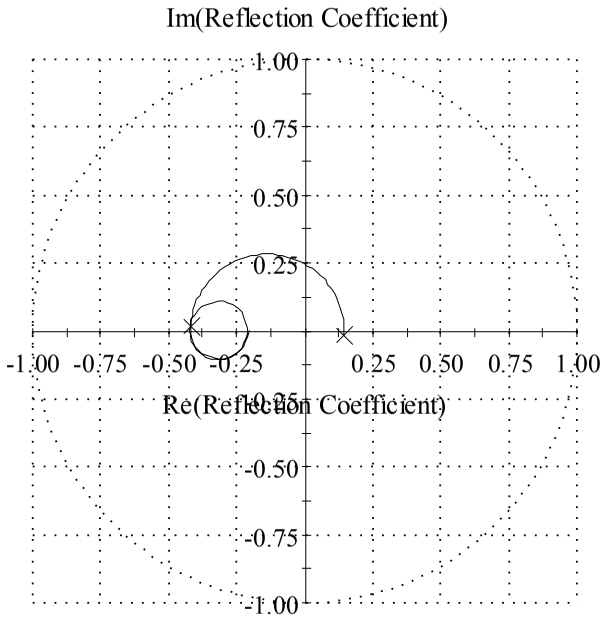

Figure 30 Results for ITO data 2 for 400-700nm

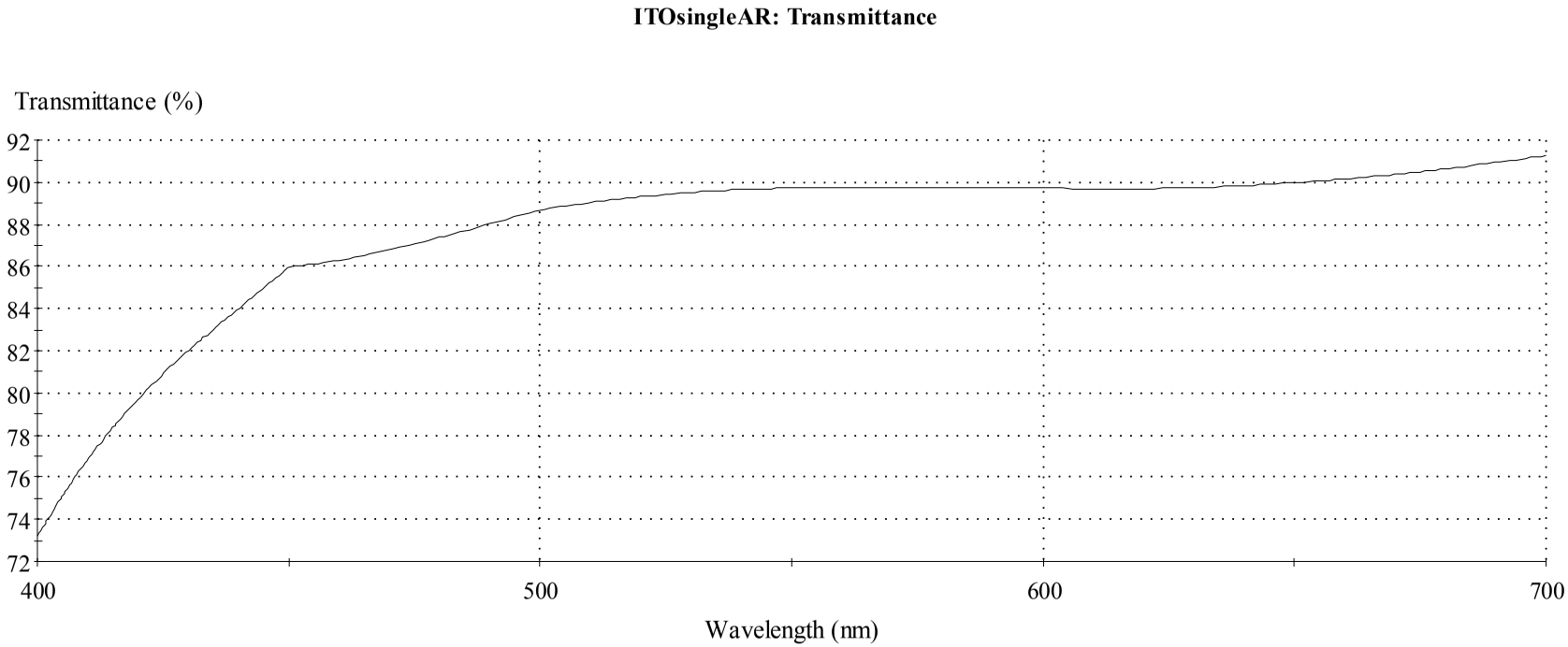

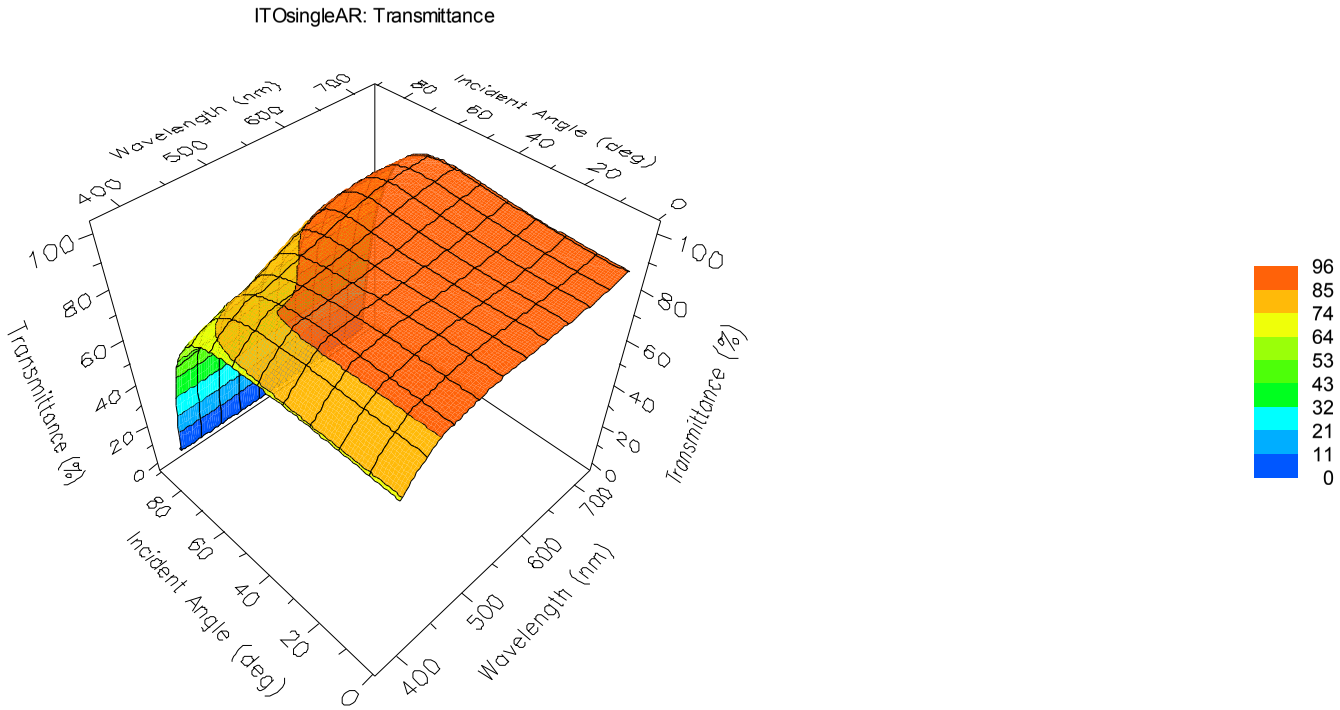
ITOsingleAR: Transmittance
Wavelength (nm)
400
500
600
700
Incident Angle (deg)
0
20
40
60
80
Transmittance (%)
0
20
40
60
80
100
96
85
74
64
53
43
32
21
11
0

ITOsingleAR: Reflection Coefficient

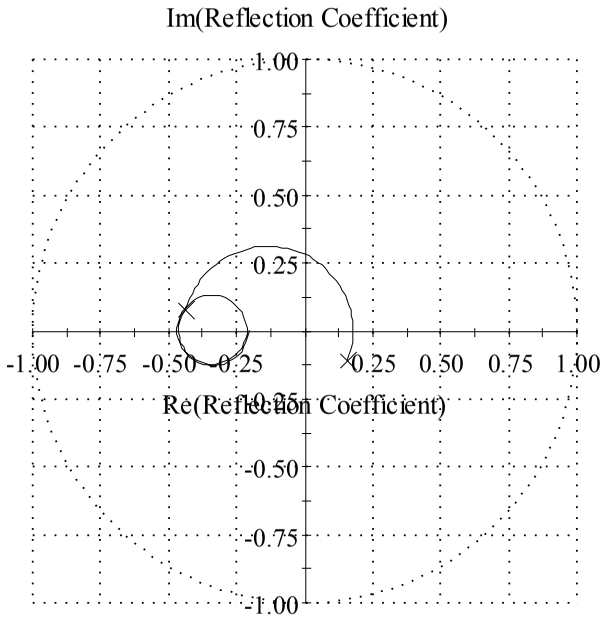

Figure 31 Results for ITO data 3 for 400-700nm

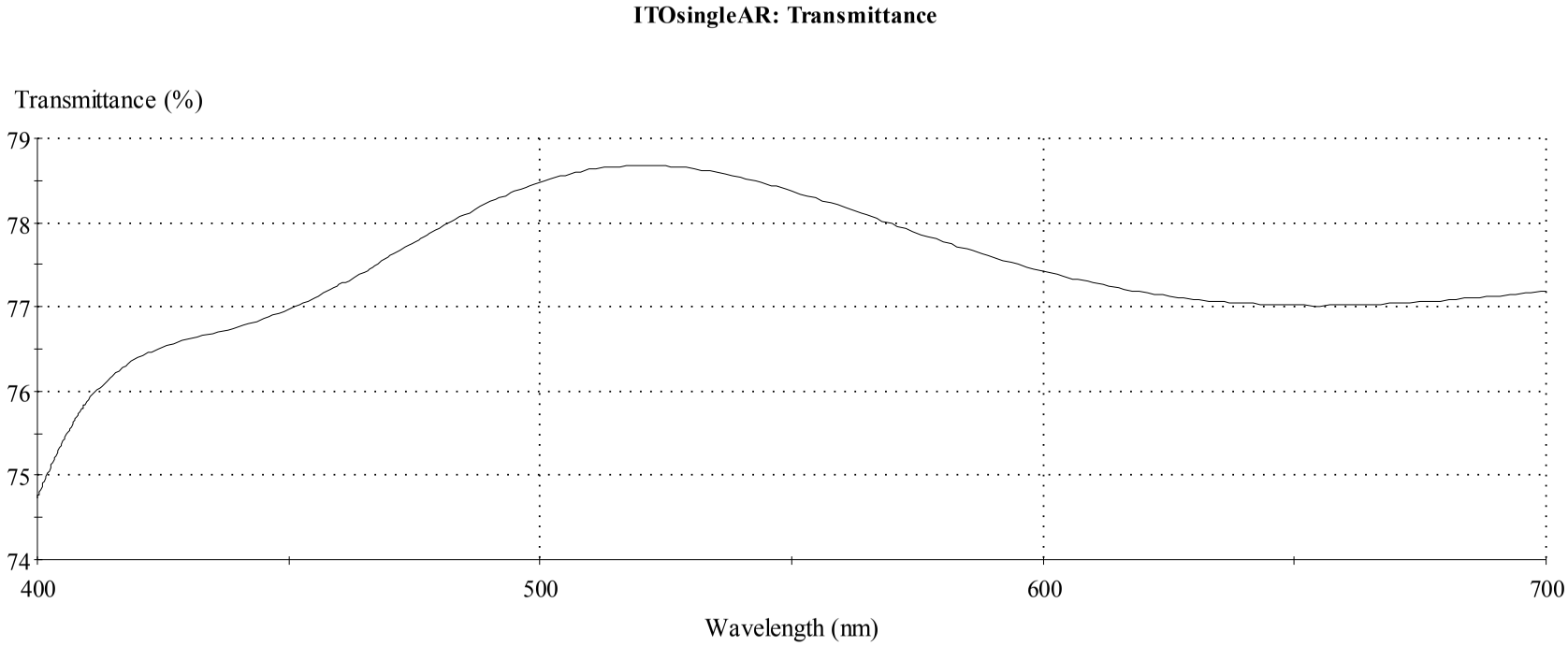

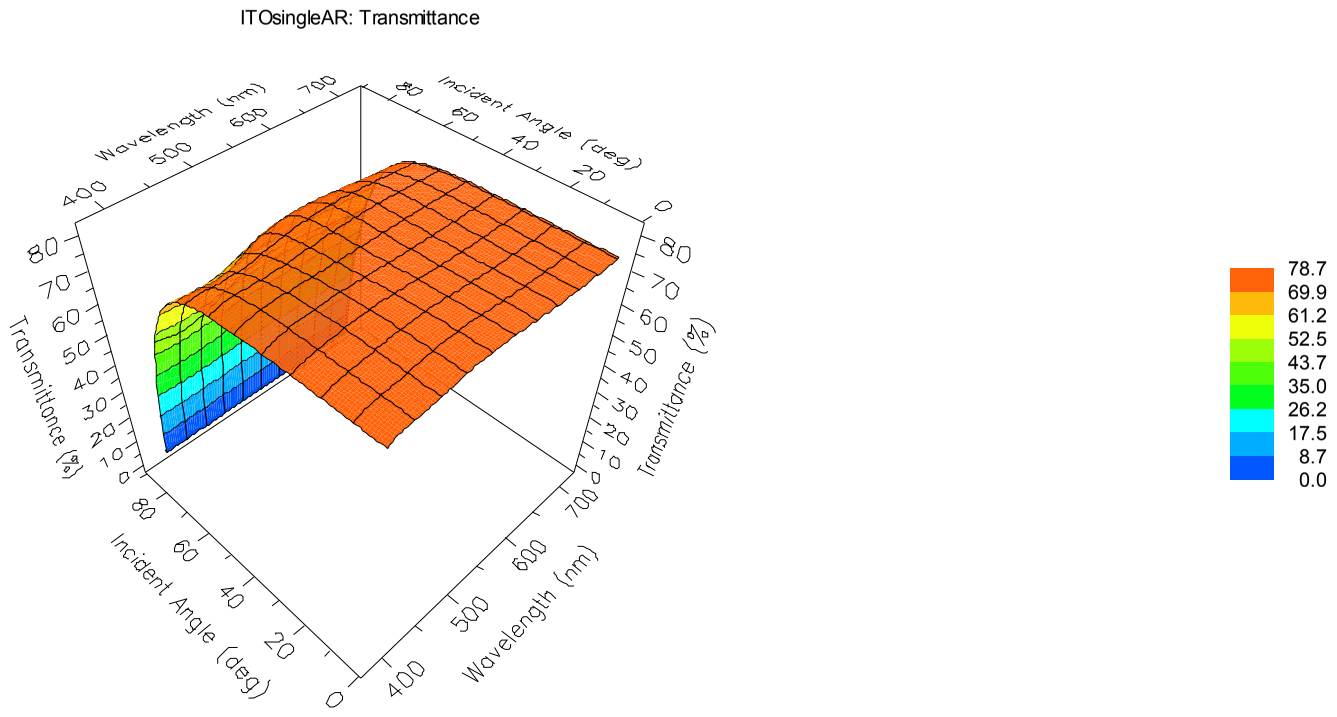
ITOsingleAR: Transmittance
Wavelength (nm)
400
500
600
700
Incident Angle (deg)
0
20
40
60
80
Transmittance (%)
0
10
20
30
40
50
60
70
80
78.7
69.9
61.2
52.5
43.7
35.0
26.2
17.5
8.7
0.0

ITOsingleAR: Reflection Coefficient

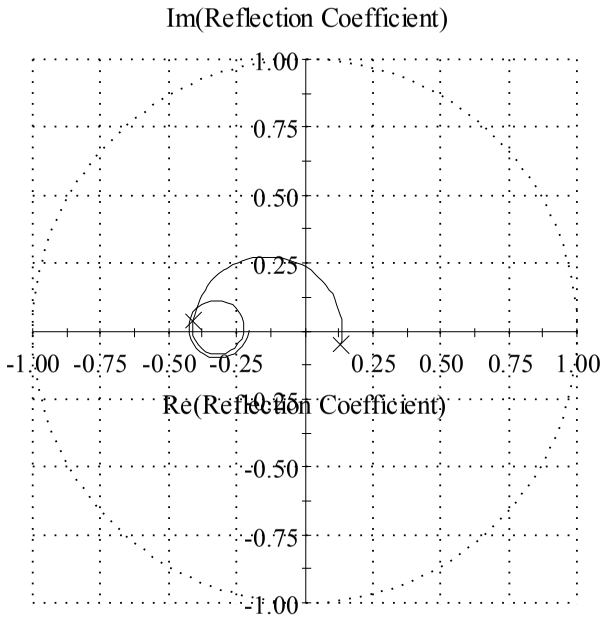

Figure 32 Results for ITO data 4 for 400-700nm

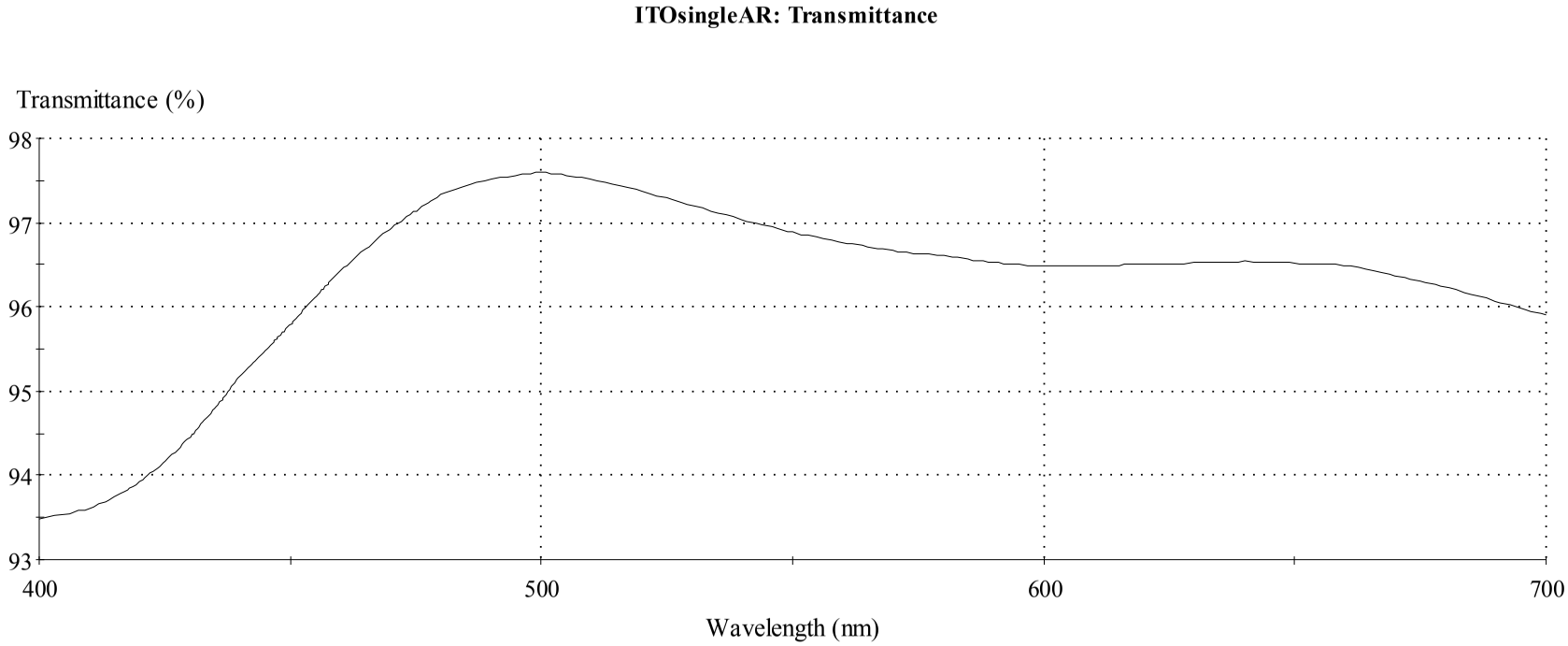

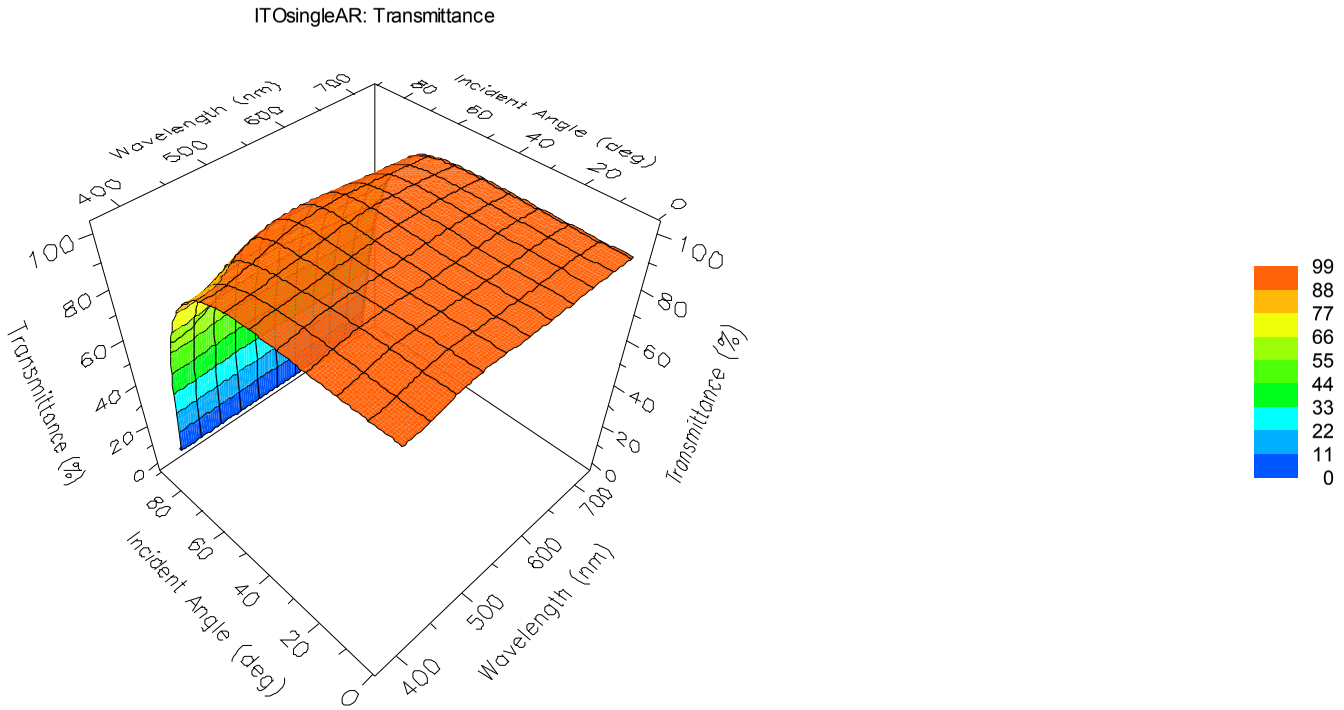
ITOsingleAR: Transmittance
Wavelength (nm)
400
500
600
700
Incident Angle (deg)
0
20
40
60
80
Transmittance (%)
0
20
40
60
80
100
99
88
77
66
55
44
33
22
11
0

ITOsingleAR: Reflection Coefficient

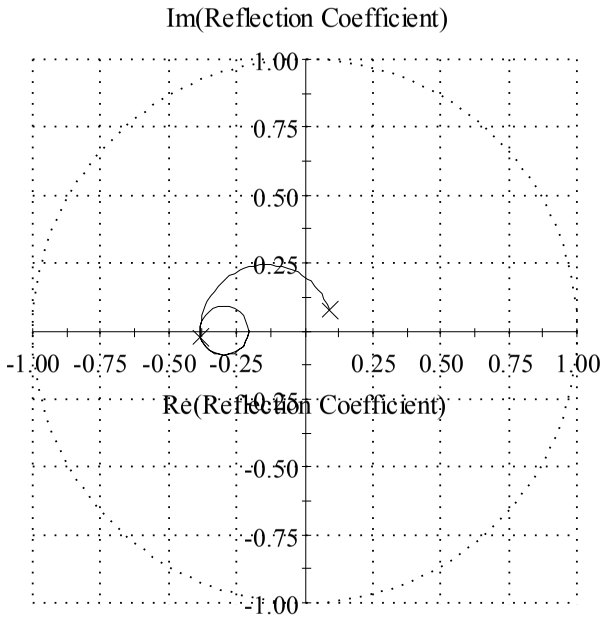

Figure 33 Results for ITO data 1 for 450-900nm

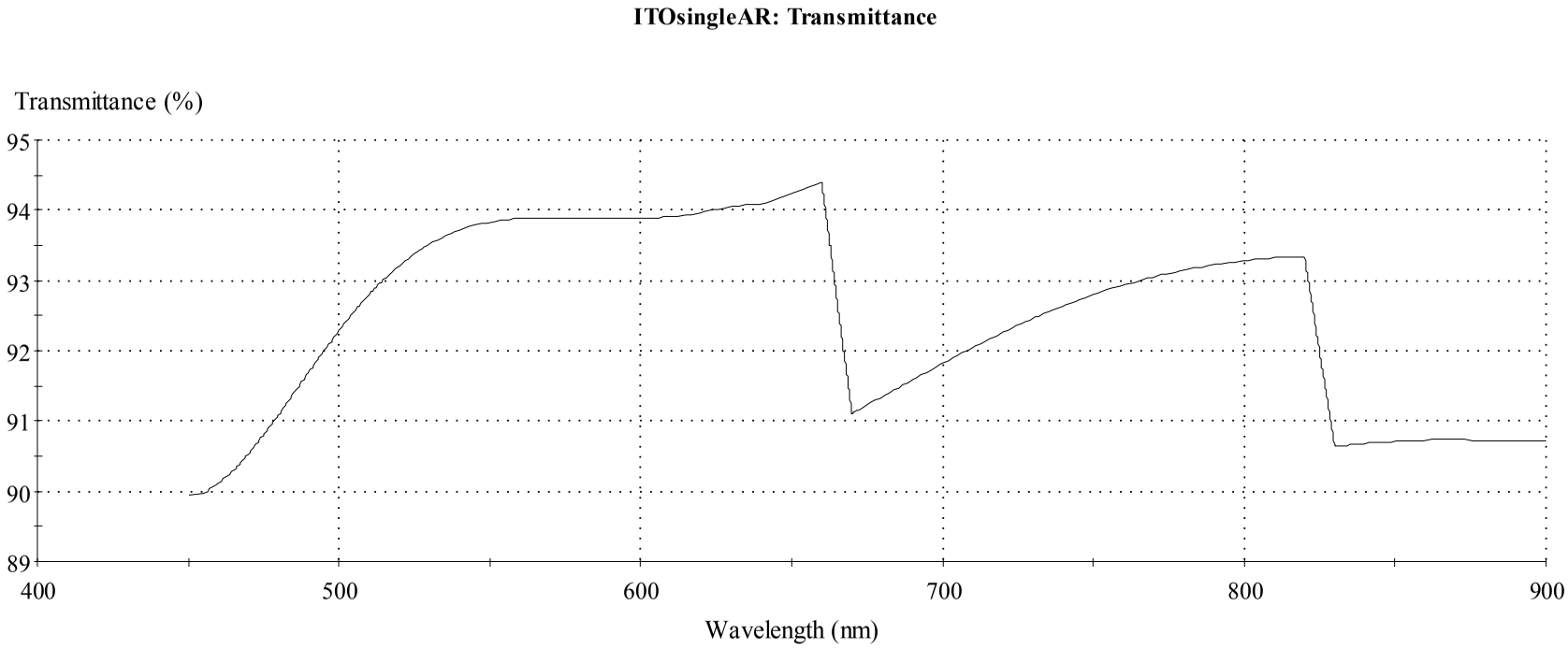

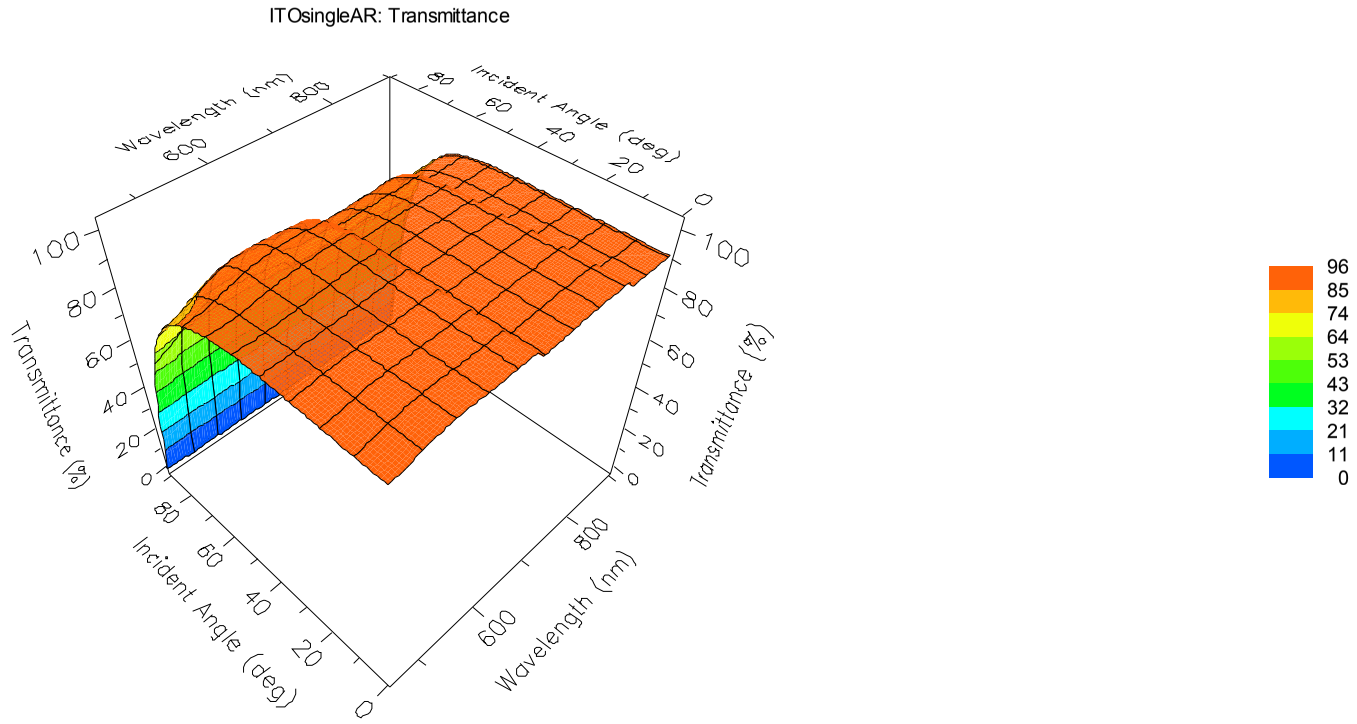
ITOsingleAR: Transmittance
Wavelength (nm)
400
600
800
Incident Angle (deg)
0
20
40
60
80
Transmittance (%)
0
20
40
60
80
100
96
85
74
64
53
43
32
21
11
0

ITOsingleAR: Reflection Coefficient

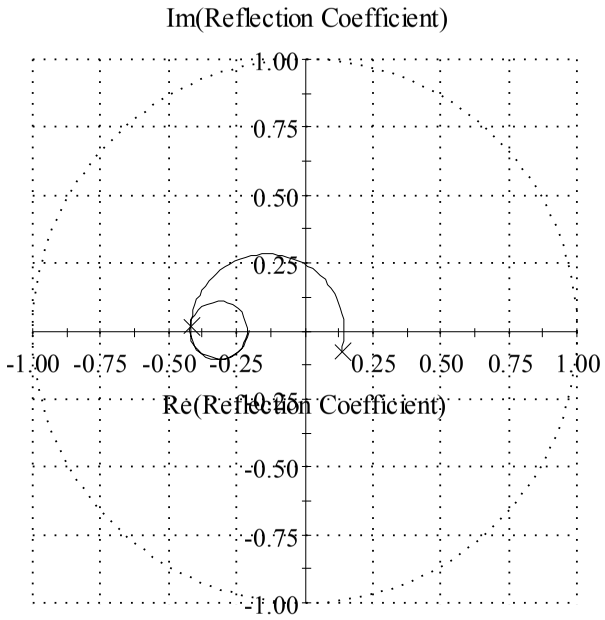

Figure 34 Results for ITO data 2 for 450-900nm

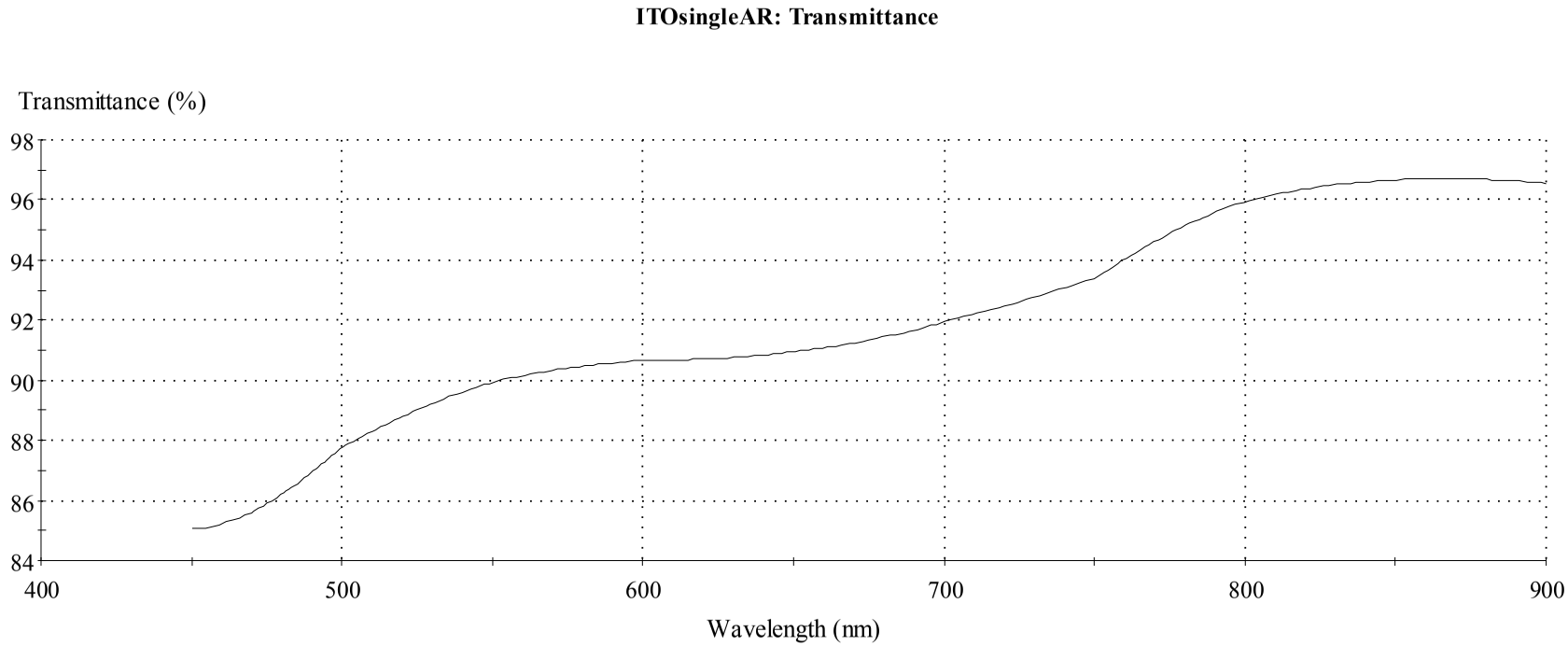

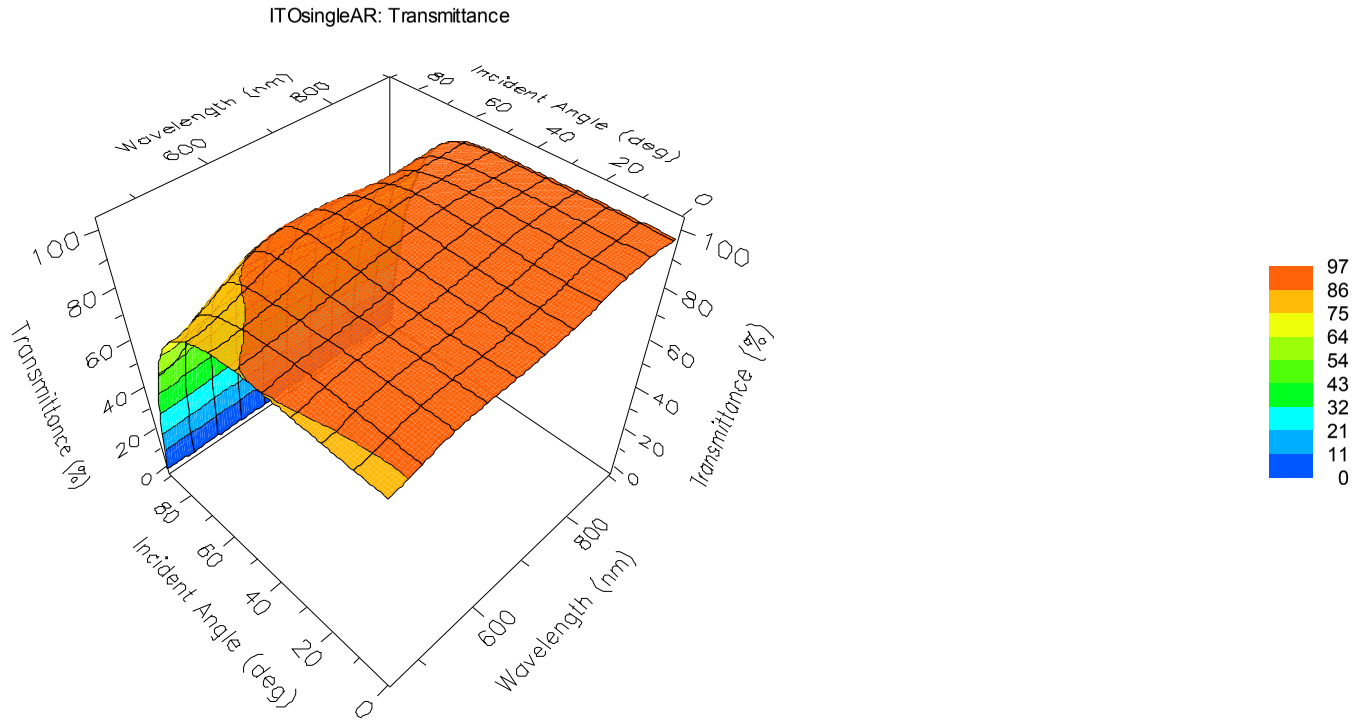
ITOsingleAR: Transmittance
Wavelength (nm)
Incident Angle (deg)
Transmittance (%)
97
86
75
64
54
43
32
21
11
0

ITOsingleAR: Reflection Coefficient

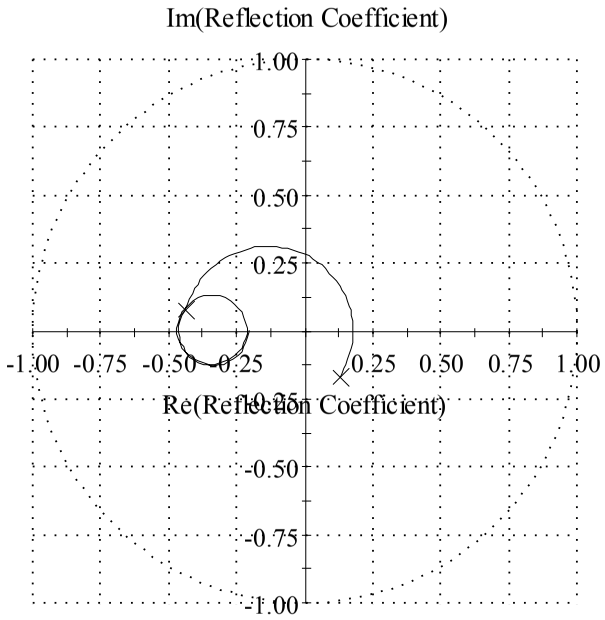

Figure 35 Results for ITO data 4 for 450-900nm

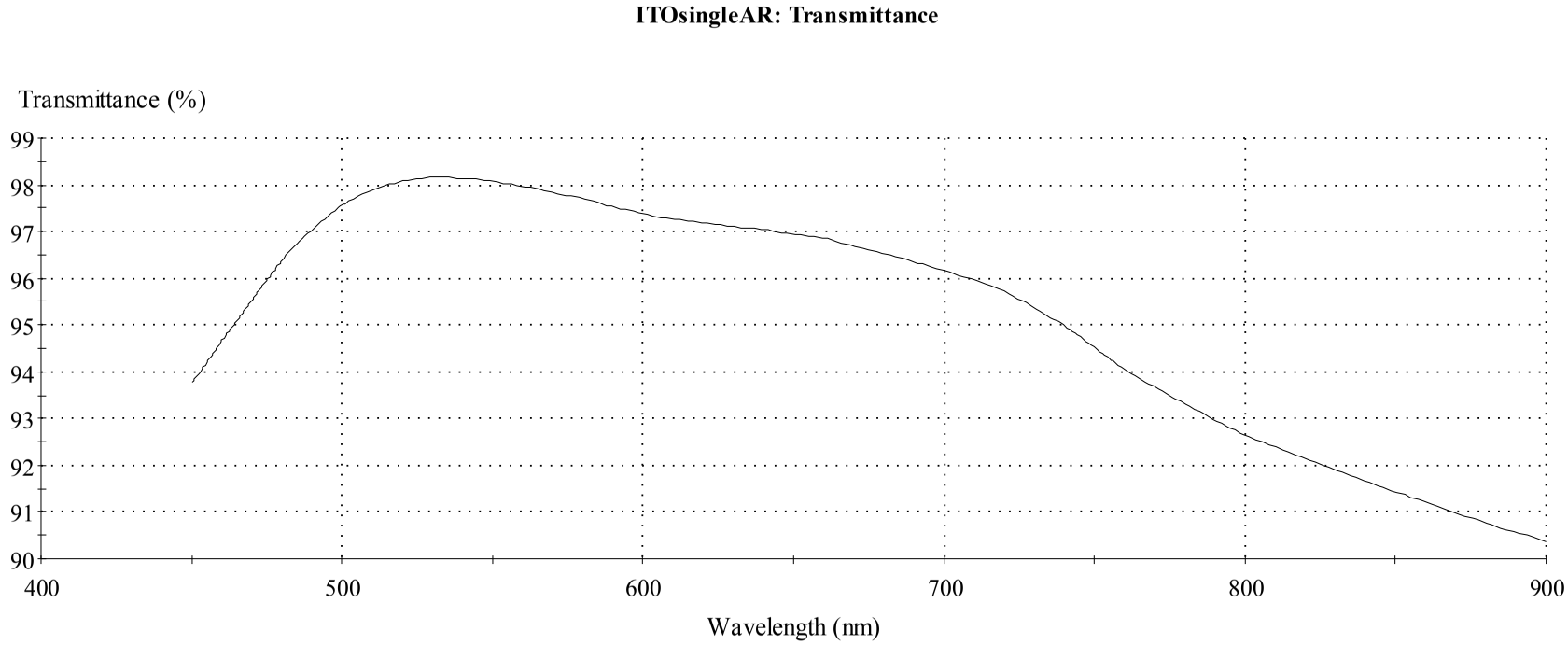

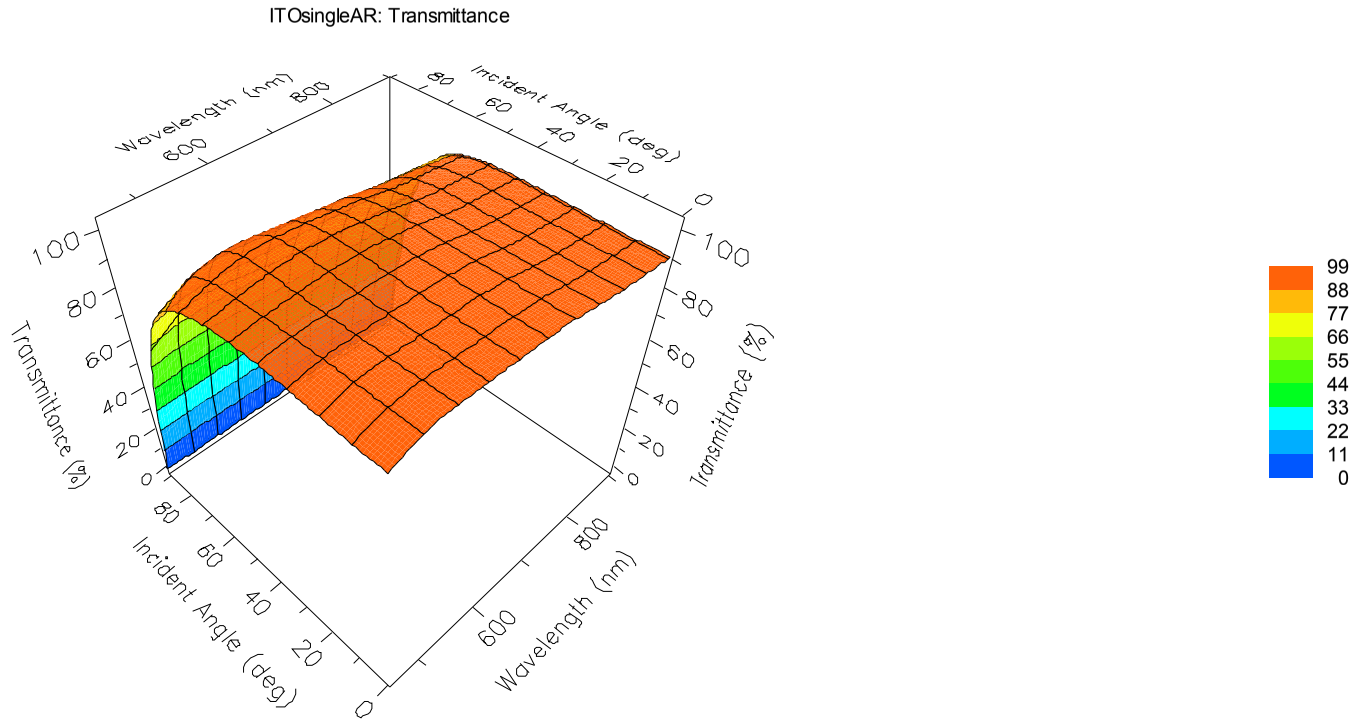
ITOsingleAR: Transmittance
Wavelength (nm)
Incident Angle (deg)
Transmittance (%)
99
88
77
66
55
44
33
22
11
0

ITOsingleAR: Reflection Coefficient

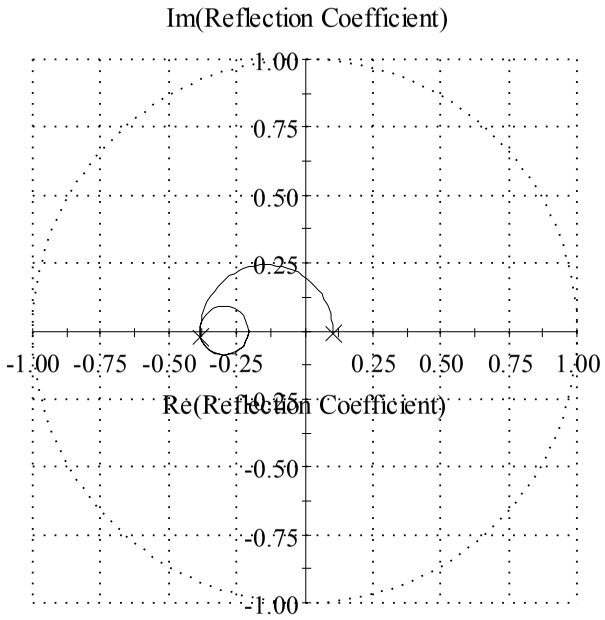

Figure 36 Results for ITO data 1 for 400-800nm

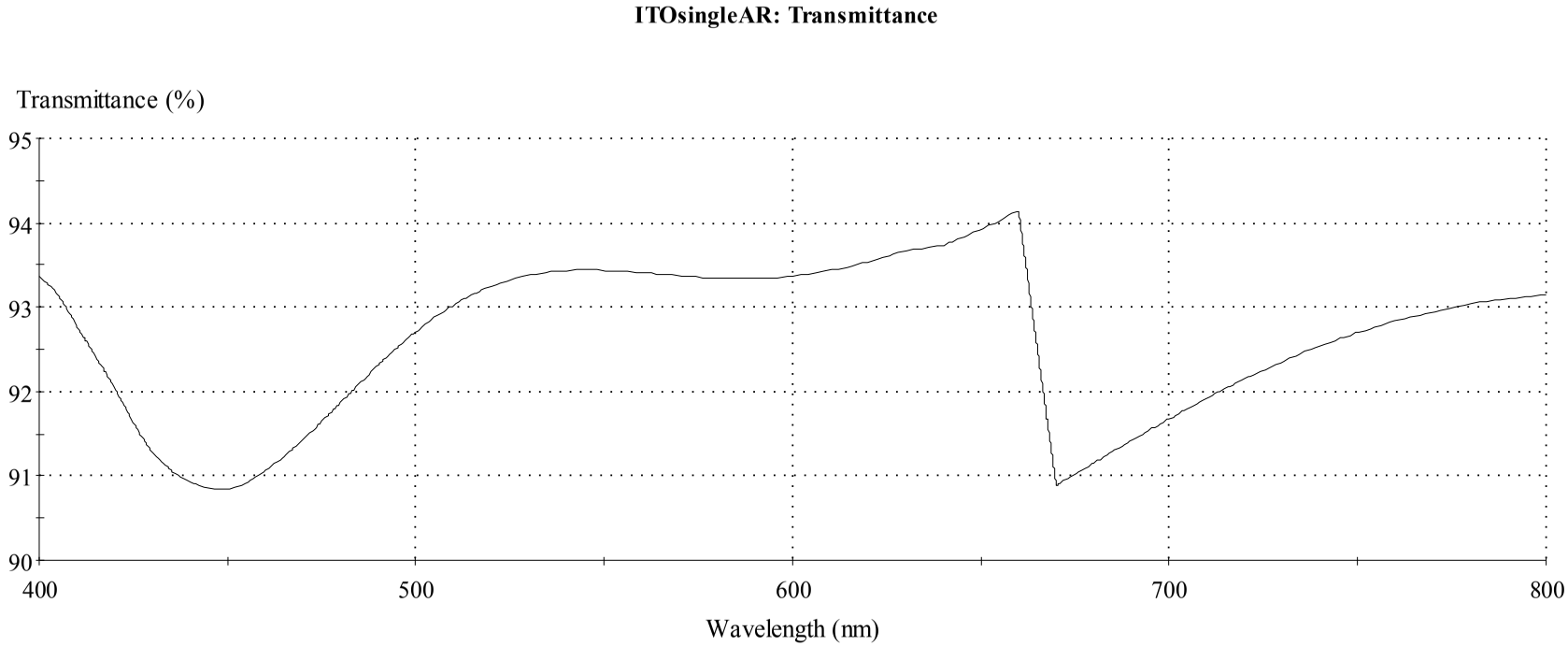

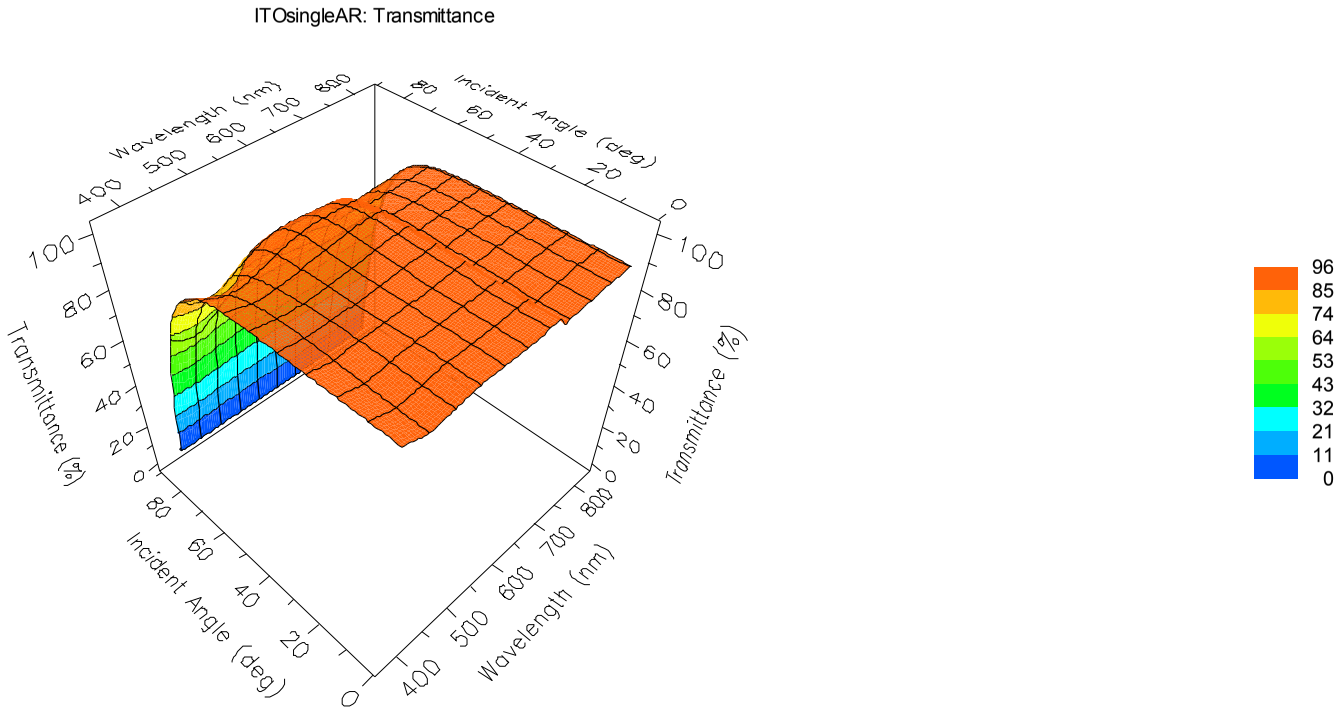
ITOsingleAR: Transmittance
Wavelength (nm)
400
500
600
700
800
Incident Angle (deg)
0
20
40
60
80
Transmittance (%)
0
20
40
60
80
100
96
85
74
64
53
43
32
21
11
0

ITOsingleAR: Reflection Coefficient

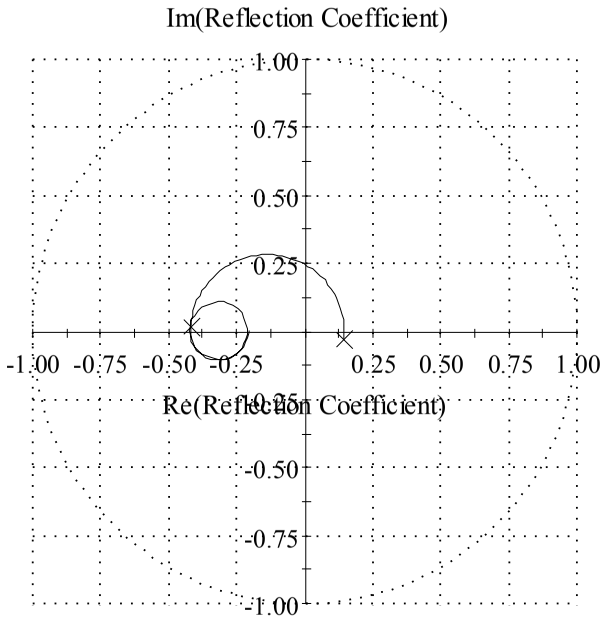

Figure 37 Results for ITO data 2 for 400-800nm

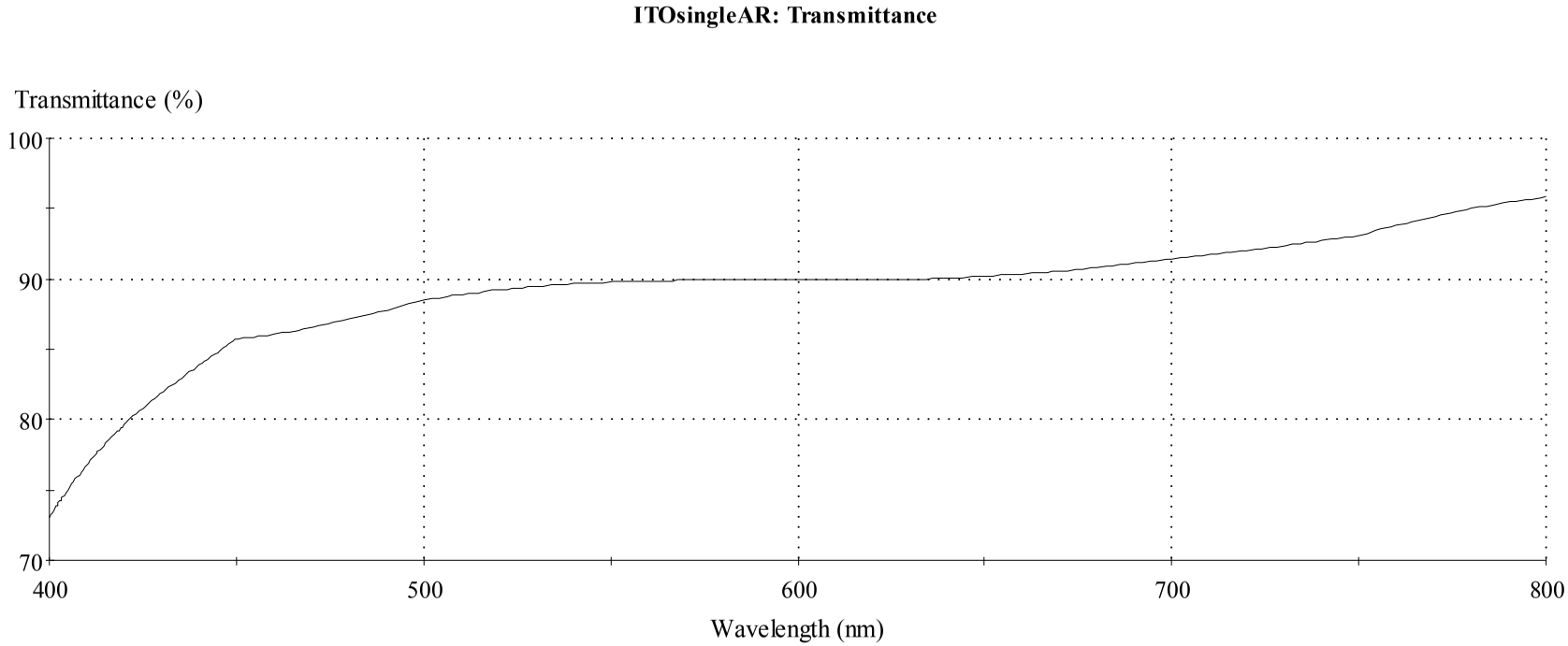

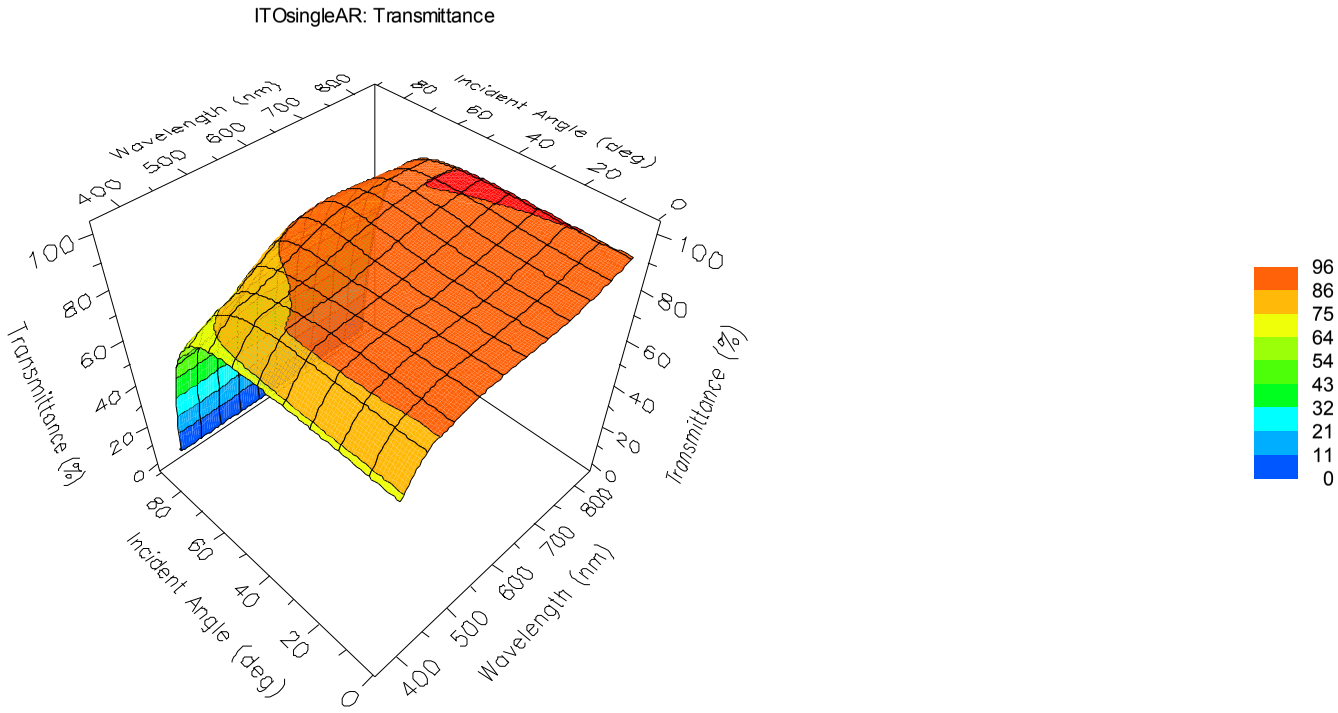
ITOsingleAR: Transmittance
Wavelength (nm)
400
500
600
700
800
Incident Angle (deg)
0
20
40
60
80
Transmittance (%)
0
20
40
60
80
100
96
86
75
64
54
43
32
21
11
0

ITOsingleAR: Reflection Coefficient

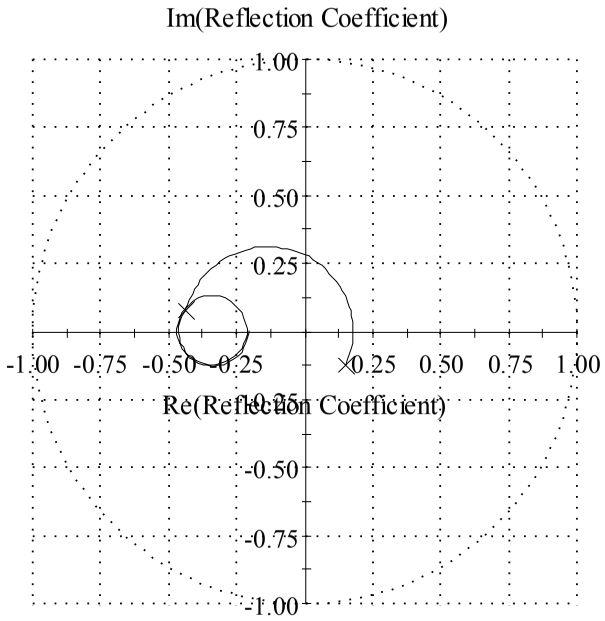

Figure 38 Results for ITO data 3 for 400-800nm

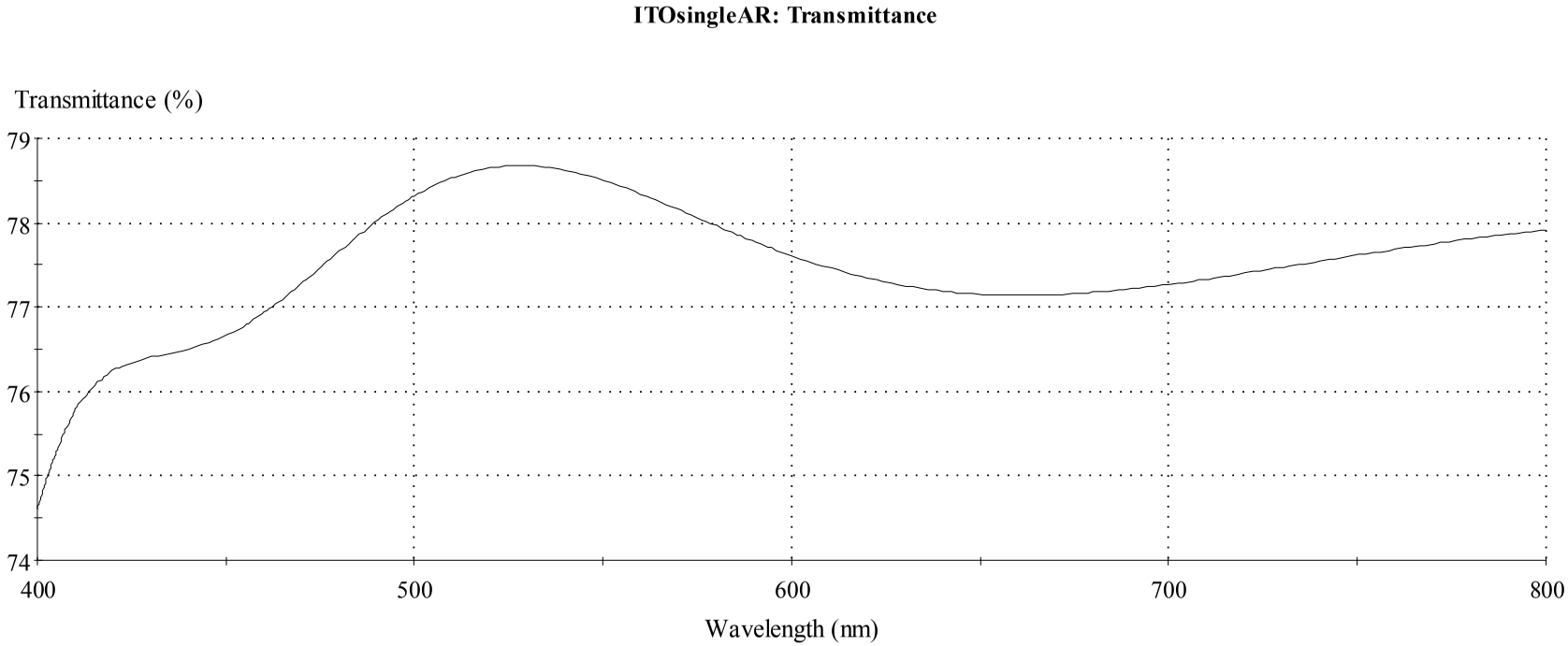

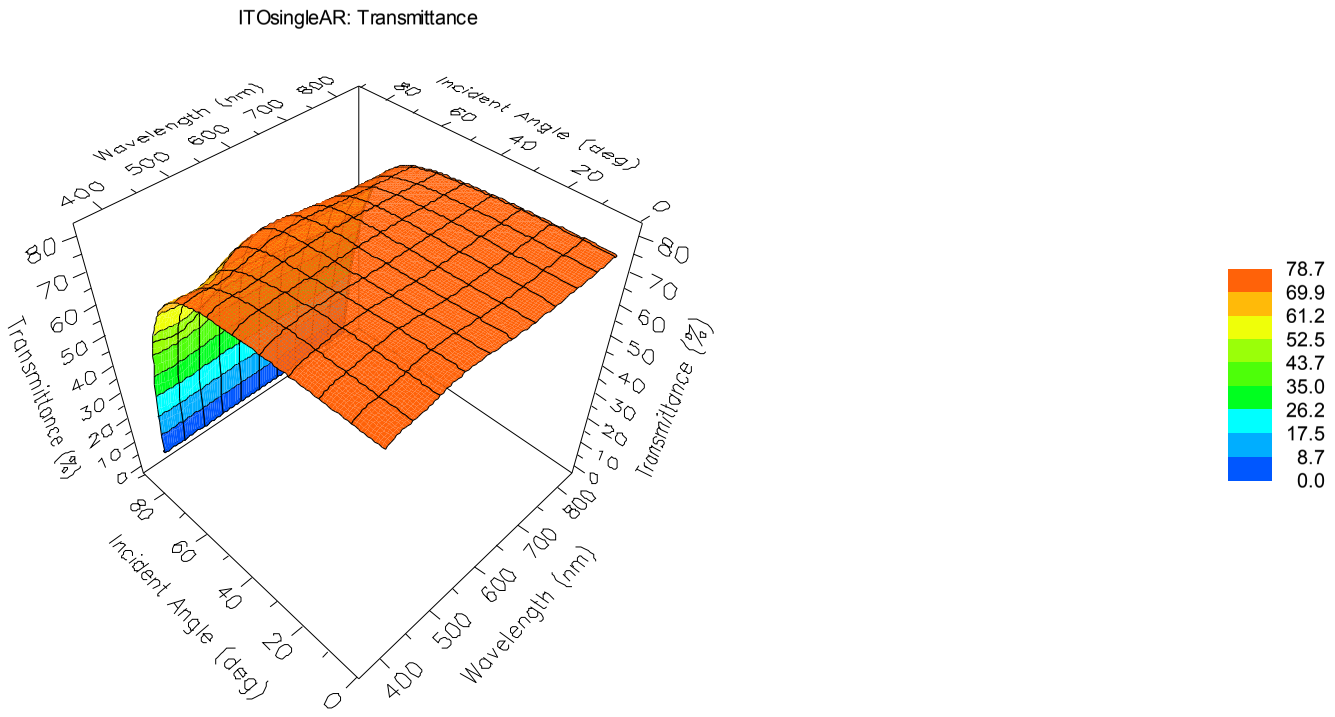
ITOsingleAR: Transmittance
Wavelength (nm)
400
500
600
700
800
Incident Angle (deg)
0
20
40
60
80
Transmittance (%)
0
10
20
30
40
50
60
70
80
78.7
69.9
61.2
52.5
43.7
35.0
26.2
17.5
8.7
0.0

ITOsingleAR: Reflection Coefficient

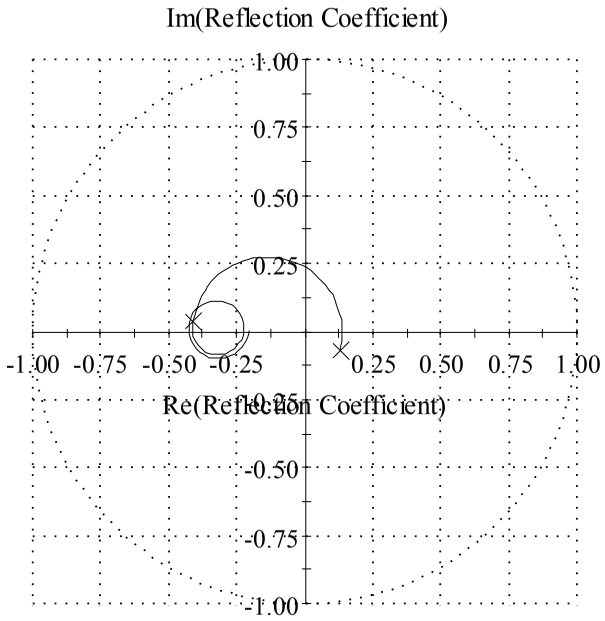

Figure 39 Results for ITO data 4 for 400-800nm

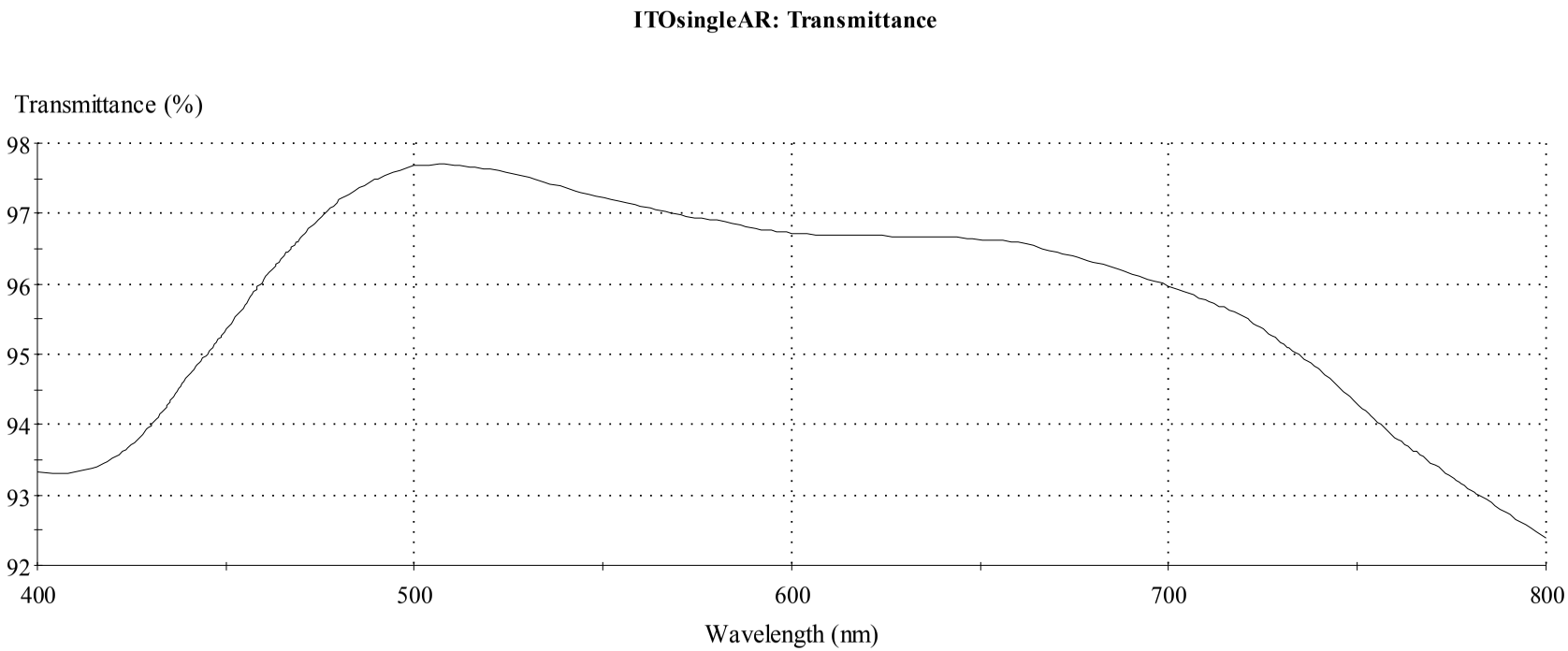

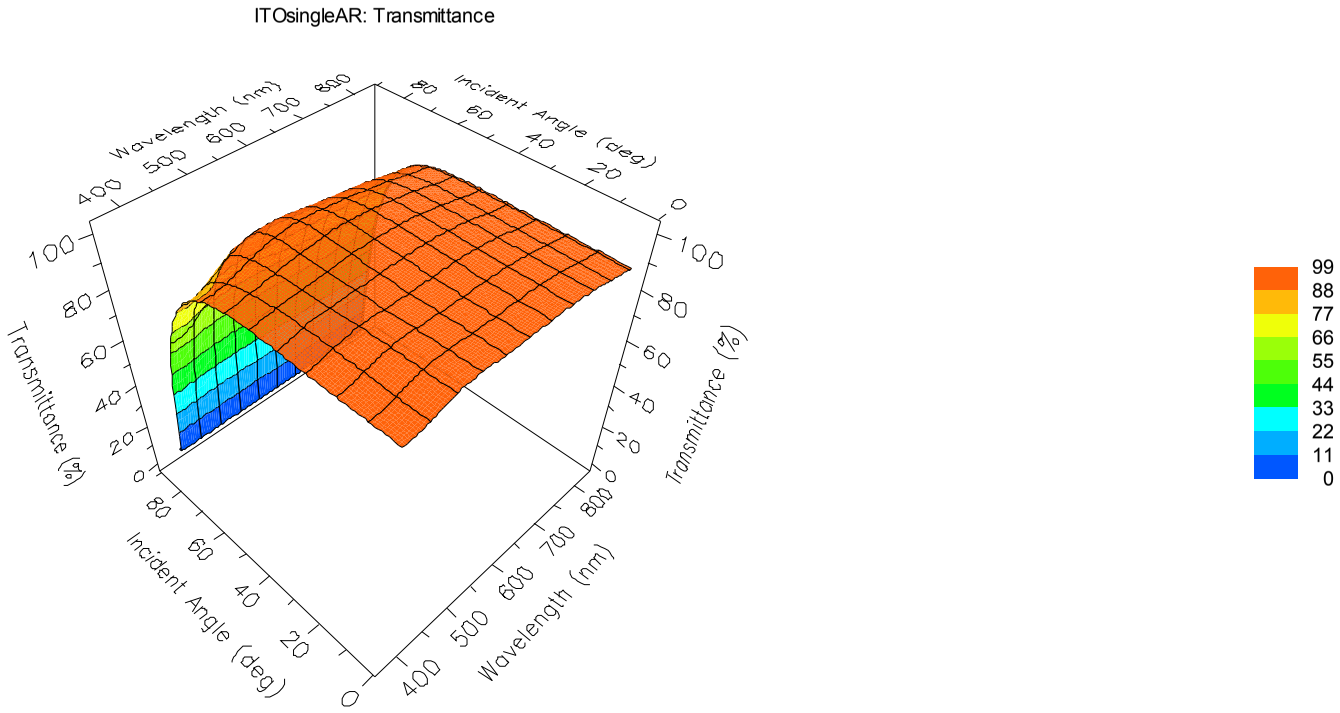
ITOsingleAR: Transmittance
Wavelength (nm)
400
500
600
700
800
Incident Angle (deg)
0
20
40
60
80
Transmittance (%)
0
20
40
60
80
100
99
88
77
66
55
44
33
22
11
0

ITOsingleAR: Reflection Coefficient

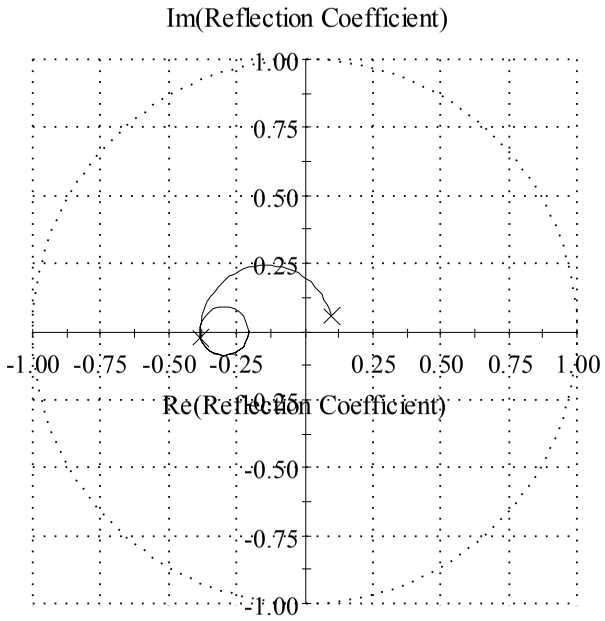

Table 15 Cryolite Results in comparison to the results obtained for the optimum refractive index

Wavelength range /nm	**ITO Thickness /kÅ**	**ITO Data**	**Cryolite layer thickness /nm**	**Average %T for Cryolite studies**	**Average %T for optimum refractive index**
400-700nm	**2**	1	**93.96**	**92.7**	**92.7**
400-700nm	**2**	2	**95.49**	**87.4**	**87.8**
400-700nm	**2**	3	**94.82**	**77.4**	**77.4**
400-700nm	**2**	4	**88.16**	**96.2**	**96.3**
450-900nm	**2**	1	**100.00**	**92.4**	**92.4**
450-900nm	**2**	2	**101.51**	**91.8**	**91.9**
450-900nm	**2**	4	**98.77**	**95.2**	**95.3**
400-800nm	**2**	1	**95.47**	**92.7**	**92.7**
400-800nm	**2**	2	**96.83**	**89.0**	**89.1**
400-800nm	**2**	3	**96.85**	**77.4**	**77.4**
400-800nm	**2**	4	**90.83**	**95.7**	**95.8**

The results in this table and the single layer studies show that Cryolite provides a very good solution. The next step from this is to consider more complex coatings to see if further improvement is observed.

5.2.8 Addition of a multi layer stack on ITO using needle synthesis

Another route to attempt to maximise %T is to investigate is the production of multi layer stacks applied on top of the ITO utilising the needle synthesis technique. This is considered below. As such good results were achieved with the Cryolite in the previous section, Cryolite will be used as one of the stack constituents. As the refractive index of Cryolite is less than that of ITO, the other material used in the stack will be TiO_2 as this has a refractive index greater than that of ITO, is a commonly used AR material and will therefore has a more substantial contrast to Cryolite. An example of needle synthesis run in progress is shown in Figure 40:

Figure 40 Needle synthesis

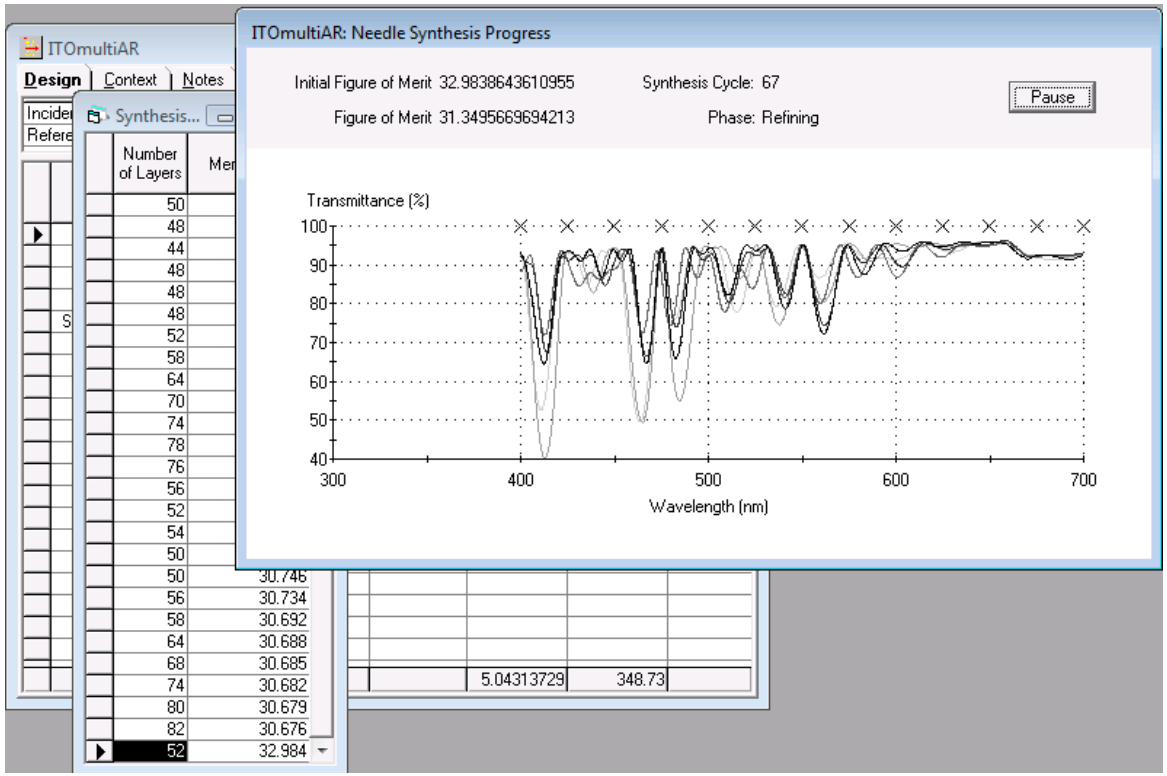

Needle synthesis is carried out in Essential Macleod by firstly stating the layers that you wish to insert 'very tiny needles' containing the substances you wish to inject. In this case, the layers are Cryolite and TiO_2 that sit on top of the ITO. The next step is to specify the materials that you want to 'inject' in these layers. Again, in this case, this is Cryolite and TiO_2. Figure 40 shows Essential Macleod running the needle synthesis technique with these parameters.

The results from the needle analysis for 400-700nm ITO data 1 are shown in Table 16. The %T graphs and the circle diagrams that result from this analysis are shown in Figure 35.

Table 16 Addition of a multilayer stack consisting of TiO_2 and Cryolite

Layer	Material	Physical Thickness (nm)
Medium	Air	
1	Na3AlF6	173.23
2	TiO2	2.74
3	Na3AlF6	321.67
4	TiO2	0.65
5	Na3AlF6	216.48
6	TiO2	2.65
7	Na3AlF6	185.36
8	TiO2	1.05
9	Na3AlF6	335.26
10	TiO2	1.22
11	Na3AlF6	11.54
12	TiO2	3.08

13	Na3AlF6	434.53
14	TiO2	4.04
15	Na3AlF6	610.72
16	TiO2	0.52
17	Na3AlF6	437.15
18	TiO2	5.35
19	Na3AlF6	173.22
20	TiO2	5.31
21	Na3AlF6	396.61
22	TiO2	1.31
23	Na3AlF6	244.3
24	TiO2	3.27
25	Na3AlF6	189.88
26	TiO2	4.21
27	Na3AlF6	603.45
28	TiO2	4.54
29	Na3AlF6	177.38
30	TiO2	2.78
31	Na3AlF6	871.92
32	TiO2	4.93
33	Na3AlF6	7.31
34	TiO2	1.06
35	Na3AlF6	178.92
36	TiO2	1.48
37	Na3AlF6	294.37
38	TiO2	0.76
39	Na3AlF6	225.72

40	TiO2	2.55
41	Na3AlF6	500.11
42	TiO2	3.41
43	Na3AlF6	152.17
44	TiO2	0.17
45	Na3AlF6	134.8
46	TiO2	2.14
47	Na3AlF6	127.57
48	TiO2	5.34
49	Na3AlF6	188.89
50	TiO2	5.66
51	Na3AlF6	751.52
52	TiO2	6.4
53	Na3AlF6	33
54	ITO	200
Substrate	Glass	

Figure 41 Results from the TiO_2 and Cryolite multilayers

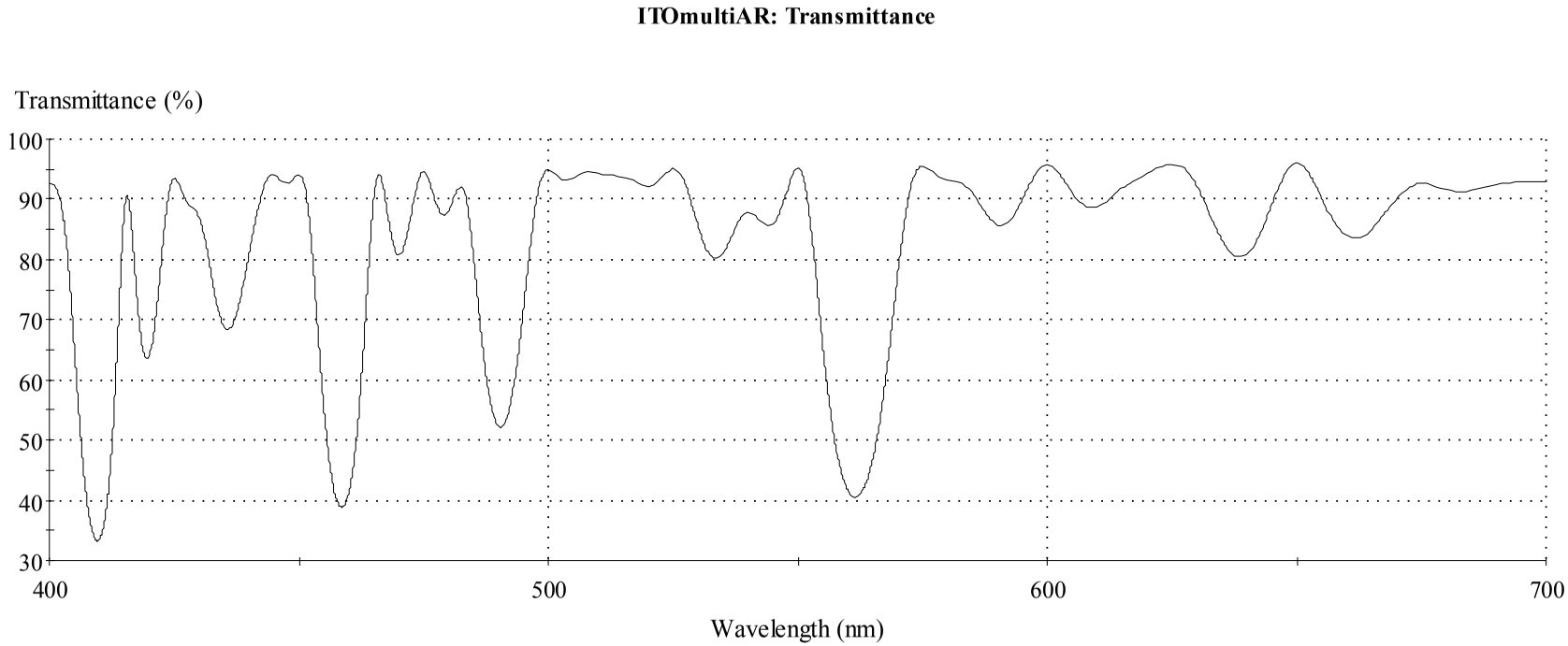

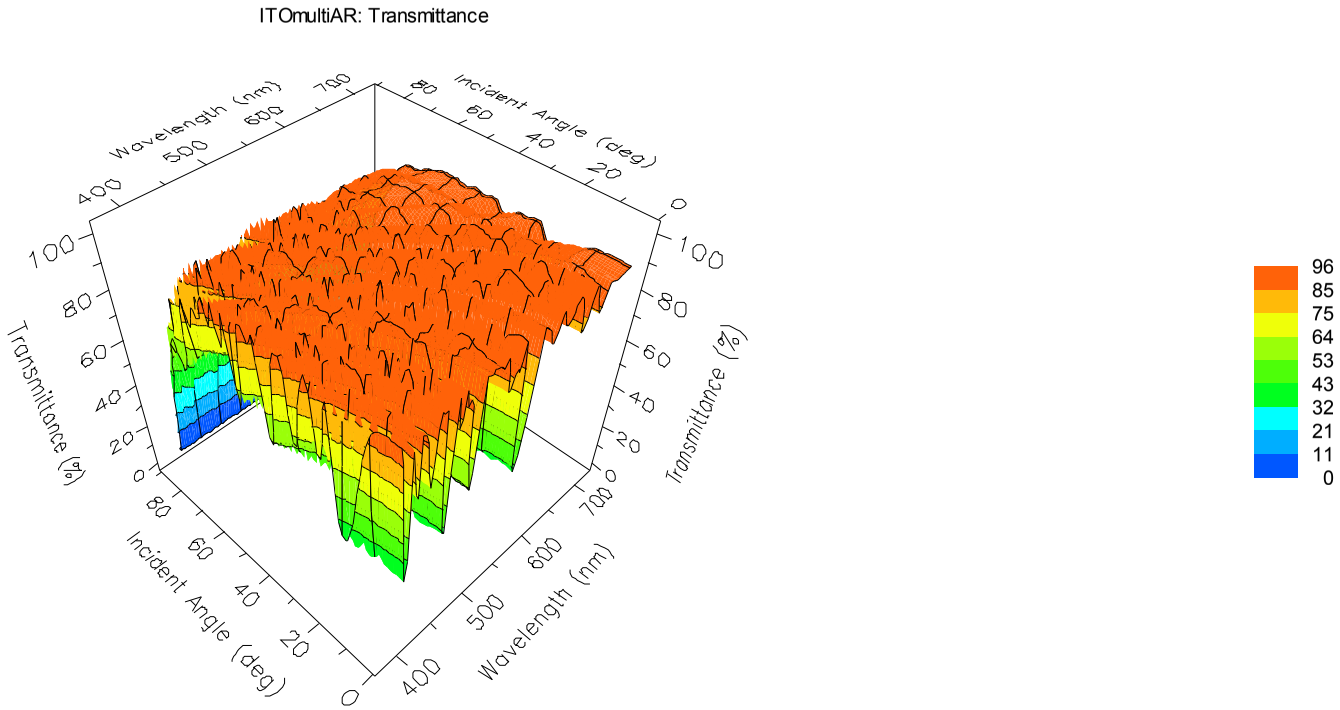
ITOmultiAR: Transmittance
Wavelength (nm)
400
500
600
700
Incident Angle (deg)
0
20
40
60
80
Transmittance (%)
0
20
40
60
80
100
96
85
75
64
53
43
32
21
11
0

ITOmultiAR: Reflection Coefficient

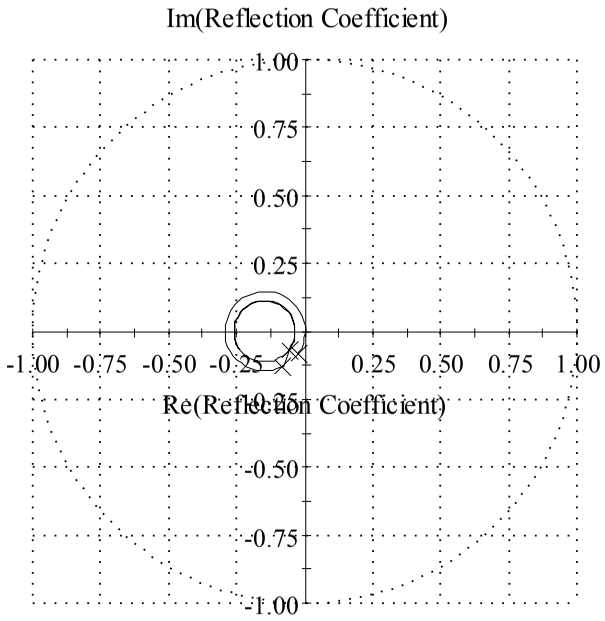

Average %T over 400-700nm for ITO data 1 = 82.2.

5.2.9 Addition of multilayer stacks using needle synthesis with ITO as one of the stack layers

The next logical step from this would be to consider having ITO and Cryolite as the stack layers to see the effects of this.

The results for 400-700nm ITO data 1 were as follows

Table 17 Multilayer stack consisting of Cryolite and ITO

Layer	Material	Physical Thickness (nm)
Medium	Air	
1	Na3AlF6	427.62
2	ITO	0.13
3	Na3AlF6	2039.36
4	ITO	0.19
5	Na3AlF6	2674.36
6	ITO	0.28
7	Na3AlF6	803.45
8	ITO	4.98
9	Na3AlF6	198.77
10	ITO	3.57
11	Na3AlF6	751.98
12	ITO	1.99
13	Na3AlF6	1383
14	ITO	4.49

15	Na3AlF6	200.03
16	ITO	1.07
17	Na3AlF6	927.81
18	ITO	3.12
19	Na3AlF6	1177.65
20	ITO	1.91
21	Na3AlF6	180.44
22	ITO	5.24
23	Na3AlF6	1158.88
24	ITO	0.17
25	Na3AlF6	1187.34
26	ITO	1.02
27	Na3AlF6	961.57
28	ITO	5.2
29	Na3AlF6	30.18
30	ITO	200
Substrate	Glass	

Figure 42 Results from the ITO Cryolite multilayers

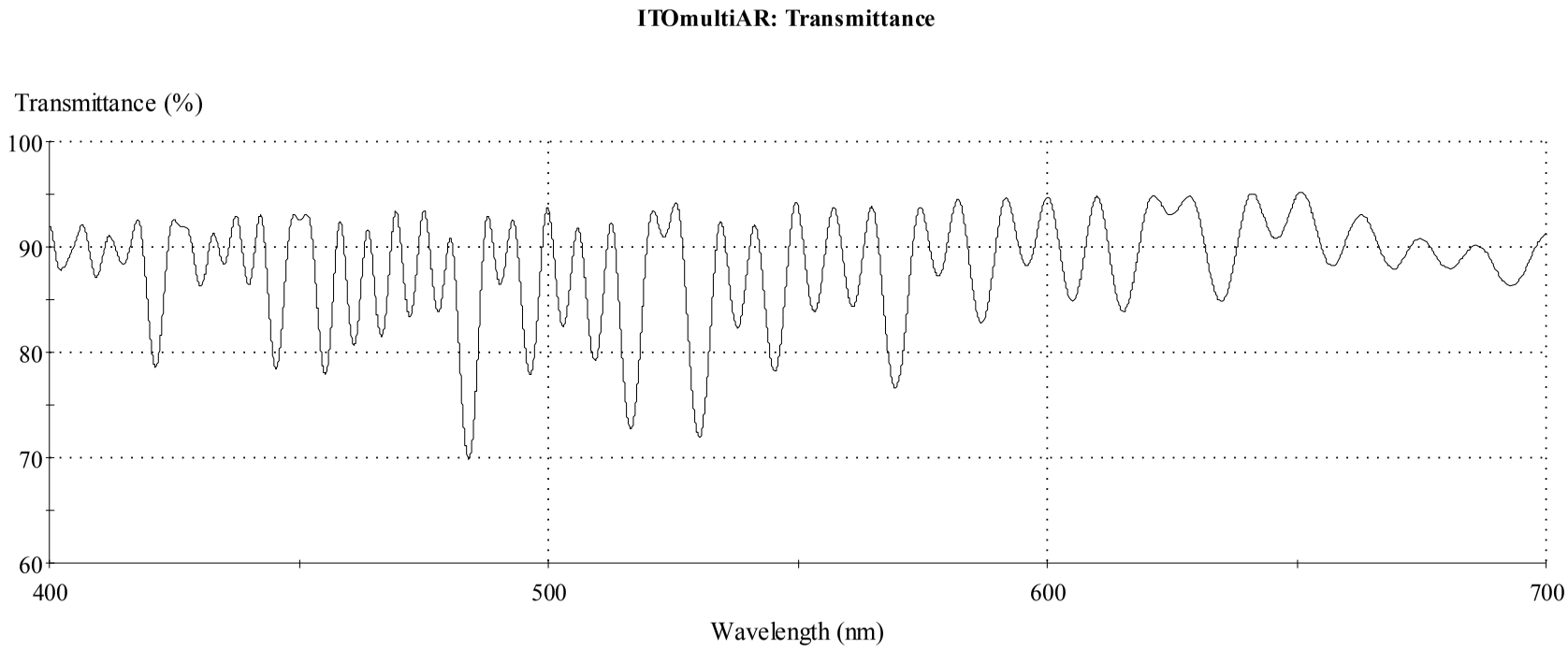

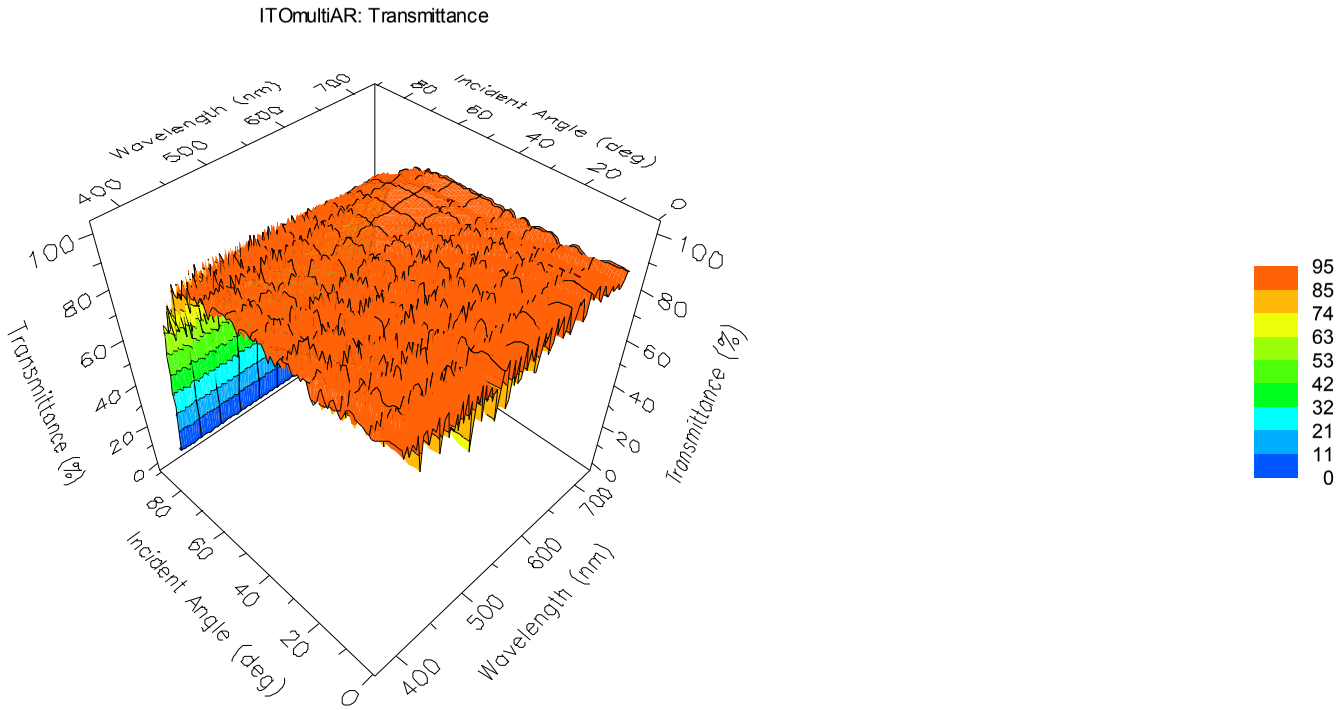
ITOmultiAR: Transmittance
Wavelength (nm)
400
500
600
700
Incident Angle (deg)
0
20
40
60
80
Transmittance (%)
0
20
40
60
80
100
95
85
74
63
53
42
32
21
11
0

ITOmultiAR: Reflection Coefficient

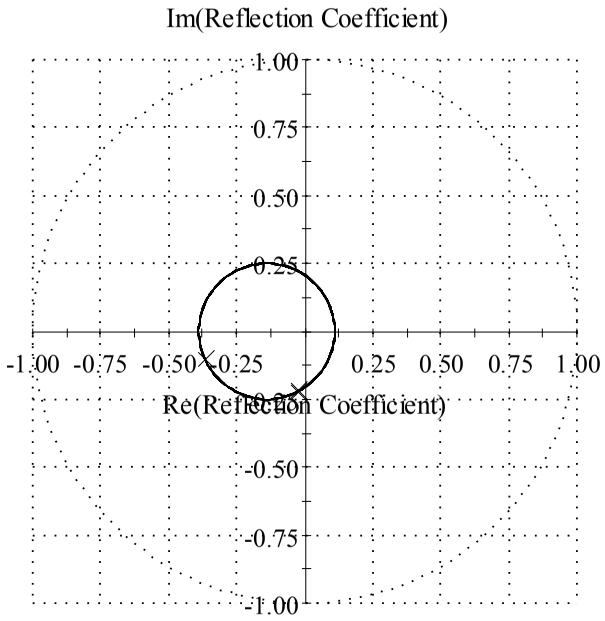

Average %T for 400 to 700nm for this design = 89.9.

It can be seen from both of these results that there is a large variation in response over wavelength. This is clearly unacceptable. The effect could be reduced by the addition of further layers, but as can be seen by the layer thicknesses given from the needle analysis, this would be a pointless exercise as some of the recommended layers are so thin that they are not practically reproducible.

6 Observations and Discussion

6.1 Consideration of the Experimental results

This section makes observations and discusses the results of the analysis of coatings produced with various conditions via Electron Beam Evaporation with and without Ion Assisted Vapour Deposition in a Leybold LAB600 at PJ Coatings.

6.2.1 Observation of the effects of deposition parameters on the output parameters when depositing a single layer of ITO via Electron beam evaporation onto a glass substrate multiple times with varying conditions

The reproducibility of the deposition conditions was evaluated statistically using the “Analysis of Variance” (ANOVA).

Table 2 provided a summary of the values of F and F_{crit} for each variable and result considered in the ANOVA analysis.

The Results considered in this ANOVA analysis were Inner Resistivity, Outer Resistivity and %T for 400-700nm, 450-900nm, 400-800nm and 700-3000nm respectively. Even though the aims are to just consider the visible and near surrounding area, 700 – 3000nm was also considered here out of interest.

The main observations from these results were as follows:

- It can be seen that each result is affected by all of the variables considered to a greater or lesser extent. The next obvious step to this analysis would be to determine relationships between each result and each variable directly. Looking at the effects on variables such as

Temperature on results produced would be interesting. To perform this, each variable would have to be altered while all the other variables were held constant in a methodical manner for numerous runs. This unfortunately was not possible in this project as the number of practical hours where the equipment was available for use was limited.

- Temperature and ITO % Composition were found to be the most significant variables overall that influenced average %T over the wavelength range 400-3000nm.

- Temperature was found to be the most significant factor influencing resistivity, although ITO % composition, Ion assistance, pressure, deposition rate, thickness and Argon flow also have considerable influence on resistivity.

- It is interesting to note that for each result considered (both transmission and resistivity), the variable that had the least significance to each result was the Anode Voltage. For the 700 to 3000nm region, this was the smallest observed difference between F and F_{crit} in the ANOVA analysis. It is interesting than the presence or absence of Ion Assistance plays more of a role on the result that the value of the Anode Voltage in each case. This implies that the value of the Anode Voltage does not play an important part in Ion Assistance when considering these wavelength ranges and the Anode Current is the variable that plays the bigger role.

- When the %T was considered for each wavelength range, the values for F were larger than the values produced from the Resistivity analysis. This indicates that the %T is more sensitive to these variables than the resistivity.

6.2.2 Determination of the ITO deposition conditions required to provide <20 Ω/□

Table 3 illustrates the parameters used to provide an ITO coating with <20 Ω/square. The results achieved are illustrated in Table 4.

The observations made from these results are as follows:

- It is Interesting to note that the desired resistivity has been obtained both with and without ion assisted deposition.
- In all of the cases considered, an ITO thickness of 2kÅ was required to obtain the required sheet resistivity.
- Without IAD, an O_2 flow of 40sccm and an Ar flow of 0sccm was required.
- With IAD, an O_2 flow of 12.8sccm and an Ar flow of 5sccm was required.

6.2.3 Determination of the ITO deposition conditions required to provide <100 Ω/□

Table 5 illustrates the parameters used to provide an ITO coating with <100 Ω/square. The results achieved are illustrated in Table 6.

It can be seen that the thickness required to produce <100 Ω/square is considerably less than the thickness required to produce <20 Ω/square thus concurring with the observations of Eite (2004).

It can be seen that the relationship is not straight forward as an ITO thickness of 100kÅ is required to produce 83 ohms per square, whereas a 200kÅ layer produces a measured value of 17 ohms per square.

6.2.4 Attempt to maximise the %T with the addition of extra layers

No effect on ITO Resistivity was observed from the addition of any of the extra coatings applied.

Table 7 illustrates the results of adding additional coatings to the ITO coating.

It can be seen that for 2kÅ of ITO, the coating applied on 140508 run 1 yielded the best practical %T results for the visible wavelength range and the immediate surrounding area. MgF_2 also produced very high %T for 0.5kÅ of ITO and the wavelength ranges considered.

Additional coatings for ITO are further considered in the Theoretical Modelling section.

6.2.5 Examination of the results of ITO deposition via IAD and sputtering to determine the difference the technique used has upon the coating produced

6.2.5.1 Atomic Force Microscopy

Atomic Force Microscopy was used to look at the surface roughness of the three samples and to determine how this is affected by the method of deposition and to observe the variation with thickness of coating.

The results of this study are illustrated in Figures 14-16.

It is interesting to note that the Average roughness (R_A) of the thick evaporation sample is over 3 times more than for the thin evaporation sample.

Yun *et al* (2004) report that Surface roughness deteriorates the conductivity and homogeneity of ITO thin films. It is for this reason that Yun *et al* (2004) etched the ITO coating surface to make it smoother. Their unetched sample had an average roughness of approximately 4.8Å, whereas the optimum etching resulted in a sample with an average roughness of approximately 3Å.

The study in this thesis reported the following average roughnesses for the samples considered:

Sputtered ITO Sample Average roughness = 11.1Å
Thin ITO Sample Average roughness = 9.2Å
Thick ITO Sample Average roughness =34.3Å.

It is interesting to note that the average roughness produced with the LAB600 and Diamond Coatings sputter sample was greater that the average roughness reported in the study of Yun *et al* (2004) where Chemical Solution Deposition was employed.

Another interesting observation that can be made from the thesis results is that the Average Roughness of the Thick ITO sample was about 3 times greater than the Average roughness of both the thin ITO sample and the sputtered ITO sample (which had similar Average roughness values). As this is a preliminary study, more work would need to be done to investigate this to see if this pattern was repeatedly observed.

Another interesting observation that has arisen from analysis of these results is that the ratio of Rq/Ra is fairly consistent for the evaporation samples and that this value is less than the value that this ratio takes for sputtering.

Figures 17-19 illustrate the SEM results.

The purpose of this section was to examine the ITO coating thicknesses produced in comparison to the thicknesses that were set with the LAB600 deposition equipment.

It can be seen from the results that the sputtered ITO sample produced a fairly even coating whose thickness was 300nm. Unfortunately, for commercial reasons, Diamond Coatings could not provide the parameters used with this coating. Looking at the LAB600 samples, it can be seen that the thickness of the thinner sample showed variation between 92nm and 131nm compared to the specified 75nm. The thickness of the thicker sample however showed a thickness of 192nm compared to the specified 200nm. It can be seen that the thicker sample produced thicknesses that were comparable to the specified thickness, but as the required coating thickness became thinner, the accuracy of the coating thickness obtained diminished.

6.3 Consideration of the Theoretical Modelling results

The table below provides a summary of the work carried out in the Theoretical modelling section.

Table 18 Summary of the thicknesses and the average %T from the theoretical studies

Study	**Wavelength range nm**	**ITO data**	**ITO Thickness nm**	**SLAR Refractive index**	**Optimum SLAR coating thickness nm**	**Average %T**
ITO thickness optimised for highest %T	400-700	1	**117.02**			**88.4**
		2	**114.43**			**84.6**
		3	**105.73**			**79.6**
		4	**120.68**			**91.5**
	450-900	1	**132.41**			**88.8**
		2	**137.78**			**76.3**
		4	**136.79**			**92.0**

	400-800	1	**116.74**			**88.1**
		2	**119.59**			**83.9**
		3	**102.15**			**79.0**
		4	**120.03**			**91.3**
ITO set at 2kÅ thickness to see effect on %T	400-700	1	**200**			**85.2**
		2	**200**			**77.8**
		3	**200**			**70.5**
		4	**200**			**89.5**
	450-900	1	**200**			**86.1**
		2	**200**			**84.0**
		4	**200**			**89.8**
	400-800	1	**200**			**86.1**
		2	**200**			**81.0**

		3	**200**			**71.4**
		4	**200**			**89.8**
Single layer of SiO_2 on 2kÅ ITO	400-700	1	**200**	**1.46180**	**86.60**	**92.2**
		2	**200**	**1.46180**	**88.67**	**87.8**
		3	**200**	**1.46180**	**87.31**	**77.1**
		4	**200**	**1.46180**	**80.75**	**95.5**
	450-900	1	**200**	**1.46180**	**89.83**	**91.8**
		2	**200**	**1.46180**	**93.73**	**91.7**
		4	**200**	**1.46180**	**88.34**	**94.3**
	400-800	1	**200**	**1.46180**	**87.20**	**92.1**
		2	**200**	**1.46180**	**89.86**	**88.9**
		3	**200**	**1.46180**	**88.28**	**77.1**
		4	**200**	**1.46180**	**82.05**	**94.9**

Single layer of TiO_2 on 2kÅ ITO	400-700	1	**200**	**2.34867**	**108.93**	**80.3**
		2	**200**	**2.34867**	**95.59**	**77.3**
		3	**200**	**2.34867**	**123.96**	**67.1**
		4	**200**	**2.34867**	**107.52**	**83.2**
	450-900	1	**200**	**2.34867**	**148.86**	**80.2**
		2	**200**	**2.34867**	**129.31**	**79.3**
		4	**200**	**2.34867**	**151.66**	**83.1**
	400-800	1	**200**	**2.34867**	**157.06**	**80.8**
		2	**200**	**2.34867**	**150.59**	**78.4**
		3	**200**	**2.34867**	**155.13**	**67.5**
		4	**200**	**2.34867**	**158.79**	**83.4**
Single layer of MgF_2 on	400-700	1	**200**	**1.38542**	**91.46**	**92.6**
		2	**200**	**1.38542**	**93.10**	**87.6**

2kÅ ITO		3	**200**	**1.38542**	**92.28**	**77.4**
		4	**200**	**1.38542**	**85.67**	**96.1**
	450-900	1	**200**	**1.38542**	**96.17**	**92.3**
		2	**200**	**1.38542**	**99.07**	**91.9**
		4	**200**	**1.38542**	**95.15**	**95.0**
	400-800	1	**200**	**1.38542**	**92.76**	**92.6**
		2	**200**	**1.38542**	**94.40**	**89.1**
		3	**200**	**1.38542**	**94.03**	**77.4**
		4	**200**	**1.38542**	**89.04**	**95.6**
Purely theoretical optimised Refractive indices of SLAR on 2kÅ	400-700	1	**200**	**1.35452**	**93.57**	**92.7**
		2	**200**	**1.42840**	**90.54**	**87.8**
		3	**200**	**1.37595**	**92.93**	**77.4**
		4	**200**	**1.32215**	**90.01**	**96.3**

ITO	450-900	1	**200**	**1.33534**	**101.63**	**92.4**
		2	**200**	**1.40263**	**98.03**	**91.9**
		4	**200**	**1.30834**	**103.14**	**95.3**
	400-800	1	**200**	**1.33967**	**96.24**	**92.7**
		2	**200**	**1.40417**	**93.24**	**89.1**
		3	**200**	**1.35570**	**96.36**	**77.4**
		4	**200**	**1.30834**	**94.06**	**95.8**
Single layer of Cryolite on 2kÅ ITO	400-700	1	**200**	**1.35**	**93.96**	**92.7**
		2	**200**	**1.35**	**95.49**	**87.4**
		3	**200**	**1.35**	**94.82**	**77.4**
		4	**200**	**1.35**	**88.16**	**96.2**
	450-900	1	**200**	**1.35**	**100.00**	**92.4**
		2	**200**	**1.35**	**101.51**	**91.8**

		4	**200**	**1.35**	**98.77**	**95.2**
	400-800	1	**200**	**1.35**	**95.47**	**92.7**
		2	**200**	**1.35**	**96.83**	**89.0**
		3	**200**	**1.35**	**96.85**	**77.4**
		4	**200**	**1.35**	**90.83**	**95.7**

Given the discrepancies between the ITO data, it is exceedingly difficult to say which set of data provides the most accurate representation. It is for this reason that the results from all of the ITO data sets was examined.

The prevalent observations from the results displayed in this table are as follows:

- It can be seen from the results that increasing the thickness of the ITO layer to 2kÅ results in a decrease in transmission. This concurs with the results observed by Eite (2004).

- The addition of a single layer of SiO_2, TiO_2 and MgF_2 respectively on top of 200nm of ITO in an attempt to maximise the average %T across all of the ranges considered produced some interesting results:

- The TiO_2 (with a refractive index greater than that of ITO) actually produced a decreased average %T in comparison to the plain layer of 200nm ITO

- The SiO_2 and MgF_2 (both with a refractive index less than that of ITO) on the other hand both enhanced the average %T observed for each range considered.

- Out of these three single layer coatings considered, MgF_2 created the best improvement of average %T overall on all of the wavelength ranges considered.

- The next step after considering the application of single layer coatings was to deduce the optimum coating thickness and optimum coating refractive index that could be used in a single layer. Optimisation processes are good tools. It must however be remembered that they are only as good as their starting point. If the wrong starting point is chosen, optimisation can result in a local maximum instead of finding the true

maximum. To minimise the chance of this, the Refractive index of MgF_2 was therefore used as the starting point as it provided the highest enhancement of average %T across the wavelength ranges of interest. This starting point was used in conjunction with Simplex optimisation in Essential Macleod to determine an optimised Refractive index and thickness for each case considered. This point has been reemphasised here as it is important to bear in mind when considering the results obtained.

- Symmetrical layer periods were used in an attempt to simulate the optimum refractive indices and thicknesses deduced previously. Unfortunately, the results from this show that the physical thicknesses required for each layer are exceedingly small making accurate deposition of such thicknesses exceedingly difficult. (This was illustrated in the Experimental section, where it could be seen that the actual thicknesses obtained compared to the thicknesses that were programmed got progressively less accurate when the thickness considered were smaller).

- As symmetrical layer periods produced results that it was difficult to apply practically, the next step was to attempt to find a commonly used coating material that had a refractive index as close to the calculated optimum refractive indices as possible.

- Studying the optimum refractive indices illustrates that the majority of the data predicts that Cryolite produces the highest average %T for the wavelength ranges considered. Cryolite was therefore modelled for all of the ITO data for the wavelength ranges of interest. 2D plots of %T versus wavelength for normal incidence were produced. Even though normal incidence is the primary consideration here, 3D plots were also shown to give more information for other angles. Circle diagrams were also produced to give a clearer picture of the effects the layers were having.

- From the Cryolite modelling, it could be seen that on the whole, Cryolite generally produces an average %T slightly smaller than for the optimum refractive index. This is to be expected as the refractive index of Cryolite moves the situation away from the optimum configuration. It is however noted that the difference between the Average %T for Cryolite and the %T for the optimum refractive index is very small which implies that Cryolite is a very good approximation to the optimum refractive indices.
- The below table compares the Material that was found to be nearest to the calculated optimum refractive index and the material that actually gave the highest average %T for the wavelength range considered.

Table 19 Comparison of the material giving the highest %T and the material nearest to the optimal refractive index

Wavelength range /nm	ITO Data	Nearest standard coating material	Material giving the highest %T on 2KÅ ITO
400-700nm	1	Na_3AlF_6 (Cryolite)	Na_3AlF_6 (Cryolite)
400-700nm	2	SiO_2	SiO_2
400-700nm	3	MgF_2	MgF_2
400-700nm	4	Na_3AlF_6 (Cryolite)	Na_3AlF_6 (Cryolite)
450-900nm	1	Na_3AlF_6 (Cryolite)	Na_3AlF_6 (Cryolite)

450-900nm	2	MgF_2	MgF_2
450-900nm	4	Na_3AlF_6 (Cryolite)	Na_3AlF_6 (Cryolite)
400-800nm	1	Na_3AlF_6 (Cryolite)	Na_3AlF_6 (Cryolite)
400-800nm	2	MgF_2	MgF_2
400-800nm	3	Na_3AlF_6 (Cryolite)	Na_3AlF_6 (Cryolite)
400-800nm	4	Na_3AlF_6 (Cryolite)	Na_3AlF_6 (Cryolite)

- It can be seen from this table that all of the predicted materials actually gave the highest average %T when considered. It can also be seen again that on the whole, Cryolite produces the highest average %T on the ranges considered on 2kÅ of ITO. Due to limited equipment access during this project, it was not possible to produce the ITO Cryolite coatings practically. This study would therefore be therefore a natural progression from this work.

- Another route taken in an attempt to maximise average %T was to investigate is the production of multi layer stacks on ITO using needle synthesis. As such good results were achieved with the Cryolite in the previous section, Cryolite was used as one of the stack constituents. As the refractive index of Cryolite is less than that of ITO, the other materials used in the stack was to be TiO_2 and Cryolite as this has a refractive index greater than that of ITO, is a commonly used AR material and therefore had a more substantial contrast to the Cryolite. The results from this however showed that some of the layers utilized in this are exceedingly thin. For reasons previously discussed, this can not

successfully be applied to Experimental TiO_2 and Cryolite work with any great accuracy. The average %T produced from this was found not to be as high as that produced with a single layer of Cryolite!!

- Another multilayer stack was modelled this time having ITO and Cryolite as the two materials in the stack to see the effects of this. Again, it could be seen from the results that some of the layers were exceedingly thin. Again, this can not successfully be applied to Experimental work with any great accuracy. The average %T is not as high as that produced with a single layer of Cryolite!!

- Cryolite seems to have produced some very encouraging results in the theoretical studies for the wavelength ranges considered. This is not the end of the story however, merely the beginning. Will Cryolite produce the results that they theory suggests? Is the next obvious question that needs to be addressed. If this hurdle is met, the next issue is that Cryolite is fairly soft (Chemical Land, 2008). This means that to make Cryolite a viable solution, a protective coating system would need to be developed to make it suitable.

6.4 Consideration of both the Experimental and Modelling results

The Experimental work carried out in this thesis shows that thick ITO layers are required to provide 20 ohms/square. The theoretical work carried out shows that the optimum transmission is obtained for lower ITO thicknesses, and the effect of increasing the thickness is to decrease the average %T across all of the wavelength ranges considered.

The Experimental work also shows that to obtain 100 ohms/square, the ITO layer required is thinner.

The results discussed above concur with the observations of Eite (2004) that increasing the thickness of an ITO coating results in an increase in conductivity.

Both the theoretical and experimental studies revealed that the average %T across the wavelength ranges considered could be increased by the addition of additional layer (s) of material.

6.5 Comparison between the work reported in the literature and this thesis

This thesis has examined the work done with coatings added to ITO coatings in an attempt to maximise %T in the visible region and used it as a starting point for further investigation into the maximisation of %T in the visible region.

The numerous papers (considered in section 2) have shown that the deposition variables considered play an important role in the results that are obtained. This thesis has carried out a more comprehensive study with the Ion Assisted Vapour Deposition parameters where more variables have been considered. The work carried out in this thesis concurs with the view that the variables used play a crucial role in the results obtained. It has been demonstrated by the results of this work that all of the variables considered effect the results obtained to a greater or lesser degree.

With all of the studies reported in the literature, the authors had either different or undisclosed sheet resistivity requirements (and thus thicknesses). Unless the required sheet resistivity matches the sheet resistivity requirements of this thesis, the work on variables illustrates that a direct comparison of the Transmission and Resistivity results can not be successfully performed as the result has been shown to be very variable dependent. It was for this reason that a direct comparison is not performed in this section. To do more work with this, the conditions given in the literature would need to be replicated to enable direct comparisons to be performed. Unfortunately, this was not possible due to the very limited practical time where the equipment was available.

6.6 More practical multilayer structures

A Multilayer structure that was applied in the Experimental section is illustrated in Table 20. This multilayer structure is more easily producible practically due to the more manageable thicknesses involved.

Table 20 Summary of the multilayers applied in the Experimental section

Date	Run	Additional Coating	ITO Thickness kA	AR Thickness kA	AR Deposition Rate A/s
140508	1	TiO2	2	0.09	2.5
		SiO2		0.46	5
		TiO2		0.28	3.5
		SiO2		0.18	5
		TiO2		0.80	3.5
		SiO2		0.16	5
		TiO2		0.26	3.5
		MgF2		1.02	10

The results of this showed an enhancement of the average %T produced in the wavelength ranges of interest. Thicknesses of this magnitude would need to be applied to the theoretical work to make a more practically achievable coating.

7 Overall Conclusions and Recommendations

7.1 Consideration of the aims and objectives of the project

It can be concluded that all of topics in the aims and objectives have been worked upon in this thesis. Obviously, the time scale dictates the amount of work that can be carried out on each topic, but it can be seen that all aims and objectives have been examined in a detail commensurate to the timescale of this project.

7.2 General Conclusions

Unfortunately, ideal ITO thicknesses that produce maximum %T requirements do not produce 20 Ohms/square. To achieve this sheet resistivity requires a thicker ITO layer. The modelling work carried out demonstrated that making the ITO layer thicker diminishes the average %T observed over the wavelength ranges considered. Application of additional coatings enhances %T. Luckily, this is not at the expense of sheet resistivity.

Cryolite has produced some very encouraging results in the theoretical studies for the wavelength ranges considered. This is not the end of the story however, merely the beginning. Will Cryolite produce the results that they theory suggests? Is the next obvious question that needs to be addressed. If this hurdle is met, the next issue is that Cryolite is fairly soft (Chemical Land, 2008). This means that to make Cryolite a viable solution, a protective coating system would need to be developed to make it usable in the application considered. It is acknowledged that MgF_2 produces only a slightly lower result than Cryolite and that MgF_2 is more durable, but it is this author's opinion that instead of avoiding Cryolite for this reason, work should be done to discover how to make it more usable, for example, a coating of a material like diamond like carbon may be

considered to enhance durability but minimizing the loss in transmission observed. It is this author's opinion that if you always do what you always did, you will always get what you have always got and it is therefore important to explore new options.

7.3 Recommendations for future work

It can be seen from this thesis that the main aims and objectives have all been worked upon in this thesis. This is not the end however, merely a foundation on the road of the quest for knowledge of ITO coatings. The author would therefore recommend the following as next steps as they naturally progress from this work:

- Practical implementation of Cryolite coating – is it as good as the theory suggests?
- Research to devise a protective coating system to make Cryolite usable in the application considered
- Further investigation into multi layer coatings for 2kÅ ITO that would produce thicknesses that are more realistically producible in practice.
- The author wishes to leave reader with the following question - Can Cryolite be beaten? – This is the ultimate question, but what is the answer.....

8 Appendices

Appendix A Parameters used with Electron beam evaporation

Date	Run	Thickness kA	Rate A/s	Material	Temp ° c	IAD	Anode Current A	Anode Voltage V	O2 flow sccm	Pressure x 10-4 mbar	Ar flow sccm	
20108	1	1.25	3.5	90 10 ITO	290	Yes	2	125	4.3	2.1	7	
20108	2	1.1	3.5	90 10 ITO	290	Yes	3	125	7.4	2.3	7	
80108	1	2	0.5	90 10 ITO	290	No	0	0	38	5	0	
80108	2	2	1	90 10 ITO	290	No	0	0	40	5.2	0	
90108	1	2	0.2	90 10 ITO	290	No	0	0	42	5.2	0	
90108	2	1	0.2	90 10 ITO	290	No	0	0	42	5.3	0	
220108	1	1	0.5	95 5 ITO	290	No	0	0	42	4.6	0	
220108	2	1	0.2	95 5 ITO	290	No	0	0	42	4.5	0	
250108	1	2	7.5	95 5 ITO	290	Yes	3	110	12.1	3.3	6	
250108	2	2	7.5	95 5 ITO	290	Yes	3	100	15.3	3.6	6	
250108	3	2	7.5	95 5 ITO	290	Yes	3	115	10.2	3.1	6	
260108	1	2.5	7.5	95 5 ITO	290	Yes	3	125	8.2	3	6	
60208	1	2	7.5	90 10 ITO	290	Yes	2	100	11.7	3	5	
60208	2	2	7.5	90 10 ITO	290	Yes	2	100	11.9	3	5	
60208	3	2	5	90 10 ITO	290	Yes	2	100	13.5	3	5	
70208	1	1.75	7.5	90 10 ITO	290	Yes	2	100	13	3.1	5	
110208	2	1.8	7.5	90 10 ITO	290	Yes	2	100	14.2	3.2	5	
220208	1	0.5	7.5	90 10 ITO	290	Yes	2	100	13.8	3.4	5	
250208	2	1	1.5	90 10 ITO	290	No	0	0	40	4.6	0	
250208	3	1.5	1	90 10 ITO	290	No	0	0	45	5	0	
260208	2	1.75	1	90 10 ITO	290	No	0	0	50	5.8	0	
270208	1	1.75	1	90 10 ITO	290	No	0	0	50	5.8	0	
270208	2	2	1	90 10 ITO	290	No	0	0	50	5.8	0	
280208	1	2.5	1	90 10 ITO	290	No	0	0	50	5.8	0	
280208	2	1.75	1.5	90 10 ITO	290	No	0	0	50	5.8	0	
10308	1	2	7.5	90 10 ITO	290	Yes	2	100	12.1	3.7	5	
30308	1	2	7.5	90 10 ITO	290	Yes	2	100	11	3	5	
50308	1	0.5	7.5	90 10 ITO	290	Yes	2	100	10.5	3.1	5	
50308	2	0.5	7.5	90 10 ITO	290	Yes	2.5	100	13	3.2	5	
50308	3	1	7.5	90 10 ITO	290	Yes	2.5	100	14.3	3.1	5	
60308	1	0.75	7.5	90 10 ITO	290	Yes	2.5	100	13.7	3.2	5	
60308	2	0.6	7.5	90 10 ITO	290	Yes	2.5	100	13.8	3.2	5	
70308	1	0.75	7.5	90 10 ITO	290	Yes	2	100	11.8	3.3	5	
70308	3	0.75	7.5	90 10 ITO	290	Yes	3	100	15.3	3.3	5	
100308	2	0.5	7.5	90 10 ITO	290	Yes	2	100	12.6	3.5	5	
110308	1	0.5	7.5	95 5 ITO	290	Yes	2	100	13.8	3.4	5	
120308	1	1	7.5	95 5 ITO	290	Yes	2	100	16	3.4	5	
90408	1	2	5	90 10 ITO	290	Yes	2	100	15.6	3.2	6	
90408	2	2	3.5	90 10 ITO	290	Yes	2	100	10.3	3.4	6	
100408	1	2	6	90 10 ITO	290	Yes	2	100	16	3.5	5	
100408	2	2	7.5	90 10 ITO	290	Yes	2	100	15.3	3.4	5	
110408	1	2	6	90 10 ITO	290	Yes	2	100	15.6	3.3	5	
70508	1	1	1	90 10 ITO	290	No	0	0	50	5.9	0	
100508	1	2	7.5	90 10 ITO	290	Yes	2	100	8.7	2.8	5	
120508	1	2	7.5	90 10 ITO	290	Yes	2.25	90	14	3.3	5	
150508	1	2	7.5	90 10 ITO	290	Yes	2.25	90	22.1	3.8	5	
160508	1	2	1	90 10 ITO	290	No	0	0	40	4.8	0	
230108	1	2	3.5	95 5 ITO	250	Yes	4	125	8.3	3	7	
230108	2	2	3.5	95 5 ITO	250	Yes	4	125	9.9	3	7	
230108	3	2	5	95 5 ITO	250	Yes	3	110	11.6	3.2	6	
240108	1	2	7.5	95 5 ITO	250	Yes	3	110	10.5	3.2	6	
240108	2	2	7.5	95 5 ITO	250	Yes	3	110	13.2	3.1	6	
240108	3	2	10	95 5 ITO	250	Yes	4	110	12.3	3.6	6	
70408	1	1.5	1.5	90 10 ITO	275	No	0	0	40	4.7	0	
70408	2	1.5	1	90 10 ITO	275	No	0	0	45	5.3	0	
80408	1	1.25	0.5	90 10 ITO	275	No	0	0	50	5.8	0	
80408	2	1.5	7.5	90 10 ITO	275	Yes	2	100	10	3.5	6	
290208	1	1.5	1.5	90 10 ITO	325	No	0	0	50	5.6	0	

9 References

Agerter, M, Al-Dahoudi N (2003) *Wet-chemical processing of transparent and antiglare conducting ITO coating on plastic substrates.* Journal of Sol-Gel Science and Technology, 27 (1), pp. 81-89

Al-Dahoudi N, Aegerter, M (2003) *Wet coating deposition of ITO coatings on plastic substrates.* Journal of Sol-Gel Science and Technology, 26 (1-3), pp. 693-697

Al-Dahoudi N, Aegerter, M (2006). *Comparative study of transparent conductive In2O3:Sn (ITO) coatings made using a sol and a nanoparticle suspension.* Thin Solid films, 502 (1-2), pp. 193-197

Amirishahbazi, M, Fallah, H, Zahedi, M (2005) *Fabrication of Indium Tin Oxide (ITO) antistatic nano-layers in the visible spectrum using DC Magnetron Sputtering.* International Journal of Nanoscience and Nanotechnology, Vol 1, No 1, pp 61-64

AtoZ of materials (undated)
http://www.azom.com/details.asp?ArticleID=2349, Accessed 06/05/08

Azo Nano (2005) *The Electroluminescent Light Sabre.* Nanotechnology News Archive. http://www.azonano.com/news.asp?newsID=1007. Accessed 26/08/08

Baouchi, A (1996) *Atomic force microscopy study of ITO coatings deposited on glass by DC magnetron sputtering.* Proceeding Annual Technical Conference – Society of Vacuum Coaters, pp. 151-156

Bashar, S (1998) *Study of Indium Tin Oxide (ITO) for Novel Optoelectronic devices. Thesis from* Department of Electronic Engineering, Kings College London.

Bertran, E, Corbella, C, Vives, M, Pinyol, A. Person, C, Porqueras, I (2003) *RF sputtering deposition of Ag/ITO coatings at room temperature.* Solid State Ionics, 165 (1-4) pp. 139-148

Bisht, H, Eun H, Mehrtens, A, Aegerter, M (1999) *Comparison of spray pyrolyzed FTO, ATO and ITO coatings for flat and bent glass substrates.* Thin Solid films, 351 (1-2), pp. 109-114

Boehme, M, Charton, C (2005) *Properties of ITO on PET film in dependence on the coating conditions and thermal processing.* Surface and Coatings Technology, 200 (1-4 Spec. Iss), pp. 932-935

Boycheva, S, Sytchkova, A, Piegari, A (2007). *Otical and electrical Characterisation of r.f. sputtered ITO fils developed as art protection coatings.* Thin Solid Films, 515 (24 spec. iss), pp8474-8478

Bunshah, R (1980) *High Rate Physical Vapor Deposition Processes.* AGARD Lecture Series No 106, Materials Coating Techniques, Neuilly Sur Seine, France p 2-1

Cerac technical publications (undated)
http://www.cerac.com/pubs/proddata/ito.htm, Accessed 06/05/08

Chen, B, Sun, X, Tay, B (2004) *Fabrication of ITO thin films by filtered cathodic vacuum arc deposition.* Materials Science and Enngineering B: Solid sate materials for advanced technology 106(3), pp. 300-304

Chen, S, Li, J (2005). *Sol-gel dip-coating technique for preparation of ITO thin film.* Zhongguo Youse Jinshu Xuebao/Chinese Journal of Nonferrous Metals, 15(1), pp. 94-99

De Bosscher, W, Dellaert, K, Luys, S, Lacres, A (2005) *ITO coating of glass for LCDs.* Information Display, 21 (11), pp. 12-15

Dever, J, Rutledge, Hambourger, O, Bruckner, E, Ferrante, R, Pietromica, A (1998) *Indium Tin Oxide – Magnesium Fluoride Co-Deposited Films for Spacecraft Applications.* Nasa contribution to the International Conference on Metallurgical Coatings and Thin Films, San Diego, California

Dobrowolski, J, Ho, F, Menagh, D, Simpson, R, Waldorf, A (1987) *Transparent, conducting indium tin oxide films formed on low or medium temperature substrates by ion-assisted deposition.* Applied Optics, Vol 26, No 24, pp5204-5210

Eite, J, Spencer, A (2004) *Indium Tin Oxide for transparent EMC shielding and Anti-static Applications.* Presented at EMCUK, Newbury. http://www.diamondcoatings.co.uk, Accessed 16/04/08

Fallah, H, Ghasemi, M, Hassanzadeh, A, Steki, H (2006) *The effect of deposition rate on electrical, optical and structural properties of tin doped indium oxide (ITO) films on glass at low substrate temperature.* Physica B: Condensed matter, 373(2), pp. 274-279

Gao, J, Sun, L, Zhng, X, Wang, Z (2001) *Deposition of ITO coating on PMMA substrate by RF magnetron sputtering.* Guangxue Jishu/Optical Technique 27(6) pp. 501-502

Gilo, M, Dahan, R, Croitoru, N (1999) *Transparent Indium tin oxide films prepared by ion-assisted deposition with a single-layer overcoat.* Optical Engineering, Volume 38, Iss 6, pp953-957

Gnehr,W, Hartung, U, Kopte, T (2005) *Pulsed plasmas for reactive deposition of ITO layers.* Proceeds, Annual Technical Conference – Society of Vauum Coaters, pp. 312 - 316

Goebbet, C, Nonninger, R, Aegerter, M, Schmidt, H (1999) *Wet chemical deposition of ATO and ITO coatings using crystalline nanoparticles redispersable in solutions.* Thin Solid Films, 351 (1-2), pp. 79-84

Han, M, Yun, Y, Choi, S (2005). *Effects of annealing condition on the preparation of Indium Tin Oxide (ITO) Thin fims via sol-gel spin coating process.* Materials Science forum, 492 – 493, pp. 325 - 330

Hatchett, P (2008), *Optical Coating Technology – MSc Ultra Precision Technologies Course notes*, Cranfield University.

Hirvonen, J (2004) *Ion Beam Assisted Deposition*. Materials Research Society Symposium Proceedings, Vol 792, p647 - 657

Hong, S, Han, J (2004) *Fabrication of indium tin oxide (ITO) thin film with pre-treated sol coating.* Journal of the Korean Physical Society, 45(3), pp. 634 – 637

Kim, K, Park, N, Kim, T, Cho, K, Lee, J, Chu, H, Sung, G (2005) *Indium Tin Oxide Thin Films Grown on Polyethersulphone (PES) Substrates by Pulsed-Laser Deposition for Use in Organic Light-Emitting Diodes.* ETRI Journal, Vol 27, No 4

Kusano, E, Kashiwagi, N, Kobayashi, T, Nanto, H, Kondo, I, Kinbara, A (1998) *Effects of CH4 addition to Ar-O2 discharge gases on resistivity and structure of ITO coatings.* Vacuum, 52(4), pp. 785-789

L-3 Wescam (2008) – http://www.l-3com.com/wescam/ Accessed 16/08/08

Lawson, K (2008) *Optical Applications of Coatings – MSc Ultra Precision Technologies Course notes.* Department of Materials Science, Cranfield University.

Lee, C, Hiau, S, Yang, Y (1999) *Characteristics of indium tin oxide (ITO) film prepared by ion-assisted deposition.* Proceedings, Annual Technical Conference – society of Vacuum Coaters, pp. 261-264

Lee, J, Park, J, Kim, Y, Chun, H, You, Y, Kim, D (2007) *Properties of ITO on PES fil in dependence on the coating conditions and vacuum annealing temperatures.* Korean Journal of Materials Research, 27(4), pp. 227-231.

Lippens, P, Segers, A, Haemers, J, De Gryse, R (1998) *Chemical instability of the target surface during DC-magnetron sputering of ITO coatings.* Thin Solid Films, 317 (1-2), pp. 405-408

Liu, C, Matsutani, T, Asanuma, T, Kiuchi, M (2003) *Structural, electrical and optical properties of indium tin oxide films prepared by low-energy oxygen-ion-beam assisted deposition.* Nuclear Instruments and Methods in Physics Research B Vol 206, pp348-352

Liu, C, Matsutani, T, Yamamoto, N, Kiuchi, M (2002) *High-quality indium tin oxide films prepared at room temperature by oxygen ion beam assisted deposition.* Euro Physics Letters, Vol 59, No 4, pp606-611

Liu, C, Mihara, T, Matsutani, T, Asanuma, T, Kiuchi, M (2003) *Preparation and characterizatoin of indium tin oxide films formed by oxygen ion beam assisted deposition.* Solid State Communications Vol 126, pp509-513

Mayr, M (1986) *High vacuum sputter roll coating. A new large-scale manufacturing technology for transparent conductive ITO layers.* Proceedings, Annual Technical Conference – Society of Vacuum Coaters, pp. 74-77

Morton, D, Dinca, A (1999) *Ion-Assisted Deposition of E-gun Evaporated ITO Films at Low Substrate Temperatures. 42nd Annual Technical Conference of the Society of Vacuum Coaters, Chicago – April 16th – 22nd*

Ngaffo, F, Caricato, A, Fernandez, M, Martino, M, Romano, F (2007) *Structural properties of ingle and multilayer ITO and TiO2 films deposited by reactive pulsed laser ablation deposition technique.* Applied Surface Science 253(15), pp. 6508-6511

Niino, F, Hirasawa, H, Koondo K (2002) *Deposition of low-resistivity ITO on plastic substrates by DC arc discharge ion plating.* Thin Solid films, 411(1), pp. 28-31

Nishio, K, Sei, T, Tsuchiya, T (1996) *Preparation and electricalproperties of ITO thin films by dip-coating process.* Journal of Materials Science 31 (7), pp. 1761-1766

NPL (2008) Table of Physical and Chemical Constants. http://www.kayelaby.npl.co.uk/general_physics?2_5/2_5_9.html Accessed 14/08/08

Pellicori, S (2002) *Common Deposition Techniques.* Cerac Coating Materials News, Vol 12, Iss 1 pp 1 – 3.

Piao, S, Liu, J, Zhang, N (2006). *Optical and electrical properties of transparent conduciton ITO films prepared by dip-coating process.* Advanced Materials research, 22-23, pp. 171-174

Pokaipisit, A, Horprathum, M, Kittiauchawal, T, Limsuwan, P (undated) *Growth and Characterization of ITO Thin Films grown by electron beam evaporation and ion assisted deposition.* 33rd Congress on Science and Technology of Thailand

Psuja, P, Strek, W (2007) *Fabrication of indium tin oxide (ITO) thin films by spin-coating deposition*. Proceedings of SPIE – The International Society for Optical Engineering, 6674, art no. 667408.

Puetz, J, Heusing, S, De Haro Moro, M, Ahlstedt, C, Aegerter, M (2005) *Gravure printing of transparent conducting ITO coatings for display applications.* Proceedings of SPIE – The International Society for Optical Engineering, 5963.

Raoufi, D, Fallah, H, Kiasatpour, A, Rozatian, A (2008) *Multifractal analysis of ITO thin films prepared by electron beam deposition method.* Applied Surface Science, 254(7), pp. 2168-2173

Sagecroft Technologies (2008) *Lightsaber.* http://www.coolest-gadgets.com/wp-content/uploads/lightsaber1.jpg Accessed 26/08/08

Shen, M., Ji, C., He, H (2006) *Investigation of sputtering coating ITO transparent elecroconductive film at lower temperature.* Ciliao Gongcheng/Journal of Materials Engineering (suppl.), pp. 17-19

Smith, D.L. (1995) *Thin-film deposition – Principles and Practice.* McGraw Hill, Boston, Massachusetts

SPO (2000) *Transparent ITO* http://www.optical-coating.com/cata_11_0.html, Accessed 26/08/08

Stetson, J (2006) *Analog Resistive Touch Panels and Sunlight Readability.* Information Display, Vol 12, No 06, pp 2-6

Strumpfel, J, May, C (2000) *Low ohm large area ITO coating by reactive magnetron sputtering in DC and MF mode.* Vacuum, 59 (2-3), pp. 500-505

Subrahmanyam (2002), *Transparent Conducting Oxide (TCO) Thin Films : Fundamentals to Frontiers*. www.geocities.com/sem_lab/subbu, Accessed 16/04/08

TakÅhashi, Y. OkÅda, S, Bel Hadj Tahar, R, NakÅno, Ban, T, Ohya, Y (1997) *Dip Coating of ITO films.* Journal of Non-Crystalline Solids, 218, pp. 129-134

Teghil, R, Ferro, D, Galasso, A, Giardini, A, Marotta, V, Parisi, G, Santagata, A, Villani P (2007) *Femtosecond pulsed laser deposition of nanostructured ITO thin films.* Materials Science and Engineering C, 27 (5-8 Spec Iss), pp. 1034-1037

Traub, L (2008) *Introduction to Optical Thin Films (Seminar notes) – Held at OpTIC, St Asaph, North Wales*

Viespe, C, Nicolae, I, Sima, C, Grigoriu, C, Medianu, R (2007) *ITO thin films deposited by advanced pulsed laser deposition.* Thin Solid Films 525 (24 Spec Iss), pp. 8771 - 8775

Wang, D, Fan, Z, Huang, J, Bi, J, Wang, Y (2006) *Symmetrical periods used as matching layers in multilayer thin film design.* Chinese Optics Letters, Vol 4, No 11, pp675-677

Wang, R, Lee, C (1999) *Design of antireflecion coating using Indium Tin Oxide (ITO) film prepared by Ion Assisted Deposition (IAD).* Proceedings, Annual Technical Conference – Society of Vacuum Coaters, pp. 246-249

Whitehouse, D (2002) *Surfaces and their measurement.* Kogan Page Science, London, UK, pp202-213

Wu, W, Chiou, B (1997) *Mechanical and optical properties of ITO films with anit-reflective and anti-wear coatings.* Applied Surface Science, 115 (1), pp.96-102

Yasui, T, Tahara, H, Yoshikawa, T (2001) *Study on deposition method of ITO thin films with large area by electron cyclotron resonance plasma sputtering. Shinku/Journal of the Vacuum society of Japan, 44(3), pp. 272-275*

Yu, Z. Xiang, L, Xue, W, Wang, H, Lu, W (2008) *The effects of process parameters on the properties of ITO films grown by ion beam assisted*

deposition using 90In-10Sn (%wt) alloy. Proceedings of SPIE – The International Society for Optical Engineering 6624, art no. 66241

Yun, Y, Choi, J, Choi, S (2004) *Surface treatment of Indium Tin Oxide (ITO) thin films synthesized by chemical solution deposition.* Journal of Ceramic Processing Research, Vol 5, No 4, pp395-398

Yun, Y, Hyun, W, Mi, J, Sung, C (2005) *Effects of sequential annealing processes on surface morphology and resistivity of Indium Tin Oxide (ITO) thin films fabricated by chemical solution deposition.* Journal of Ceramic Processing Research, 6(3), pp. 259-262

Zhou, J (2005) *Indium Tin Oxide (ITO) Deposition, Patterning and Schottky contact fabrication.* Thesis from Department of Microelectronic engineering, College of Technology, Rochester Institute of Technology, New York